POLITECHNIKA LUBELSKA

MONOGRAFIE

Computational Methods in Engineering Science

redakcja
Zbigniew Czyż
Marcin Badurowicz

Lublin 2019

Computational Methods in Enginering Science

Monografie – Politechnika Lubelska

Politechnika Lubelska
Wydział Mechaniczny
ul. Nadbystrzycka 36
20-618 LUBLIN

Computational Methods in Enginering Science

redakcja:
Zbigniew Czyż
Marcin Badurowicz

Wydawnictwo Politechniki Lubelskiej
Lublin 2019

Recenzent:
prof. dr hab. inż. Mirosław Wendeker, Politechnika Lubelska

Publikacja wydana za zgodą Rektora Politechniki Lubelskiej

ISBN: 978-83-7947-386-1

Wydawca: Wydawnictwo Politechniki Lubelskiej
www.biblioteka.pollub.pl/wydawnictwa
ul. Nadbystrzycka 36C, 20-618 Lublin
tel. (81) 538-46-59

SPIS TREŚCI

Zbigniew Czyż[1]

HELICOPTER MAIN ROTOR AERODYNAMIC SIMULATION USING CFD METHOD

Keywords: numerical analyses, helicopter main rotor, computational fluid dynamics, aerodynamic characteristics, drag force

Abstract

Today's progress in the development of rotorcrafts is mostly associated with optimisation of rotorcraft performance achieved by active and passive modifications of main rotor assemblies and a tail propeller. The solution to actively change aerodynamic characteristics assumes a periodic change of geometric features of blades depending on flight stages. Changing geometric parameters of blade warping enables optimisation of main rotor performance depending on helicopter flight stages. This numerical research with Ansys Fluent investigates the characteristics of the drag and lift force as a function of angle of attack for the profile of the blades. In order to obtain quantitative and qualitative data to solve this research problem, it was necessary to carry out a number of numerical analyses. This design concept assumes a three-bladed main rotor with a chord of 0.07 m and radius R = 1 m. The value of rotor speed is a calculated parameter of an optimisation function. A number of performance analyses as a function of rotor speed have been performed.

1. Introduction

The development of aircraft rotors construction is related to performance optimisation of the main rotor and tail rotor assemblies [9]. Numerous studies are being carried out to improve aerodynamics of aircrafts [14, 17, 20] or to reduce its fuel consumption [6]. The change of geometric properties of the elements of the rotorcraft depending on the flight stages, is the subject of many research papers [4, 7, 15]. Such an approach in the case of the blade, through the use of active and passive modifications, allows to increase the aerodynamic performance of rotorcraft [16, 18].

The angle of attack of a given section of the helicopter's rotor blade depends on the flight speed, current rotor azimuth, distance between the profile and the rotor axis, rotor's oscillation with respect to the horizontal and vertical hinge and given angle of general pitch controlled by the pilot. The range of attack angles achieved by different blade sections and their forced variability caused by control influence complexity of aerodynamic phenomena occurring on the main rotor. All of this makes aerodynamic loads acting on the blade, which are transferred to the fuselage to allow flight, very variable [10]. The literature [5, 11] presents a study

[1] Polish Air Force University, Faculty of Aviation, 35 Dywizjonu 303 Str., 08-521 Dęblin, Poland, z.czyz@law.mil.pl

of helicopter aerodynamics and flight mechanics mainly for fixed flight conditions. In the papers [1, 12] and [13], models of aerodynamic phenomena occurring on the main rotor were presented. The formulas enabling determination of the position of the main rotor cone and calculation of global forces and moments generated by the rotor were given.

The paper [19] presents experimental results of turbulence tests from helicopter rotor in the hover mode. The investigations were carried out with a model of a rotor in a T-1K wind tunnel at the Kazan Aviation Institute. The rotor consisted of four identical blades. The Q-criterion was used to identify peak vortices for a 2D case. The results were compared with two different turbulence models. In work [8] vortices were identified using Q-criterion, which defines vortices as connected spatial regions, where the Euclidean norm of the vorticity tensor dominates over the rate of strain tensor. Visualisation of the flow field around the research object was carried out on the basis of Dantec PIV system. More on imaging anemometry can be found in the paper [3].

2. Research object

Figure 1 shows the view of the blade with general dimensions. This blade was made based on profiles NACA 24018, NACA 23012 and NACA 2309. The blade chord is 0.07 m. The location of given profiles along the blade length is reserved and constitutes "know-how" of the project. Between the above mentioned sections, there is an approximation from one profile to another by using, for example, the function of multi-sections solid.

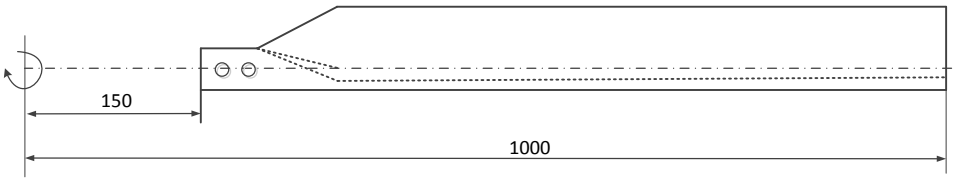

Fig. 1. View of the blade with general dimensions

The blade is based on three different aerodynamic profiles, which are approximated between the characteristic cross-sections indicated in figure 1 and provide a modification of two adjacent profiles. Therefore, it is important to determine transitional characteristics for the derivative profiles located between the main ones. 2D models were made for eight blade cross-sections starting from 0.3R to 1R every 0.1R. For each of sections numerical calculations were carried out in the range of angles of attack from 0° to 16° every 4°. This is a theoretical range for setting the angles of attack of the entire blade. Due to the number of measurement points, it was decided to carry out calculations from blades zero position and not from aerodynamic aerofoils zero position. This is justified by the

fact that the subject of the article is to test the supporting rotor and not individual aerodynamic profiles.

At work [2], calculations on engine load for prerotation of the main rotor of an autogyro were carried out. The calculations were performed in an analytical manner based on the available aerodynamic characteristics of the NACA 9-H-12 profile on which the rotor blade was based. In this case, three different profiles were used, which significantly extends the calculation, but the algorithm of operation remains unchanged.

3D model has been prepared in CATIA V5 program. Figure 2 shows the blade with applied aerodynamic profiles in control sections placed every 0.1 m. This blade is a research object and, at the same time, an initial model for further research. It contains torsional angles of individual sections, which are verified by the calculations carried out in this article.

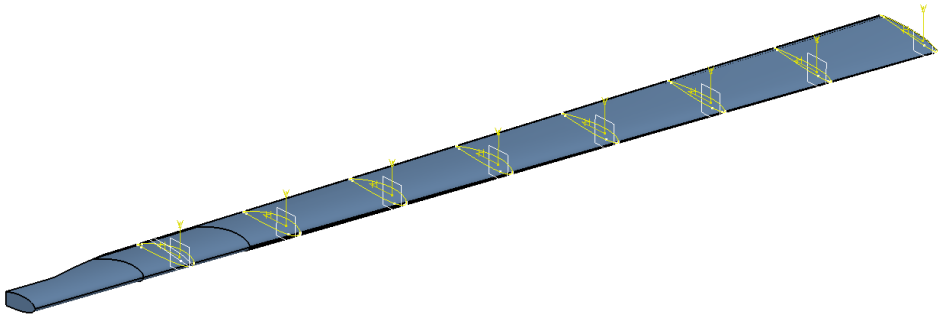

Fig. 2. View of 3D blade model with aerodynamic profiles

3. Numerical method and boundary conditions

Because the rotor blade is based on three different profiles and there are intermediate profiles between the three profiles (after approximation), the aerodynamic characteristics of profiles distributed evenly along the blade must first be developed. For this purpose, it was decided to divide the blade into sections starting from R = 0.3 m every 0.1 m. Each section is represented by a profile appropriate to the section, e.g. R/Ro = 0.3; 0.4;...; 1. 2D calculations were carried out for each section to determine the value of the lift force coefficient and the drag force coefficient. They will be used to calculate aerodynamic forces acting on the rotor as described in the work [2]. When the rotor rotates at an exemplary rotational speed of 1600 rpm, individual sections of the blade reach a different peripheral speed. Values of the peripheral speed at which the lift force and drag force coefficients of profiles placed on an individual radius are calculated and presented in table 1.

The calculations were carried out as two-dimensional. As a solver, the pressure-based solver was selected. In the solution settings as momentum equation

algorithm and default SIMPLE algorithm was selected. For the equations of momentum, energy, dissipation energy of turbulence, kinetic energy of turbulence, interpolation schemes of the second row were chosen. The convergence calculation solution for the above mentioned equations, as well as the pressure and the velocity on the plane of the symmetry were monitored during the simulation.

Tab. 1. Peripheral speed value in the considered sections

Radius R/Ro	Velocity at radius R [m/s]
0.3	50.24
0.4	66.99
0.5	83.73
0.6	100.48
0.7	117.23
0.8	133.97
0.9	150.72
1	167.47

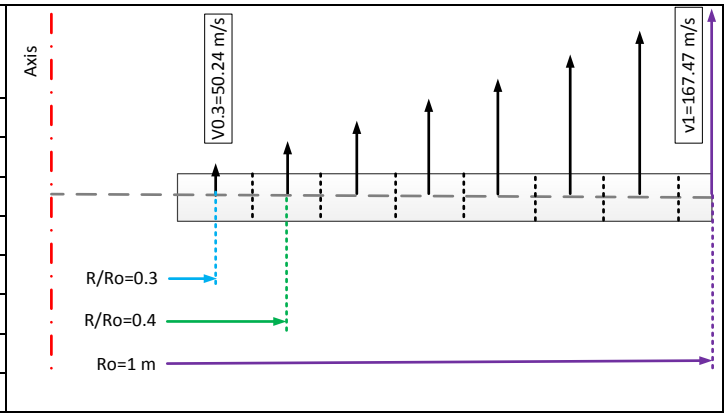

The calculations were carried out for turbulent intensity 1%, turbulent viscosity ratio 2 and temperature 288 K. For prepared geometry, the 2D mesh were calculated with 28 572 elements and 17 049 nodes (figure 3). The maximum skewness value is 0.76.

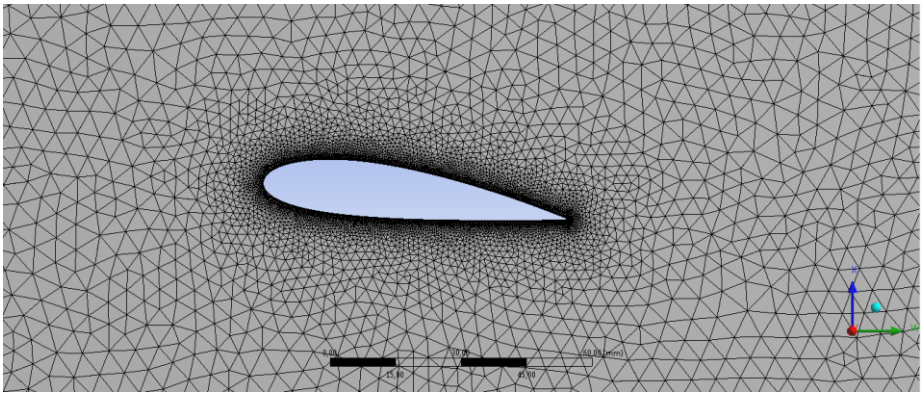

Fig. 3. View of the 2D computational grid for R = 0.3 m

In addition, a preliminary 3D model of the main rotor was developed for aerodynamic characteristics testing. Individual blades were prepared as solid models and then modified to facilitate preparation of the calculation grid (figure 4).

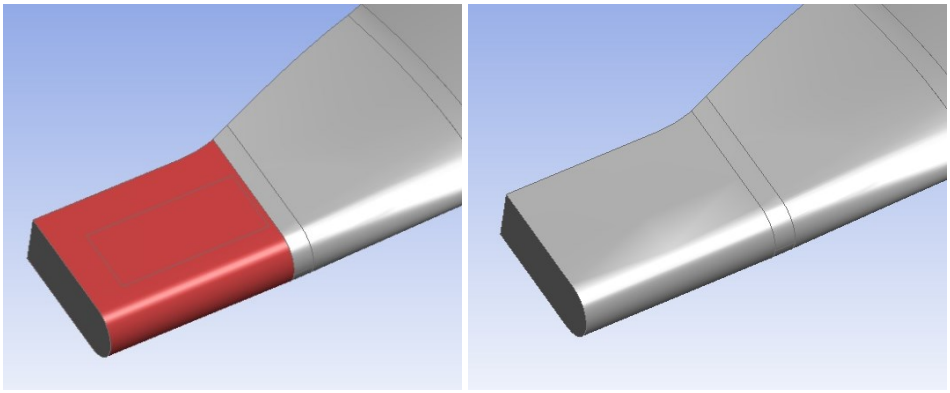

Fig. 4. Simplifying the rotor blade surface using the merge function

Figure 5 shows a view of the complete 3D model of the support rotor, based on which the computational model was developed. Sliding mesh layers on each other and the exchange of information between them without having to connect the nodes of each cell is guaranteed by the use of interfaces. This situation required to choose interfaces cooperating with each other, so it was necessary to create a pair of interfaces on the contact place, one for each of the adjoining.

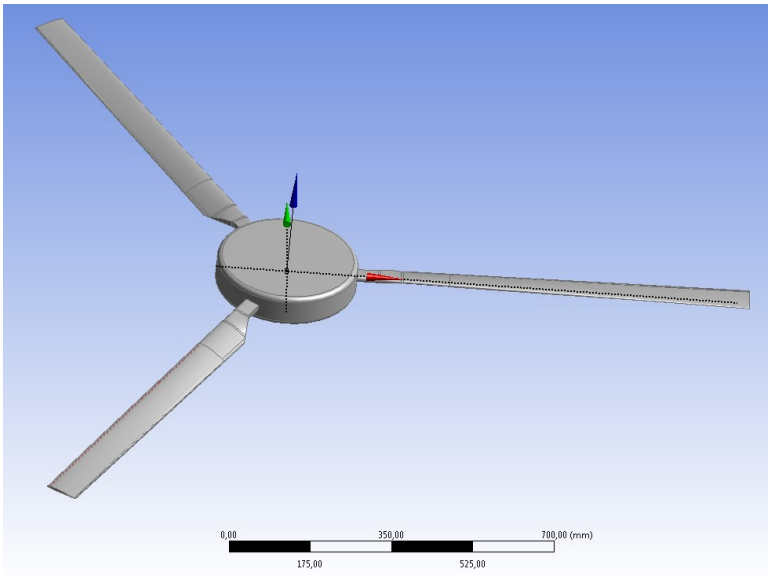

Fig. 5. View of the complete rotor for numerical calculations

For the Mesh Motion simulation using computational solver Fluent, flow phenomena simulation with transient time conditions was prepared. Due to the nature of flow, to solve the phenomena of turbulence, equation of energy and turbulence were assumed. In all analyses, the turbulence model Realizable k-ε

(RKE) was used. Calculations were carried out for a rotational speed of 1400–1800 rpm.

The flowing gas was the ambient air for which the ideal gas model was adopted. As a reference pressure, a normal pressure with a value of 101 325 Pa was assumed. In the simulations, following boundary conditions were assumed:

- inlet: pressure-inlet, air pressure at the inlet 101 325 Pa;
- pressure-outlet, air pressure at the outlet was equal to ambient pressure: 101 325 Pa;
- turbulent intensity: 10%;
- turbulent viscosity ratio: 10;
- time step: 0.000609 s;
- number of time step: 5000.

4. Results and discussions

Figure 6 shows the aerodynamic characteristics obtained by calculations of aerodynamic profiles used. Individual characteristics have been described in the legend as subsequent sections, e.g. 0.3R, i.e. R = 0.3 m, etc.

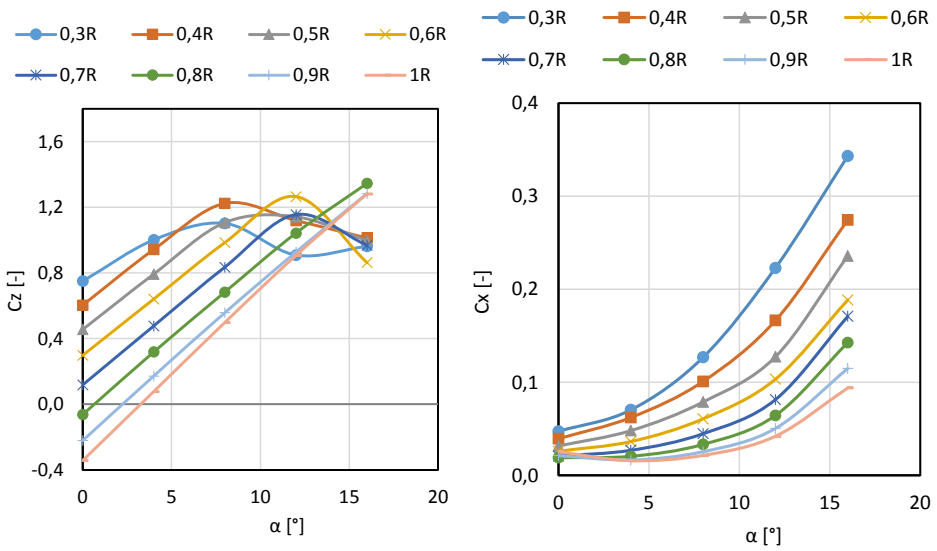

Fig. 6. The characteristics of the lift force coefficient (left) and drag force coefficient (right) as a function of the angle of attack α

In order to calculate the power demand and torque of the drive system of the tested rotor, the forces acting on individual blades should be determined. The general formula for the drag force (necessary to determine the torque) is shown in equation (1) where C_D is the drag force coefficient, ρ – air density, A – reference surface area, υ – blade peripheral speed.

$$F_D = 0.5 \cdot C_D \cdot \rho \cdot A \cdot v^2 \quad (1)$$

To calculate the total thrust generated by the rotor, firstly the lift force of a single blade should be determined. The formula for lift is illustrated by the following dependence (2). According to the calculation algorithm based on division into sections, in order to calculate the lift force of the first section (counting from the rotor axis), it is necessary to consider the lift force factor C_L for the profile located in the section R = 0.3 m (3).

$$F_L = 0.5 \cdot C_L \cdot \rho \cdot A \cdot v^2 \quad (2)$$

$$F_{L0,3} = 0.5 \cdot C_{L0.3} \cdot \rho \cdot A \cdot v_{0.3}^2 \quad (3)$$

Based on (3), the total lift generated by a single blade will be described as (4):

$$F_L = 0.5 \cdot \rho \cdot A \cdot (C_{L0.3} \cdot v_{0.3}^2 + C_{L0.4} \cdot v_{0.4}^2 + C_{L0.5} \cdot v_{0.5}^2 + C_{L0.6} \cdot v_{0.6}^2 + C_{L0.7} \cdot v_{0.7}^2 + C_{L0.8} \cdot v_{0.8}^2 + C_{L0.9} \cdot v_{0.9}^2 + 0.5 \cdot C_{L1} \cdot v_1^2) \quad (4)$$

Similarly, the torque of one blade (5) and the power of the propulsion system from equation (6) can be determined.

$$M = F_{D0.3} \cdot R_{0.3} + F_{D0.4} \cdot R_{0.4} + F_{D0.5} \cdot R_{0.5} + F_{D0.6} \cdot R_{0.6} + F_{D0.7} \cdot R_{0.7} + F_{D0.8} \cdot R_{0.8} + F_{D0.9} \cdot R_{0.9} + F_{D1} \cdot R_1 \quad (5)$$

$$P = \frac{M \cdot n}{9549.3} \text{ [kW]} \quad (6)$$

Figure 7 shows an exemplary velocity contour and pressure contour around the blade profile for a radius R = 0.3 m, peripheral speed v = 50.24 m/s and an angle of attack α = 12°.

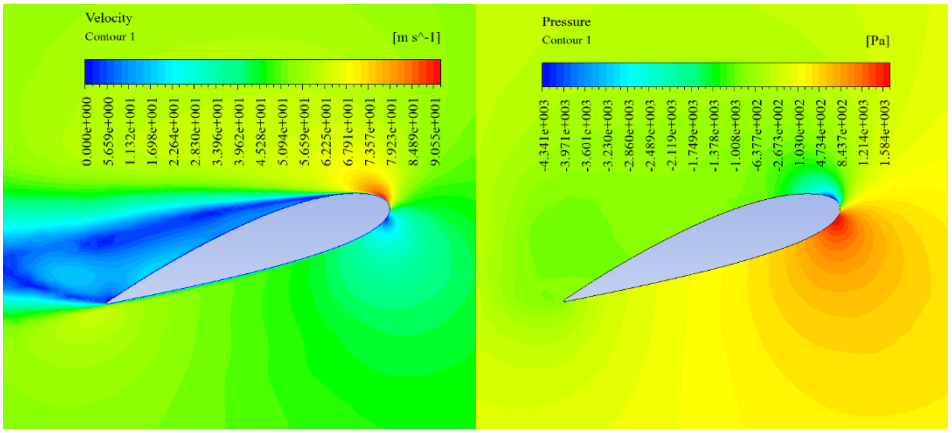

Fig. 7. Velocity contour (left) and pressure contour (right) around blade profile for R = 0.3 m, v = 50.24 m/s, α = 12°

Figure 8 shows the velocity contour and pressure contour around the blade profile for a radius R = 1 m, peripheral speed v = 167.47 m/s and an angle of attack α = 12°.

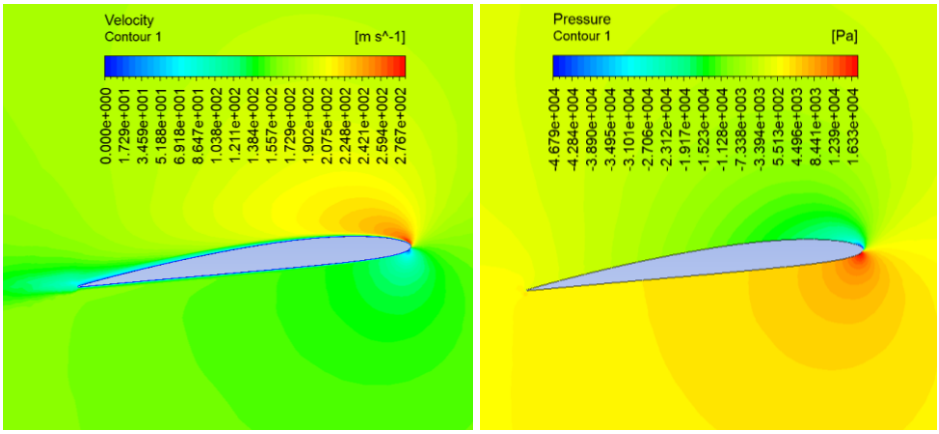

Fig. 8. Velocity contour (left) and pressure contour (right) around blade profile for R = 1 m, v = 167.47, m/s, α = 12°

Figure 9 shows the dependence of the demand for the power of the propulsion system on the angle of attack of the rotor blades and the mass for the considered rotor speeds in the range from 1400 rpm to 1800 rpm.

Figure 10 shows the dependence between the torque as a function of the angle of attack of the rotor blades and the mass for the considered rotor speeds in the range from 1400 rpm to 1800 rpm.

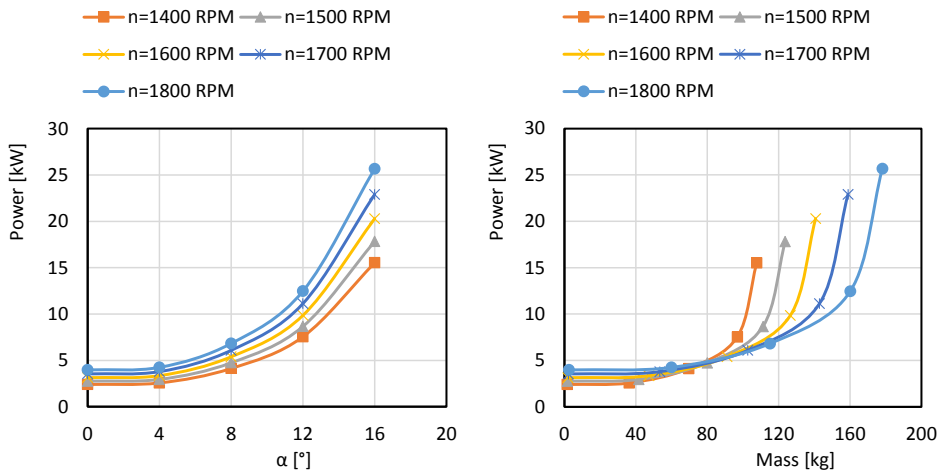

Fig. 9. Demand for power of the rotor drive system as a function of angle of attack (left) and as a function of weight (right)

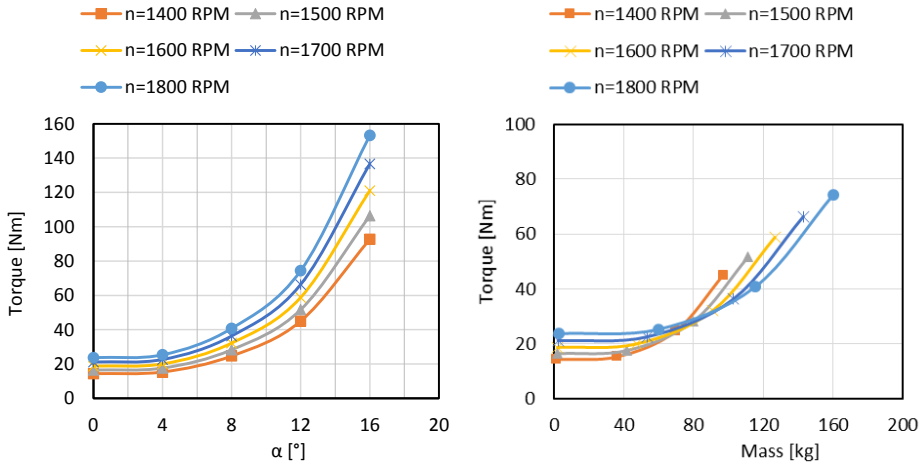

Fig. 10. Demand for torque of the rotor propulsion system as a function of the blade angle (left) and as a function of weight (right)

Based on the calculations carried out using the mesh motion method, very similar results of power demand and torque were obtained in relation to the thrust presented as the lifting mass. Three-dimensional calculations were carried out for the selected rotation speed n = 1600 rpm. Figure 11 shows the pressure contour on the surface of the tested rotor.

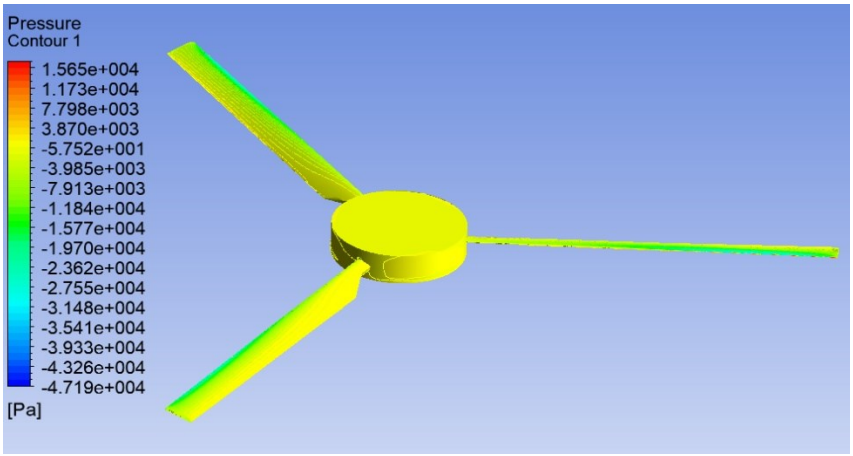

Fig. 11. View of the pressure contour of main rotor

A comparison of obtained results is shown in figure 12. For the rotational speed n = 1600 rpm in the first method based on 2D analysis, the angle of attack α = 12° resulted in a thrust force equal to 1241.8 N. For the mesh motion method, it is only 936.7 N which is a difference of 24.6%. The reduced value of the thrust force in relation to the angle of attack of the rotor blades for the mesh motion method may result from the influence of the number of blades on the results obtained. The phenomenon of aerodynamic interference of blades interacting with each other can have a negative effect. The first method based on 2D analysis does not consider the negative impact of the blades. Subsequent tests including wind tunnel tests will allow to verify current calculations.

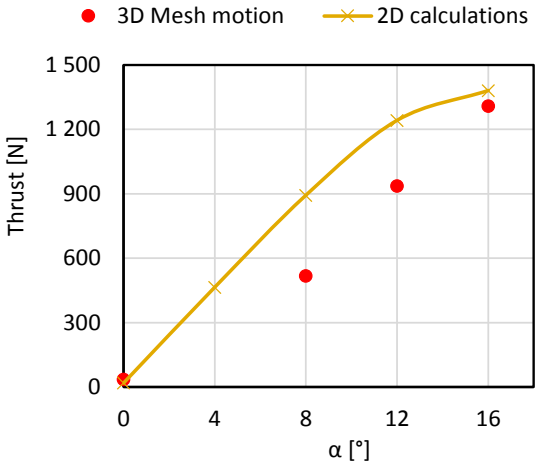

Fig. 12. Comparison of obtained power demand values for n = 1600 rpm

5. Conclusion

The research performed on helicopter rotor blades is the initial stage of work on a new rotor, to increase the aerodynamic performance of rotorcraft. The work involved calculations of thrust and demand for torque and power of helicopter main rotor propulsion system. The calculations were carried out for rigid rotor blades with a diameter of 2 m. The rotor is to be dedicated to the unmanned helicopter with a take-off mass up to 150 kg. Based on the results obtained (Fig. 9), it was found that only at a rotational speed of 1700 and 1800 rpm sufficient thrust has been achieved. In the considered range of blade angles of attack from 0° to 16° degrees for a rotational speed of 1800 rpm, a thrust force corresponding to 150 kg of mass at $\alpha = 11°$ was obtained. The power demand for these conditions is 10.5 kW and for torque 67 Nm. To achieve the same thrust for a rotational speed of 1700 rpm, power demand increases to 14 kW, torque is 85 Nm and blade angle $\alpha = 13°$. In the future, wind tunnel testing is planned to validate numerical models.

Acknowledgement

This work has been financed by the Polish National Centre for Research and Development under the LIDER program. Grant Agreement No. LIDER/45/0177/L-9/17/NCBR/2018.

References

[1] A. R. S. Bramwell, G. Done, D. Balmford, "Balmford, Bramwell's Helicopter Dynamics", *Oxford: Butterworth-Heinemann*, 2001.

[2] Z. Czyż, T. Łusiak, D. Czyż, D. Kasperek, "Analysis of the Pre-Rotation Engine Loads in the Autogyro", *Advances in Science and Technology Research Journal*, vol. 10(31), pp. 169–176, 2016, https://doi.org/10.12913/22998624/64015.

[3] Z. Czyż, W. Stryczniewicz, "Investigation of Aerodynamic Interference in a Multirotor by PIV Method", *Advances in Science and Technology Research Journal*, vol. 12(1), pp. 106–114, 2018, https://doi.org/10.12913/22998624/86475.

[4] A. Fortini, A. Suman, M. Merlin, G. L. Garagnani, "Morphing blades with embedded SMA strips: An experimental investigation", *Materials and Design*, vol. 85, pp. 785–795, 2015, https://doi.org/10.1016/j.matdes.2015.07.175.

[5] A. Gessow, G. C. Myers, "*Aerodynamics of the helicopter*", F. Ungar Pub. Co. 1952.

[6] Ł. Grabowski, K. Siadkowska, K. Skiba, "Simulation Research of Aircraft Piston Engine Rotax 912", *MATEC Web of Conferences*, vol. 252, 05007, 2019, https://doi.org/10.1051/matecconf/201925205007.

[7] S. Gudmundsson, "The Anatomy of the Airfoil", *General Aviation Aircraft Design*, 2014, https://doi.org/10.1016/B978-0-12-397308-5.00008-8.

[8] G. Haller, "An objective definition of a vortex", *Journal of Fluid Mechanics,* vol. 525, pp. 1–26, 2005, https://doi.org/10.1017/S0022112004002526.

[9] A. Kovalovs, E. Barkanov, S. Ruchevskis, M. Wesolowski, "Optimisation Methodology of a Full-scale Active Twist Rotor Blade", *Procedia Engineering*, vol. 178, pp. 85–95, 2017, https://doi.org/10.1016/j.proeng.2017.01.067.

[10] G. Kowaleczko, T. Kwaśniak, M. Nowakowski, M. Michalczewski, "Analysis of aerodynamics and main rotor loads under stalled conditions of helicopter's main rotor during the pull-up manoeuvre", *Journal of Konbin*, vol. 48(1), pp. 7–29, 2018, https://doi.org/10.2478/jok-2018-0045.
[11] A. Kusyumov, S. Kusyumov, S. Mikhailov, E. Romanova, K. Phayzullin, E. Lopatin, G. Barakos, "Main rotor-body action for virtual blades model", *EPJ Web of Conferences*, vol. 180, 02050, 2018, https://doi.org/10.1051/epjconf/201818002050.
[12] R. N. Liptrot, "Helicopter Dynamics and Aerodynamics", *P. R. Payne. Pitman*, London, 1959. 442 pp. Illustrated. 84s. The Journal of the Royal Aeronautical Society, vol. 63(585), 553, 2016, https://doi.org/10.1017/S0368393100071728.
[13] G. D. Padfield, "Helicopter Flight Dynamics: The Theory and Application of Flying Qualities and Simulation Modelling", *Blackwell Publishing*, 2007.
[14] V. A. Pastrikakis, R. Steijl, G. N. Barakos, J. Małecki, "Computational aeroelastic analysis of a hovering W3 Sokol blade with gurney flap", *Journal of Fluids and Structures*, vol. 53, pp. 96–111, 2015, https://doi.org/10.1016/j.jfluidstructs.2014.06.014.
[15] R. Raczynski, "The use of co-simulation methodology in the project of PZL SW-4 helicopter adaptation to maritime version", *In 45th European Rotorcraft Forum*. Warsaw, 2019.
[16] P. Sarkar, R. Raczynski, "Recent Progress in Flow Control for Practical Flows", *In P. Doerffer, G. N. Barakos, & M. M. Luczak (Eds.), Springer*, pp. 126–135, 2017, https://doi.org/10.1007/978-3-319-50568-8.
[17] A. K. Sehra, W. Whitlow, "Propulsion and power for 21st century aviation", *Progress in Aerospace Sciences*, vol. 40(4–5), pp. 199–235, 2004,
https://doi.org/10.1016/j.paerosci.2004.06.003.
[18] A. Y. N. Sofla, S. A. Meguid, K. T. Tan, W. K. Yeo, "Shape morphing of aircraft wing: Status and challenges", *Materials and Design*, vol. 31, pp. 1284–1292, 2009, https://doi.org/10.1016/j.matdes.2009.09.011.
[19] R. Stepanov, S. Mikhailov, "Experimental investigation of main rotor wake", *MATEC Web of Conferences*, vol. 115, 02013, 2017, https://doi.org/10.1051/matecconf/201711502013.
[20] D. P. Wells, "NASA Green Flight Challenge: Conceptual Design Approaches and Technologies to Enable 200 Passenger Miles per Gallon", *Environmental Protection*, pp. 1–17, 2011, https://doi.org/10.2514/6.2011-7021.

Szymon Molski[1], Paweł Lonkwic[2], Hubert Ruta[3], Tomasz Krakowski[4]

CRITICAL POINTS BY USING STRESS ACTIVE ANALYSIS OF STRUCTURE POINTS

Keywords: FEM, active points, stability, elevator, elevator frame, traction lift

Abstract

The article presents the Finite Element Method used to evaluate the bracket-type structure in terms of stress accumulation in the places of structural notches. Frequently, the presence of structural notches causes a local increase in stresses. The active points of stresses allow the evaluation of the structure with regard to its stability. The comparison of results obtained from the stress numerical calculations without analysing stress active points and with the use of this method is presented herein.

1. Introduction

Reliability of results received in numerical calculations often seems to be questionable. Especially, when a simple structure is calculated by means of numerical calculations, and significantly higher results are received, as compared to approximate values suggested by our engineering intuition.

In principle, numerical modelling comes down to the reflection of real geometry of a product. The purpose of such an approach is to:

- eliminate prototype production,
- analyse production capabilities,
- eliminate assembling errors,
- analyse the product strength under applied load.

The world literature authors describe the use of finite element method in various fields of mechanical engineering. The article [4] discusses the application of finite element method to the numerical analysis of welding heat source. In the

[1] AGH University of Science and Technology The Faculty of Mechanical Engineering and Robotics, Department of Machine and Transport Engineering, Al. Mickiewicza 30, 30-059 Cracow, Poland, molski@agh.edu.pl

[2] The State School of Higher Education in Chełm The Institute of Technical Sciences and Aviation, 54, Pocztowa Street, 22 – 100 Chelm, Poland, plonkwic@pwsz.chelm.pl

[3] AGH University of Science and Technology The Faculty of Mechanical Engineering and Robotics, Department of Machine and Transport Engineering, Al. Mickiewicza 30, 30-059 Cracow, Poland, hubert.ruta@agh.edu.pl

[4] AGH University of Science and Technology The Faculty of Mechanical Engineering and Robotics, Department of Machine and Transport Engineering, Al. Mickiewicza 30, 30-059 Cracow, Poland j, krakowsk@agh.edu.pl

publication [3] authors present numerical research results for energy absorption capability of energy absorbents in the form of thin-walled poles with a square section with cavities, subject to axial impact loads. Research covered impact of geometric parameters and position of strain initiators in the form of cylindrical dimples in corners on behaviour of the structure and energy absorption properties. The article [2] details the numerical analysis of the semitrailer frame structure with variable length and increased carrying capacity intended for transportation of excessive cargos. Conducted research aimed at developing adequate FEM numerical models facilitating identification of structure strain and deformation in operational conditions.

In the publication [15] the authors described the use of numerical methods to evaluate buckling of a thin-walled profile in the shape of a C-beam subject to axial pressing. In the publication [10] the authors used numerical simulations to evaluate the strain of safety gear structure in the passenger lift. The results of numerical simulations were compared with the results of a physical experiment that has given concurring results.

The author of publication [14] depicted a problem of I-shaped profile optimisation. The optimisation process was conducted with the use of Abaqus program. The numerical analysis of a strictly statistical problem was based on the finite element method. The scope of analysis covered also determination of stresses and displacements in the profile, as well as structure typology optimisation. A different approach to structure engineering is presented in the publication [1]. The authors described impact of selected operational parameters on the distribution of stresses/deformations of a piston crown in the diesel engine. The use of FEM method allowed the explanation of wear mechanism, which in general leads to damages on the surface of piston crowns. Results obtained from operational research confirm presence of cracks and chipping in places of maximum stresses and deformations. The authors of the publication [5] discussed preliminary results of FEM analysis covering an impact of an experimental machining and chipping head on a rock. A strong impact of FEM grid on quality and accuracy of simulation was established. Moreover, the finite element method is more and more often used to simulate the effects of the magnetic field. Publications [9], [8] show results of numerical analysis for the magnetic field distribution when designing magnetic circuits in measuring probes used in magnetic testing of steel ropes. The author of the publication [13] presents the possibility to apply the finite element method in analysis and measurements of values describing the magnetic field. Measurements were taken in the QuickField program. According to the author, the use of simulation method in the field of inductance allows to evaluate model performance in defined external conditions and introduce structural modifications. In the publication [19] the author presented the use of FEM method to analyse the results of simulation of stresses and deformations in the electric motor housing on the basis of which, as the author claims, it was possible to optimise the housing. In the publication [11] the authors

described the results obtained in the analysis of the safety gear structure by means of the Finite Element Method and Abaqus software. In the publication [22] the authors discussed the method of modelling a composite profile, which was subject to axial pressing. Numerical simulation results were compared with the results received from tensile testing. The authors of article [6] present their own original FEM application for strength analysis and three-arm puller geometry optimisation. The designed puller was modelled with the use of Solid Works environment software. Strength test simulation results for stresses were presented, so were results of calculation of deformations and displacements occurring during the operation of the puller. Authors in the article [21] detail the application of ABAQUS program for the numerical simulation of the rectangular extruded profile forming process. The numerical model considered a change in friction factor and in mechanical properties, as well as a change in orientation in relation to the rolling direction. The objective of the paper [18] was to carry out strength testing of coach bodies in the situation of its overturning to the side or turning upside down. Examination of the process of hitting the road surface and deformation of body framework is supposed to allow the assessment of passengers' safety and body strength of this type of vehicles. The Abaqus software was used in simulation. In the publication [12] the authors described the results of numerical simulation applied to assess some displacements of the machine tool body used for the extruded joints and operated in equal geometric configurations. In the publication [17] the authors used the Finite Element Method available in Catia program to evaluate the strain of a carrying frame in a heavy vehicle. Stiffness of frame elements under load was also evaluated. Applicability of the Finite Element Method is much more extensive in technology, not only for purposes connected with mechanical engineering but also in different fields of technology. The author in the publication [7] showed the numerical simulation of cutting process, considering the phase of ductile fracture. Fracture growth was modelled by deleting, in next steps, deformation of these elements in case of which the critical value of the specified factor has been exceeded. A joint study describing the application of the finite element method to engineering structure is compiled in [16]. Authors present the use of this method in load carrying structures affected by various load cases.

In numerical modelling it is frequent that significant geometrical details are ignored. These are the details that affect not only proper assembly but also disturb the numerical analysis results. One of such details is the place where one surface joins the other. It is called a notch in the machines structure. When performing numerical calculations for the structural notch, the value of stresses is much higher than it is in reality.

2. Numerical model of a bracket-type part

The numerical model of a bracket-type part is presented in figure 1. A characteristic feature of the presented theoretical model is no radius on bracket bend.

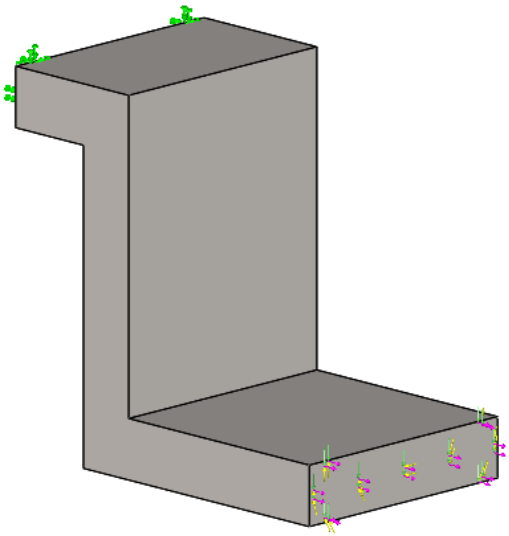

Fig. 1. The numerical model of a bracket-type part (the authors' private source)

For the purpose of theoretical numerical analysis, the bracket was restrained by eliminating all freedom degrees, three translational and three rotational ones (Lx=Ly=Lz=0 i Rx=Ry=Rz=0). Elimination of freedom degrees is illustrated in figure 1 as green arrows. In order to represent the distribution of stresses in the place of a notch, the bracket had to be subject to complex load. To achieve the assumed objective, three types of load have been selected:

- tensile force of 250N value (pink),
- shearing force of 250 N value (green)
- torque of 2 Nm value (yellow)

Values of individual loads have been matched by iterating successively simulation calculations so that stress active points occur.
In order to present the place where stresses are accumulated, the denser mesh was used in the area of a zero radius presented in figure 2.

A solid mesh was used in the model. The mesh was based on the curvature mixed with Jacobian determinants in the nodes of 1mm size. The denser mesh was used in the places with a structural notch. Also, an element of 0.45 mm size was defined. The model with applied Finite Element mesh is presented in figure 3.

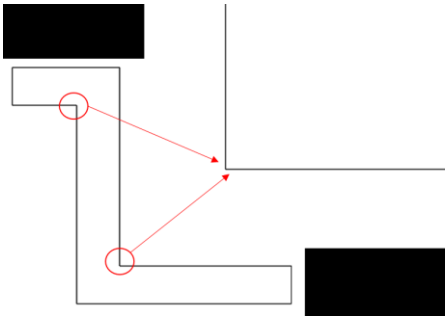

Fig. 2. The geometrical model with a linear structural notch (the authors' private source)

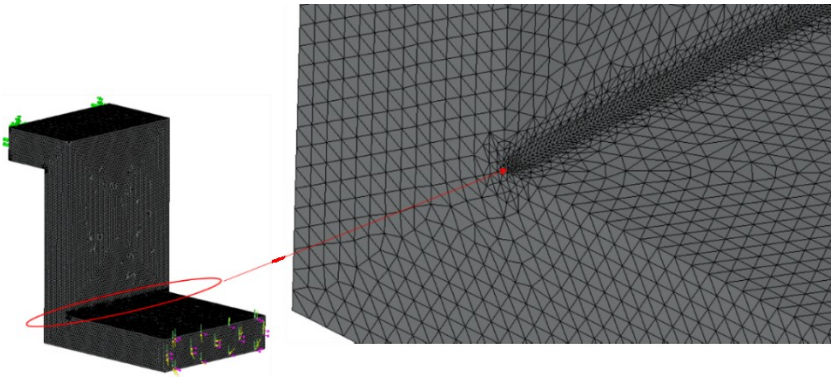

Fig. 3. The geometrical model with applied Finite Element mesh and a denser mesh used in the structural notch area

The bracket has been designed to be made from steel with the following mechanical properties:

- Young's modulus E = 210 GPa,
- Poisson's ratio $\nu = 0.3$,
- material density $\rho = 7860$ kg/m3,
- yield point $R_e = 230$ Mpa

The result of numerical calculations for the bracket subject to the complex load are presented in figure 4. While analysing the received stress distribution it can be noticed, that the colour of the volume majority ranges from dark blue to light blue. This illustrates on the stresses scale that the value of stresses in the modelled part should be on the level of app. 60 MPa. However, the maximum value of stresses reached in the analysed part is on the level of 131 MPa. That value exceeds significantly the stresses in the remaining volume of the model. When the place of the structural notch is enlarged (Fig. 5), it is noticeable that there are stress-active points on the edge between two surfaces. They reach significantly higher values than the remaining values of stresses in the part model.

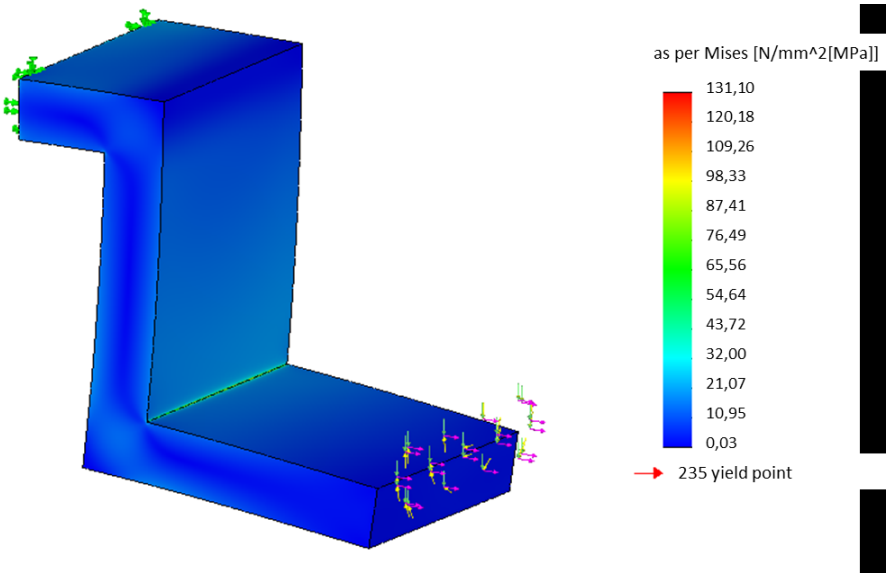

Fig. 4. The discrete model with nodular stresses distribution

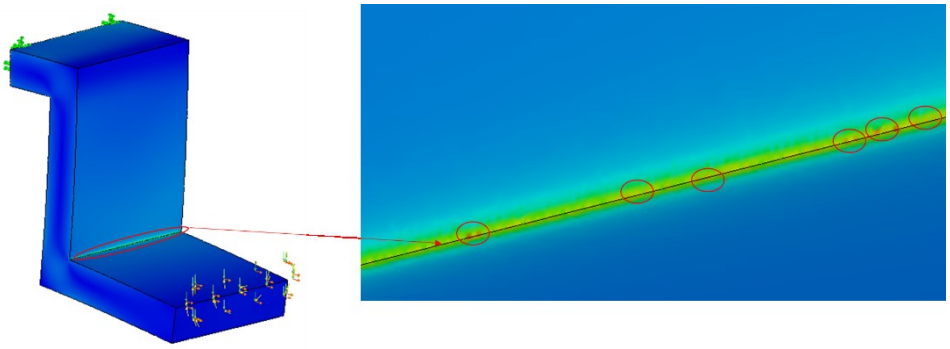

Fig. 5. The stress active points distribution

Distribution of stress values in the structural notch is presented in figure 6. To eliminate unwanted phenomenon of stress accumulation in the modelled parts, the temporary notches should be used. These are for example: undercuts, curvatures and edge chamfers. These are the notches where potentially some stress accumulations appear [[20]]. The example described above has been changed by using the temporary notches on edges where stress-active points were present. The change involved adding 2 mm curvature, which is illustrated in figure 7.

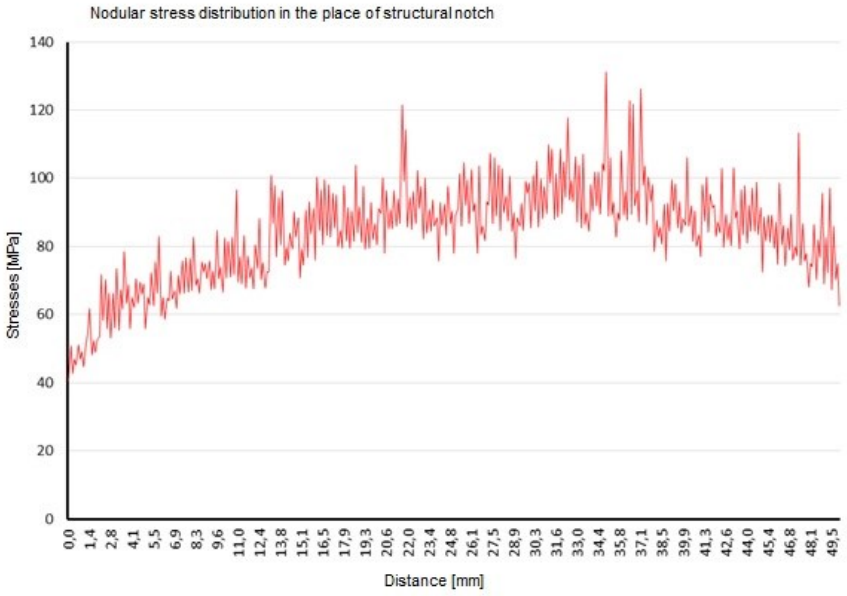

Fig. 6. Diagram of stress distribution as a function of model edge length

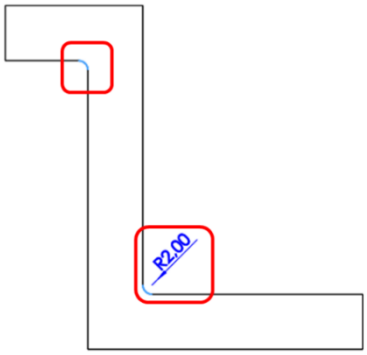

Fig. 7. The numerical model after geometrical modifications

After implementing some changes to the model geometry, it is not possible to reanalyse the numerical calculations until the new mesh is prepared. In the presented case, the mesh was made with the same properties as these described in the above case. Moreover, in the areas of edges with modified geometry, the function to control the mesh was eliminated. From the point of view of structure mechanics, stress accumulation will appear also in the analysed area of our part, but it will be directed to the certain area, and not to the spot fluctuations of values. The numerical model of the analysed part and the values of stresses are displayed in figure 8.

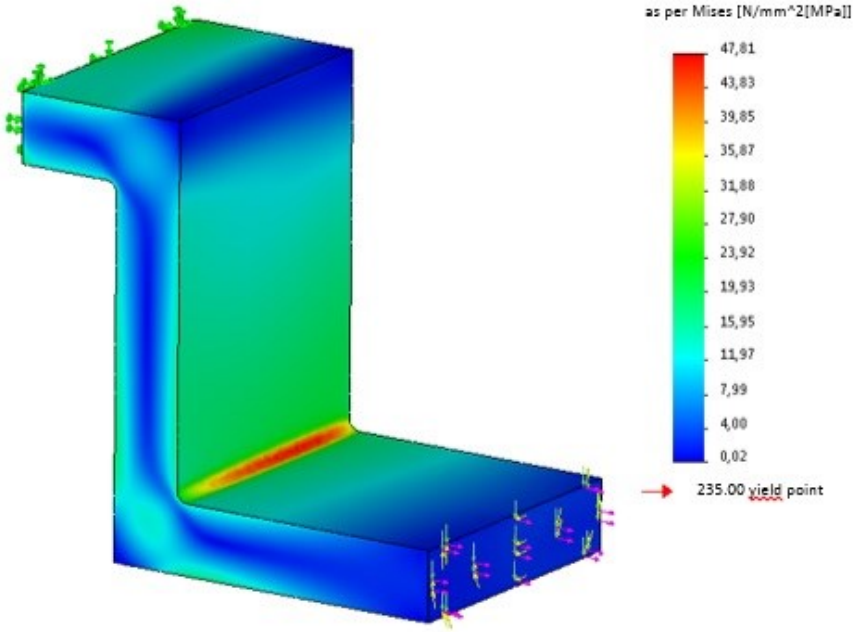

Fig. 8. The model after geometry modifications with the recalculated values of stresses

As presented in figure 7, maximum values of stresses in the analysed model, due to the rounded corner are 47.8 MPa. These values are more probable from the production's point of view.

In the case shown in figure 3, maximum stresses, according to the Huber von Mises's hypothesis, of 131 MPa have been achieved under the set load. The temporary notch applied in the bracket structure allowed to reduce the maximum stresses to 47.8 MPa. By analysing figure 7, it can be noticed that the distribution of stresses in the place of bracket bend on the assumed radius is more uniform than in the case of non-rounded edges.

When analysing the above case, a fundamental aspect of structural analysis is to adopt the right procedure that would ensure the most authentic geometrical condition of the part and the condition of stresses under load. figure 8 presents the scenario for the above mentioned case.

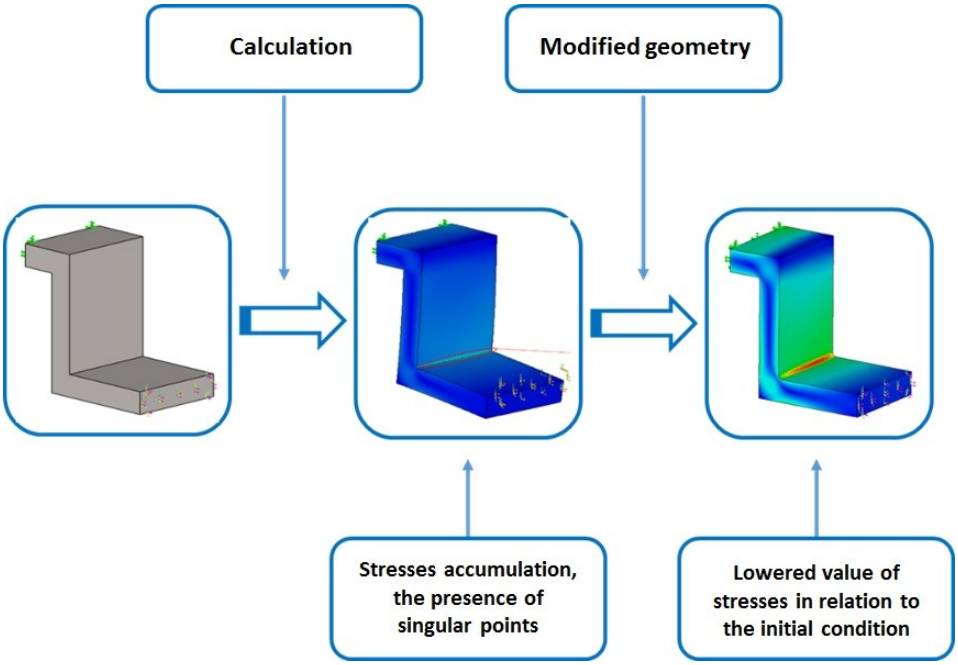

Fig. 9. The scenario adopted to analyse the case with the stress singular points

3. Conclusion

Theoretical considerations on the introduction of a temporary notch in place of a structural notch and elimination of stress active points allow formulation of the following conclusions:

- While modelling the part it is crucial to consider the fact whether it is feasible to manufacture a theoretically modelled part in the workshop conditions. The values of stresses generated due to the incorrect geometry shall also be considered.
- Numerical tools such as active point analysis used to investigate the conditions of stresses facilitate making proper decisions on modelling the right geometry of the part.
- Introducing a temporary notch to the examined bracket structure allowed the reduction of stresses from 131 to 47.8 MPa, i.e. by 63%, whereas increasing the radius would reduce the value of maximum stresses.
- Owing to the structural notch elimination, a safety factor of the bracket has increased from 1.79 to 4.91.
- In real structures, a high safety factor demonstrates the possibility to increase the load of the structure or to reduce its sections.

- On the basis of obtained results of numerical calculations, changes in the load of the structure or in sections must be correlated with the applicable safety factors for particular categories of structure.
- Knowledge of structure load conditions provides an answer in the form of distribution of stresses with values approximate to actual operation conditions.
- Revealing stress active points in the general analysis may provide the basis for conscious use of temporary notches in order to reduce the level of stresses.
- Analysing the presented case, it can be stated that the results received by means of numerical methods provide quite realistic results.
- Numerical analyses reduce the prototyping costs and limit the cost connected with time spent for structure design and preparation.

References

[1] H. Bąkowski, Z. Stanik, "Wykorzystanie analizy MES do wyjaśnienia wpływu czynników eksploatacyjnych na awaryjne zużycie tłoka w silniku o zapłonie samoczynnym", *Mechanik*, vol. 4, pp. 298–299, 2010.

[2] H. Dębski, G. Koszałka, M. Ferdynus, "Wykorzystanie mes w analizie struktury nośnej ramy naczepy o zmiennych parametrach eksploatacyjnych", *Eksploatacja i Niezawodność – Maintenance and Reliability*, vol. 14, no. 2, pp. 107–114, 2012.

[3] M. Ferdynus, M. Kotełko, J. Kral, "Energy absorption capability numerical analysis of thin-walled prismatic tubes with corner dents under axial impact", *Eksploatacja i Niezawodność*, vol. 20, no. 2, pp. 252–259, 2018.

[4] J. Goldak, A. Chakravarti, M. Bibby, "A new finite element model for welding heat sources", *Metallurgical Transactions B*, vol. 15 (299). 1984, https://doi.org/10.1007/BF02667333

[5] J. Jonak, J. Podgórski, Z. Szkudlarek, "Numerical simulation of rock separation processby catting prissing head", vol 4, pp. 54–57, 2004.

[6] K. Kukiełka, M. Trąbka, E. Reiter, "Analiza wytrzymałościowa i optymalizacja ściągacza trójramiennego z wykorzystaniem oprogramowania CAE", *Autobusy*, pp. 161–169, 2013.

[7] S. Kut, "Modelowanie fazy pękania ciągliwego w procesie wykrawania w ujęciu MES", *Acta Mechanica et Automatica*, vol. 2 (4), pp. 62–66, 2008.

[8] J. Kwaśniewski, H. Ruta, "The design of magnetic circuits taking into account measuring application", *Przegląd Elektrotechniczny*, no. 9a, pp. 60–64, 2011.

[9] J. Kwaśniewski, T. Krakowski, H. Ruta, Sz. Molski, M. Pypno, K. Ratuszny, "Qualitative assessment of the working condition of ropes in rope attachments", *Applied Mechanics and Materials*, vol. 683, pp. 45–49, 2014.

[10] P. Lonkwic, P. Różyło, H. Dębski, "Numerical and experimental analysis of the progressive gear body with the use of finite-element method", *Eksploatacja I Niezawodność – Maintenance and Reliability,* vol. 17 (4), pp. 544–550, 2015. http://dx.doi.org/10.17531/ein.2015.4.9.

[11] P. Lonkwic, P. Różyło, "Theoretical and experimental analysys of loading impact from the progressive safety gears on the free fall method", *Advances in Science and Technology Research Journal*, vol. 10(30), pp. 103–109, 2016, https://doi.org/10.12913/22998624/62628.
[12] T. Markowski, J. Mucha, W. Witkowski, "FEM analysis of clinching joint machine's C-frame rigidity", *Eksploatacja i Niezawodność – Maintenance and Reliability*, vol. 15 (1), 21–57, 2013.
[13] M. Matyjaszczyk-Nowak, "Wykorzystanie metody elementów skończonych w modelowaniu pola magnetycznego", *Techniczne Zakłady Naukowe im. gen. W. Sikorskiego w Częstochowie*, pp. 642–647, 2014.
[14] P. Różyło, "Optimization of I-section profile design by the finite element method", *Advances in Science and Technology Research Journal*, vol. 10 (29), pp. 52–56, 2016.
[15] P. Różyło, A. Teter, H. Debski, et al., "Experimental and Numerical Study of the Buckling of Composite Profiles with Open Cross Section under Axial Compression", *Appl Compos Mater 24*, 2017, https://doi.org/10.1007/s10443-017-9583-y.
[16] E. Rusiński, J. Czmochowski, T. Smolnicki, "Zaawansowana metoda elementów skończonych w konstrukcjach nośnych", *Oficyna Wydawnicza Politechniki Wrocławskiej*, Wrocław 2000.
[17] A. Supardjo, Agus, W. Tri, "Finite element analysis of truck frame by using CATIA V5", *AIP Conference Proceedings*, 030029, 2018.
[18] A. Szosland, M. Mariański, "Badania wytrzymałości typowych nadwozi autobusów przy bocznym przewróceniu się pojazdu", *Archiwum Motoryzacji*, 2013, DOI: 10.5604/1234754X.1066723 s. 115–126.
[19] M. Śladowski, "Zaawansowane metody obliczeń numerycznych naprężeń i odkształceń na przykładzie analizy korpusu silnika elektrycznego do kombajnu ścianowego KA200", *Zeszyty Problemowe – Maszyny Elektryczne*, vol. 82, pp. 87–91, 2009.
[20] The Internet source: https://solidmania.com/solidworks-simulation-wykrywanie-karbu-punktu-aktywnych-naprezen-punktu-osobliwego-naprezenia/
[21] T. Trzepieciński, S. Warchoł, "Optymalizacja kształtu wsadu w procesie kształtowania wytłoczek z wykorzystaniem MES", *XI Forum Inżynierskiego ProCAx*, Sosnowiec, pp. 1–7, 2012.
[22] P. Wysmulski, H. Dębski, P. Różyło, K. Falkowicz, "A study of stability and post-critical behaviour of thin-walled composite profiles under compression", *Eksploatacja i Niezawodność – Maintenance and Reliability*, vol. 18 (4), pp. 632–637, 2016, http://dx.doi.org/10.17531/ein.2016.4.19.

Karolina Czyż[1], Michał Derkacz[2], Jakub Smołka[3], Edyta Łukasik[4], Maria Skublewska-Paszkowska[5]

SPEECH RECOGNITION APIS IN THE CONTEXT OF USING ENGLISH AS A SECOND LANGUAGE

Keywords: speech recognition, non-native speaker, API, comparison

Abstract

Speech recognition systems are applied in many different solutions (e.g. web and mobile applications for language learning or voice assistants). They are frequently used by non-native speakers. Speech recognition accuracy or its tolerance to pronunciation imperfections may be an important aspect.

This article compares four APIs for speech recognition: Web Speech API, Microsoft Speech Service, Watson Speech to Text and Android SpeechRecognizer. The aim was to determine which API best recognises the speech of a person who uses English as his/her non-native language. The tests involved two groups of participants: (1) persons with modest language skills (level A1-A2), (2) people whose language level was at least B1. The participants read a set of sentences. Their speech was processed by each API included in the comparison. The results were assessed using (1) the percentage of incorrectly recognised words, (2) the word error rate, (3) the Levenshtein distance, (4) the number of incorrectly recognised words in a sentence. The best API for more advanced English speakers is the Watson Speech to Text service. The best API for non-fluent English speakers is Android SpeechRecognizer.

1. Introduction

Today, the knowledge of foreign languages is not only a welcome but also a desirable skill. It allows for communicating with people around the world. Sometimes the ability to communicate with people from other countries is an inevitable necessity (as in a job requirement). At the same time, people have less and less time to spend time on conventional language courses. They can get by with web or mobile language learning applications. Speech recognition systems are used in some apps to verify the user's pronunciation. Voice assistants

[1] Lublin University of Technology, Institute of Computer Science, Nadbystrzycka 36b Lublin, Poland, k.a.czyz@hotmail.com
[2] Lublin University of Technology, Institute of Computer Science, Nadbystrzycka 36b Lublin, Poland, derkaczes@gmail.com
[3] Lublin University of Technology, Institute of Computer Science, Nadbystrzycka 36b Lublin, Poland, jakub.smolka@pollub.pl
[4] Lublin University of Technology, Institute of Computer Science, Nadbystrzycka 36b Lublin, Poland, e.lukasik@pollub.pl
[5] Lublin University of Technology, Institute of Computer Science, Nadbystrzycka 36b Lublin, Poland, maria.paszkowska@pollub.pl

also use speech recognition. Due to the limited number of supported languages, many users have to control and communicate with such assistants using non-native languages. Automated translation systems also require accurate speech recognition. In all those cases speech recognition accuracy for non-native speakers with different levels of language skills is important.

2. Automatic speech recognition

Automatic speech recognition is applied in many areas. One of them is language learning applications. There are many such applications on the market, but pronunciation practice is not their strong point. Applications only offer audio recordings to be listened to by the user, or their speech recognition systems are uncomfortable. There are a few solutions that help the users verify their pronunciation but some may not be available to the particular user because they are too expensive (e.g. Busuu) or, they are applications for communication between users (e.g. HelloTalk), without the possibility of developing vocabulary or grammar in the traditional form of exercises and tasks [1].

Another application of speech recognition systems is automated translation. A personalised translation listening system is proposed in [2]. The systems classify users by age after inputting speech. It gives the translated result back to the user, speaking at an emphasised speech based on the user's age. The system performs age recognition, speech recognition, language recognition, Google machine translation, and returns the results with the help of TTS web services.

2.1. Phonology

Every language in the world has characteristic features that make it unique. These include prosody (intonation, emphasis and rhythm), pronunciation and vocabulary. Since most speech recognition research is conducted on people whose tested language is their native language, speech recognition services learn primarily a "pure" version of the language; free from distortions caused by the influence of a speaker's native-language on his/her pronunciation in the language in question.

Unfortunately, a person's speech characteristics in a foreign language depend strictly on his/her native language. The transfer of the melody of the native to a foreign language is a natural phenomenon. In addition, this phenomenon is even more pronounced if the person's foreign language skill is low. Research shows that the speech processing model for native speakers may be useless in the case of non-native speakers [3].

A completely different problem is the creation of a common phonetic alphabet for the speech recognition service in the case of the different speech characteristics of users. Two conflicting issues should be considered here: correctness and efficiency. To make speech recognition work correctly, each type of pronunciation should be implemented separately, but such a solution would require significant

resources. On the other hand, unifying the phones will make speech recognition system unable to process the required amount of input data still to function properly [4].

Apart from creating a separate phonetic alphabet for each type of pronunciation, there is one more solution. It consists in assuming that persons who speak a foreign language will use mainly the phonemes of their native language and transfer them to a foreign language. Thanks to this assumption, the amount of data can be halved. This is because the phonetic model of the user's native language is combined with the language model and the dictionary of the foreign language [5].

2.2. Decoder

The main element of a speech recognition system is a decoder [4]. The decoder analyses the provided sample and, based on the computed confidence level, selects the most likely sentence. The decoder does this analysis on the basis of data accumulated in the acoustic model, the pronunciation model and the language model.

The acoustic model is used to define the basic units of speech, which can be phonemes, syllables or complete (but simple) words. The pronunciation model is responsible for the definition of units of such as syllables, words, or expressions, consisting of units of the acoustic model. The language model is used to determine the structure and syntax of a language, using the vocabulary contained in the dictionary of the pronunciation model [4].

2.3. Automatic speech recognition systems

Automatic Speech Recognition (ASR) systems have a common structure both for users who speak a foreign language and for speakers who speak their native language. The only difference is that in the first case, ASRs may have an additional element that takes into account (manually or automatically) the accent of the person speaking. With this information, the system can select and apply appropriate speech processing models [6].

Speech recognition systems can be continuous or discrete. Continuous systems apply to users who speak full sentences or use phrases arranged in a sequence that the ASR is able to interpret. Discrete systems have a separate acoustic model for each word [7].

An ASR can also be classified as a user-dependent or user-independent system. User-dependent systems rely on data provided by the user and are able to interpret sounds only after the user has previously set up the system. An independent system does not require any initial input from the user to function properly [7].

Developments in neural-network-based acoustic and language modelling allow for advancing accuracy of speech recognition systems. Using (1) a CNN-BLSTM acoustic model with a set of models of other architectures, (2) character-

based and dialog session aware LSTM language models in rescoring, (3) a two-stage approach for system combination, (4) a confusion network rescoring step after system combination allowed for achieving a 5.1% word error rate on the 2000 Switchboard evaluation dataset [8].

Studies suggest [9] two different technologies can be used for conversational systems, one for Web systems and other for systems running on mobile devices. They authors focused on the HTML5 Web Speech API (Web SAPI), and the Android Speech APIs.

Another study [10] recognises that speech recognition is an important part of a speech interface that includes spoken dialogue function. They compare the speech recognition performance of two systems: Kaldi and Google Cloud Speech API. WER and RTF indicators are used for the evaluation of the speech recognition performance of each system.

Yet another work [11] approaches the subject of speech recognition from robot voice control point of view. The authors divide the speech recognition system into two categories: open-source and closed source. For their comparison, the following systems were selected: Dragon Mobile SDK, Google Speech Recognition API, Siri, Yandex SpeechKit, Microsoft Speech API, CMU Sphinx, Kaldi, Julius, HTK, iAtros, RWTH ASR and Simon. The comparison is mainly focused on accuracy, API, performance, speed in real-time, response time and compatibility.

In addition to the development of new speech recognition applications and designing experiments focused on selecting the best systems, there is also work aiming to automate speech recognition system testing. In the study by Këpuska et al. [12] the authors propose a tool that can be used to test and compare commercial speech recognition systems, such as Microsoft Speech API and Google Speech API, with open-source speech recognition systems such as Sphinx-4. They used WER as an indicator of speech recognition performance.

3. Speech Recognition APIs

The four APIs used in the presented research are briefly described in the following subsections.

3.1. Web Speech API

Web Speech API is a solution for web applications, used to recognise and synthesise speech. This interface communicates asynchronously with the speech recognition service by sending data between the user and the service [13]. It is currently available on the Google Chrome browser and should soon be available on Mozilla Firefox (at the moment of this writing it is considered experimental).

For the purposes of the research described in this article, the Web Speech API has been set up as follows: (1) the speech language was set to English, (2) continuous processing was enabled (so that the service records sound even if the user stops speaking) and (3) return of intermediate results was allowed.

3.2. Watson Speech to Text API

Originally, Watson was a supercomputer created by IBM to win the American game "Jeopardy!". Currently, Watson is a leader in the commercial use of artificial intelligence in advertising, education and finance.

Watson has a speech processing service called Watson Speech to Text API. The results of speech processing are returned in the JSON format. Watson has three interfaces for communicating with the speech recognition service. The research uses an asynchronous HTTP interface that does not block queries to the service [14].

Like Web Speech API, Watson API has been configured to record continuous speech and to display intermediate results. In addition, this API adds a confidence indicator to the final result.

3.3. Microsoft Speech Service

Speech Service is a Microsoft service that includes all available speech processing products such as Bing Speech API, Speech Translator, Custom Speech and Custom Voice.

Speech Service can work in three modes: conversation, dictation and interaction. This study used the dictation mode because it does not require any interaction between the software and the user [15]. In addition, this API has been configured to process continuous speech and to display intermediate results.

3.4. Android Speech Recognizer

SpeechRecognizer is a class built into the Android system used by applications for speech processing. It is the foundation for voice control of numerous mobile applications.

Like other APIs, SpeechRecognizer sends resources to a remote server for speech processing. However, due to the fact that it was created for a mobile system, it is not suitable for speech recognition in dictation mode, because such an operation would significantly burden the battery and bandwidth [16].

In the conducted research, English was set as the recognition language and no intermediate results or confidence indicators were displayed.

4. Testing the quality of speech recognition

Speech recognition through a programming interface can be difficult for two reasons. The first problem is the difference between the pronunciation of syllables in native and foreign languages. Bilingual persons tend to transfer the characteristic sound of one language to another, rendering it difficult to understand by software.

The second problem is the confusion of words and their meaning [17]. The systems that are most susceptible to this type of error are systems that

(in addition to processing natural language) try to understand it. Their goal is to find the context in the sentence and react to the user's request, which may be impossible in the event of erroneous recognition of the command given by the user [18].

To determine the differences in the effectiveness of the compared APIs, the Levenshtein distance and the word error rate were used. Both these values describe how much the input text (recognised from speech) differs from the original text.

4.1. Word Error Rate

The Word Error Rate (WER) indicates how many words in a sentence have been changed. These changes may concern such modifications as: insertions, deletions, substitutions or transformations (incorrect recognition) of words.

The word error rate is given by [19, 20]:

$$WER = \frac{S+D+I}{S+D+C} \tag{1}$$

where: S – number of substitutions, D – number of words removed, I – number of words inserted and C – number of correctly recognised words.

4.2. The Levenshtein distance

The Levenshtein distance determines how much the output word differs from the input word. Like the word error rate, it focuses on insertions, deletions and substitutions, but instead of analysing the entire sentence, the Levenshtein distance analyses individual words [21].

To calculate the Levenshtein distance, one should count the number of transformations in the input word required to obtain the output word. The transformations taken into account are: substitutions, deletions and insertions. For example, the words Saturday and Sunday have Levenshtein distance of 3, because first, the letters ‘a’ and ‘t’ have to be deleted and then ‘r’ has to be substituted for ‘n’.

Levenshtein's distance is a very quick way for measuring the difference between short character sequences. In the presented research it was used for original and recognised sentences.

5. Research

The research concerning the selection of the best speech recognition API was carried out on a group of 10 people, each of whom had the task of reading 3 sentences for each of the compared APIs. The group of participants consisted of 5 people who spoke English and 5 people who did not. None of them had lived

abroad previously nor was living abroad at the time of research. The native language of the participants was Polish.

In order to make the recognition task even more difficult, the test sentences constructed in such a way that problematic phenomena appear in them. The phenomena are [22]:

- homophones – words with the same pronunciation but different spelling and meaning,
- alliteration – repeating sounds,
- words easy to distort, due to the difficult-to-pronounce conglomeration of letters or those with a completely different spelling than the pronunciation.

Sentences and phrases used for testing were: (1) red roses with thorny stems, (2) two tiny toads ate fat flying flies, (3) plenty plain plates in the pantry, (4) what you write isn't right, (5) he sells mangoes from his cell, (6) the motel maid made the bed, (7) the blue paper blew away, (8) painting pretty picture, (9) I dared the deer to hurt my dear duck, (10) sinful singer's speaking sonnets, (11) I hear the humming here, (12) you're not allowed to talk out loud in the library, (13) the bride walked down the aisle on a sunny isle, (14) I've always wanted to be a bee, (15) pretty puppets for two puppies.

6. Test results

The results, composed of the results of both speaker groups, indicate that the best speech processing API is Watson Speech to Text with 84% of the correctly recognised words. The second one is the Web Speech API, with a result of 79%. The third is Android SpeechRecognizer and Microsoft Speech Service, both with a result of 76% (table 1).

Tab. 1. Percentage of correctly recognised words by the speech recognition services

API	Web Speech API	Microsoft Speech Service	Watson Text to Speech	Android Speech Recognizer
%	79.66	82.70	85.74	77.69

Source: own work

More detailed results show that the percentage of words recognised correctly by Watson Speech to Text in the group of users familiar with English is above average (92%). However, in speech recognition in users without good English skills, Watson Speech to Text achieved significantly lower results (only 75%). In this group of users, Android SpeechRecognizer achieved the best results of 76% (figure 1).

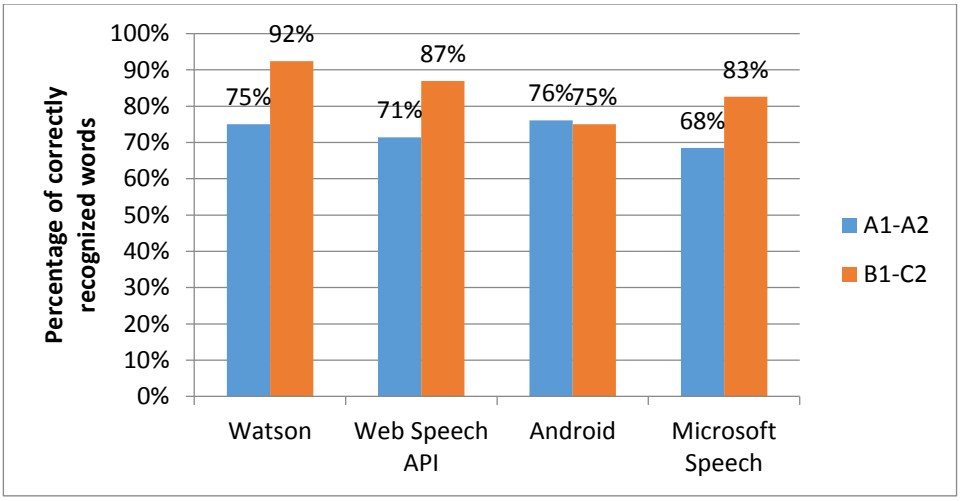

Fig. 1. Percentage of correctly recognised words by the speech recognition services by user group

On the basis of the word error rate, it can be seen that the lowest number of errors (WER equal to 0.12) were made by Watson Speech to Text for a group of users who know English well. The values of this indicator, in the same user group, for Web Speech API, Android SpeechRecognizer and Microsoft Speech were correspondingly: 0.18, 0.28 and 0.19 (figure 2).

Android SpeechRecognizer is the only service that can understand users who are not fluent in English as well as the users who know English well. Perhaps this is due to the popularity of the Android OS. Google is likely to create language models based on sample recordings from different countries with different voice characteristics. In the United States alone, Android has to recognise not only accents from different states but also accents of many minorities.

While the results of Android SpeechRecognizer differed only slightly when it came to the sum of misinterpreted words, in the case of the word error rate the difference is much significant. Surprisingly, the speech of users who claim better English skills was harder for the service to interpret. For this group the WER value reached, as mentioned, the value of 0.28 as opposed to 0.21 for non-fluent users (figure 2).

The word error rate is closely related to the Levenshtein distance. It can be observed that the distance value is the lowest for Watson Speech to Text when listening to users who speak English. Its average value is approximately 0.5.For users who do not speak the language, the best (lowest) Levenshtein distance, was achieved by Android SpeechRecognizer (approximately equal to 3 - figure 3).

The worst, in the case of users who do not speak English well, is Web Speech API and Microsoft Speech Service. For these services, the average value of the Levenshtein distance is more than 6 characters (figure 3).

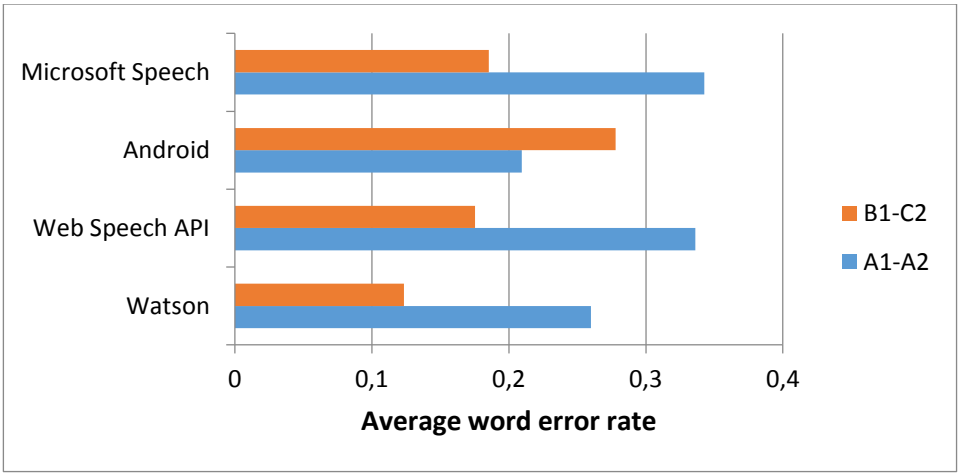

Fig. 2. Word error rate for individual services by user group

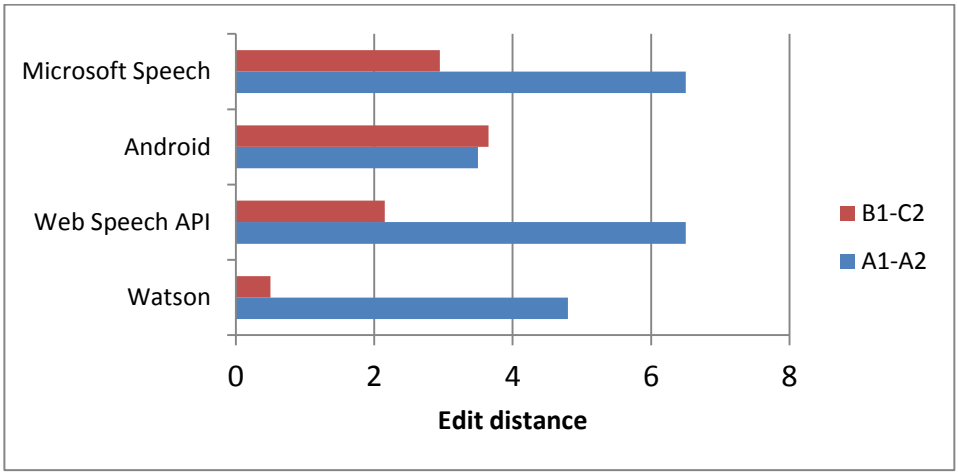

Fig. 3. Edit distance for individual APIs by user group

Additionally, the effectiveness in the interpretation of entire sentences was assessed. The most sentences – 5 – were recognised flawlessly by Watson Speech to Text. The lowest number of sentences – only 2 – were recognised correctly the Web Speech API. Both Microsoft Speech Service and Android SpeechRecognizer achieved the result of 3 correctly recognised sentences (table 2). Interestingly, speech recognition services usually recognised incorrectly 6 or more words in a sentence (table 2).

Tab. 2. Number of sentences in which 0, 2, 4 and more than 6 words were incorrectly recognised, grouped by speech recognition services

Number of sentences	Web Speech API	Microsoft Speech Service	Watson Text to Speech	Android Speech Recognizer
0	2	3	5	3
2	1	0	0	1
4	3	2	3	2
>=6	9	10	7	8

Source: own work.

The sentences that were flawlessly recognised are sentences that are quite short and do not contain difficult sounds. In addition, they are phrases containing homonyms that are clearly separated by other words and, having examined the context of the entire sentence, the speech recognition service can determine which one of the possible results should be selected.

7. Conclusions

Although at first it may seem that the best speech recognition API is Watson Speech to Text API, after analysing the results, it may be concluded that Watson, although it has its advantages, does not meet the needs of one of the two user groups.

In the case of users who have not had contact with a foreign language or their level of language skills is low, one should use the API, which it is directed towards the average user and, most importantly, is able to understand them. Android SpeechRecognizer meets this condition.

Probably, Watson's AI models were trained using high-quality native speaker speech samples. This is the likely reason why it is not able to understand the user whose pronunciation is different from those from the training dataset – they speak with an accent.

However, one cannot deny that Watson Speech to Text coped very well with speech recognition in users who are more advanced in English. Its effectiveness may be the result of using artificial intelligence, which based on the context, was able to determine more confidently which words should be selected from the possible recognition results.

Keeping in mind the current interest in speech recognition, which is developing intensively, one can expect that speech recognition will soon be more widely adopted in language learning applications.

The integration of speech recognition service with natural language interpretation software could lead to the development of an application offering a real language course. Such software could conduct a conversation with the user. Ask him/her questions and then check the correctness of the answers.

References

[1] S. Writtenhouse, "The 8 Best Language Learning Apps That Really Work", *MakeUseOf* [Online], 2019, Available: https://www.makeuseof.com/tag/five-free-apps-help-learn-foreign-language/.

[2] J. Do-won, K. Dong-Ju, "Personalized Translation Listening System for Age Groups", *Procedia Computer Science*, vol. 4, 2011.

[3] I. Bada, J. Karsten, D. Fohr, I. Illina, "Data Selection in the Framework of Automatic Speech Recognition", *ICNLSSP 2017 – Int. Conf. Natural Language, Signal and Speech Processing 2017*, pp. 1-5, Casablanca, 2017.

[4] S. Kunzmann, V. Fischer, "Multilingual acoustic models for speech recognition and synthesis", *2004 IEEE Int. Conf. Acoustics, Speech, and Signal Processing*, Montreal, Canada, 2004.

[5] D. van Leeuwen, R. Orr, "Speech Recognition of Non-native Speech Using Native and Non-native Acoustic Models", *Proc. the ESCA workshop Multi-lingual Interoperability in Speech Technology (MIST)*, 1999.

[6] A. Neri, "Automatic speech recognition for second language learning: how and why it actually works", *Proc. ICPhS*, Barcelona, pp. 1157-1160, 2003.

[7] S. J. Arora, R. Singh, "Automatic Speech Recognition: A Review", *Int. J. Computer Applications*, vol. 60 (9), pp. 34–44, 2012.

[8] W. Xiong, "The Microsoft 2017 Conversational Recognition System", *Microsoft AI and Research*, 2017.

[9] M. McTear, Z. Callejas, D. Griol, "Implementing Speech Input and Output", *The Conversational Interface*, Springer, Cham, 2016.

[10] T. Kimura, T. Nose, S. Hirooka, Y. Chiba, A. Ito, „Comparison of Speech Recognition Performance Between Kaldi and Google Cloud Speech API", *Recent Adv. Intelligent Information Hiding and Multimedia Signal Processing. IIH-MSP 2018. Smart Innovation, Systems and Technologies*, vol. 110. Springer, Cham, 2019

[11] R. Matarneh, S. Maksymova, V. Lyashenko, N. Belova, „Speech Recognition Systems: A Comparative Review", *IOSR J. Computer Engineering*, vol. 19, pp. 71–79, 2017

[12] V. Këpuska, G. Bohouta, „Comparing Speech Recognition Systems (MicrosoftAPI, GoogleAPI and CMU Sphinx", *Int. J. Engineering Research and Application,* vol. 7, no. 3, pp. 20–24, 2017

[13] MDN Web Docs, "Web Speech Concepts and Usage", 2019, [online] available: https://developer.mozilla.org/en-US/docs/Web/API/Web_Speech_API

[14] IBM Cloud Docs, "Getting started tutorial", 2019, [online] available: https://console.bluemix.net/docs/services/speech-to-text/getting-started.html#gettingStarted

[15] Microsoft Azure, "What are the Speech Services?", 2019, [online] available: https://docs.microsoft.com/en-us/azure/cognitive-services/speech-service/overview

[16] Android Developers, "SpeechRecognizer", 2019, [online] available: https://developer.android.com/reference/android/speech/SpeechRecognizer.

[17] T. T. Ping, "Automatic Speech Recognition for Non-Native Speakers", Université Joseph-Fourier - Grenoble I, 2008.

[18] T. J. Hazen, S. Seneff, J. Polifroni, "Recognition confidence scoring and its use in speech understanding systems", *Computer Speech and Language*, vol. 16, 2002.

[19] A. Ali, S. Renals, “Word Error Rate Estimation for Speech Recognition: e-WER”, *Proc. 56th Annual Meeting Association for Computational Linguistics*, Melbourne, Australia, vol. 2, pp. 20–24, 2018.
[20] R. Makowski, “Automatyczne rozpoznawanie mowy: wybrane zagadnienia”, *Oficyna Wydawnicza Politechniki Wrocławskiej*, 2011.
[21] A. Ogawa, A. Nakamura, “Joint estimation of confidence and error causes in speech recognition”, *Speech Communication*, vol. 54, no. 9, 2012.
[22] G. Di Fabbrizio, T. Okken, “Speech Mashups”, *Semantic Mashups*, Springer, Berlin, Heidelberg, 2013.

Jolanta Słoniec[1], Anna Kaczorowska[2]

SUPPORTING THE DECISION-MAKING PROCESS ON THE INTRODUCTION OF IT OUTSOURCING IN THE ORGANISATION

Keywors: IT outsourcing, decision making, artificial intelligence, case study

Abstract

IT outsourcing (ITO) is permanently present in organisations operating in the conditions of the global economy. The number of organisations using ITO is growing rapidly and new companies and organisations are still facing a dilemma whether to outsource functions related to the functioning of IT systems or to continue to perform these functions within the enterprise. Deciding on the use of IT outsourcing is not easy. The aim of the article is to present the course of the decision-making on the introduction of IT outsourcing to the organisation. The research problems were formulated as follows: What is the course of the process of deciding on the introduction of ITO to the organisation? Is it possible to support the process of deciding on the application of ITO in the organisation through the use of artificial intelligence (AI)? What benefits will the use of AI bring to the decision-making process? The article shows that the use of AI is possible and that it can bring tangible benefits. At the same time, a case study of enterprises was presented, in which IT outsourcing was successfully implemented and used. The use of artificial intelligence will help support the decision-making process regarding the introduction of IT outsourcing and making more accurate predictions. However, a growing need in assessing forecasts is predicted and the process cannot be performed by IT solutions but by human employees.

1. Introduction

25 years ago, the era of the so-called "new economy" began, that is, the economy based on an increasing share of knowledge and information. The growing importance of the two caused the development of information and communication technologies, contributing simultaneously to the ongoing globalisation. Digitisation has revolutionised the economy both on the macro and micro scale. The progress of information technologies has caused rapid development in the use of computers in the activities of organisations and enterprises. It also triggered the intensive development of IT outsourcing, that is outsourcing activities related to the functioning of internal IT systems. IT outsourcing, in today's sense, has been in operation for around 25 years. During this period, there has been an increase in the number of organisations using ITO.

[1] Lublin University of Technology, Department of Enterprise Organization, Faculty of Management, 20-618 Lublin, Nadbystrzycka Str. 38, Poland, j.sloniec@pollub.pl
[2] University of Lodz, Department of Computer Science, Faculty of Management, 90-237 Lodz, Matejki Str. 22/26, Poland, anna.kaczorowska@uni.lodz.pl

There has also been a rapid development of IT outsourcing itself through the emergence of new trends in three areas: technological, organisational and social [1]. In the technological area, novelties in ITO development concerned the use of cloud computing and the development of the technology itself (robotisation and automation, the use of artificial intelligence, the use of advanced spreadsheets). In the organisational area, new developments in ITO development included the use of crowdsourcing and reverse outsourcing. And in the social domain new developments in ITO concerned the emergence of new professions (related to security engineering, architecture and big data analysis), forms of employment (body leasing, team leasing, remote work) and intensive expansion of ITO suppliers in Asia and Central and Eastern Europe. The increase in the number of organisations using ITO and the ITO development trends have attracted the interest of other businesses considering the implementation of the changes in question. Enterprises are increasingly often faced with the decision-making dilemma whether to start using ITO or not, the process that this article sets out to present.

2. IT outsourcing in Poland

Outsourcing is not a new phenomenon, neither in the world nor in Poland. It emerged in the twentieth century, but its elements can be traced back to educational institutions (colleges, universities, institutes) run by Christian orders commissioned by rulers and in the logistics and archiving of Alexander Hays's company from the 17th century. Under the current name and meaning, the concept came into practice of management sciences in the 1980s, and to the theory of management in the1990s [2]. All companies use outsourcing as they have suppliers and cooperators. The phenomenon of outsourcing spread during the development of craft production in the 18th century, which was when a system of cooperative relations was created, NB currently referred to as outsourcing connections. The industrial revolution of the late 19th and early 20th century contributed to the development of large industrial enterprises and, at the same time, meant that the importance of craft manufactories significantly decreased.

The scale of the outsourcing phenomenon has been reduced. Only the emergence of new ones and the development of existing management concepts in the 1960s and 1970s made the concept of outsourcing revive as well. The precursor of the new wave of outsourcing development as a phenomenon, in particular, IT outsourcing is R. Perot, whose company offered a paid implementation of IT functions to Frito-Lay enterprise. It was the management of IT equipment. In the 1980s, the process of external procurement of parts for cars was called outsourcing by General Motors.

At the same time, it should be noted that from the 1960s and 1970s, the work of shared employees has been in use across industries: the employee would perform the same tasks in a number of companies. However, what distinguishes

employee outsourcing is the nature of the latter. While small companies have benefited from and still are benefiting from shared work, outsourcing is used by all enterprises, and IT outsourcing is also used by companies with large and well-developed IT departments [3]. Initially, IT outsourcing was employed primarily in the areas of non-critical information, peripheral for the company – its loss did not cause a decline in competitiveness. Then, IT outsourcing began to take over the domains with access to key information essential for the competitiveness of the company or organisation [4]. Information on banking operations is considered to be key, sensitive and has previously been stored and processed inside the company; since the 1990s, it has been no longer. Financial, insurance, health, communication and retail information are among the most frequently processed as part of IT outsourcing [5]. This phenomenon can be explained by the change of direction and the attitude to the use and management of information, as well as the use of information technologies. Taking this view into account, outsourcing can be considered as an evolving data processing utility, much as e.g. the phone service or a power supply service. The infrastructure we use is of secondary relevance; what is in our interest is the possibility of conducting a conversation or switching on an electrical device. In addition, anyone using data or information, expects to be able to download it. Therefore, companies no longer waste power and resources to build the infrastructure and can use them with higher efficiency [3]. Due to its universal availability and ease, as well as the cost of its acquisition, information loses its strategic importance[6].

Already in the 1990s, it was predicted that widespread availability of information would cease to be a lasting competitive advantage [7].

The phenomenon of globalisation also affects the development of outsourcing through:

- The trend among enterprises to localise their production processes where production factors are cheaper. This is the phenomenon of so-called global outsourcing, i.e. when software is created and developed in countries with highly qualified IT employees and where the remuneration for work is relatively low (India – a leader on the global outsourcing market – being the best example) [8].
- Increased acceptance of the Internet as a communication medium, which affects the phenomenon of application outsourcing – tendencies to create and use applications via the Internet, instead of installing them in the local environment [9].

The increase in the scope and size of IT outsourcing services was mentioned by many authors of research already in the 1990s [4, 10-12]. They stated that this increase would also take place in the subsequent years, which they believed had been confirmed by the results of the IT market analysis.

3. Deciding, decision-making process - stages and characteristics

The theory of decision making considers it in relation to the motivation and subjective assessment of the likelihood of events assessed positively or negatively [13, 14]. According to the theory, the decision is an internal act that is a free choice of one of the possible future behaviours. The decision is the result of deciding, which is the transformation of intentions into goals [13]. By decision, we call the choice of one action from a certain number of activities that we think are possible at the moment, or a conscious abstention from choosing – which is also a choice! [15]. The central problem of the decision-making theory is: What principle to follow in choosing the action knowing what can be done and what the effects may be, but what effects will be unknown, because the real state of nature is unknown? [16].

Deciding is making a non-random choice in action. The set of elements from which we choose in the decision-making process is doubly limited: firstly, the resources of our knowledge and, secondly, our conviction about the attainability or feasibility of a given variant of action [16].

Making decisions can be considered in a broad and narrow sense [17].

In a broad sense, this is a process that consists of:

- Registration and evaluation of information,
- Identification of the decision problem and application of the adopted selection criterion,
- Determining and issuing decisions,
- Registration of information about its implementation.

In a narrow sense, decision-making is a stage in the decision-making process and means a conscious act of the will of the decision-maker making non-random selection of one from a set of possible variants of solutions to the decision-making process.

The above definitions present the determinations of decision-making and decisions. The decision is made as a result of the decision-making process.

According to Finkenlstein, the effective decision-making process is divided into the following stages [18]

- Identify the decision,
- Gather information,
- Identify alternatives,
- Weigh the evidence,
- Choose among alternatives,
- Take action,
- Review your decision.

Both divisions of the decision-making process into stages may be applicable in the situation of making decisions about the use of IT outsourcing in the organisation. The next section will present the characteristics of the decision-making process on the implementation of the IT outsourcing of the organisation.

4. Characteristics of making decisions about introducing IT outsourcing in the organisation

While characterising the decision to introduce IT outsourcing in the organisation, reference was made to the established division of the process into stages.

- Registration and evaluation of information.

At the beginning of the stage, the data collection process (data acquisition) is carried out. Subsequently, the data is processed into information. When deciding on the introduction of IT outsourcing in an organisation, the information applies to:

- The internal state of the organisation and its IT department.
- The state of the organisation and its IT department is considered in three aspects: (1) organisational – processes taking place in the organisation and its IT department, the functions and activities performed, current and future organisation needs related to the functioning of IT systems, (2) personnel – employment, qualifications and skills of employees, (3) financial – costs related to the functioning of the internal IT department.
- Supply and offer of companies providing outsourcing services.
- Trends in IT development and IT outsourcing.

- Legal, economic and organisational conditions related to the use of IT outsourcing.

Collecting information entails costs and requires time. It should be noted that digital technology developed on the basis of the "new economy" resulted in the reduction of communication costs and seeking information, also in the area of searching for information on IT outsourcing.

The collected information is subject to assessment/judgment. The assessment is issued prior to the action (ex ante) and it is more or less probable due to the theoretical basis on which it was issued [16].

In carrying out the assessment, it is also possible to predict the development of accidents as a result of the intended actions. Predictions base on research, experiments or observations that affect the development of the phenomenon. When introducing IT outsourcing in the organisation, the anticipation consists in constructing possible scenarios for the developments in the internal and external situation of the organisation. Both positive and negative scenarios should be considered, as well as that the developments can be neutral. Therefore, a forecast of the future situation is made. Assessments and forecasts are usually supplied by managers and/or specialists (IT specialists) and are rather seldom outsourced (experts). The development of digital technologies has meant that as artificial intelligence improves, the values of human prognostic skills will decrease with machine predictions becoming a cheaper and better substitute for human predictions [19]. However, the importance of human skills related to the assessment of the situation will increase. Judgment complements prediction and,

therefore, when the cost of forecasts decreases, the demand for judgment will increase. For this reason, human judgment will be needed in a larger extent [19].

The boundary between assessment and prediction is not clearly defined – certain tasks requiring judgment will be transformed into a series of forecasts. Nevertheless, it is expected that the value of human prediction skills will drop, and the value of skills related to judgment will increase [19].

The development of artificial intelligence will have some impact on the automation of making predictions about the consequences of introducing IT outsourcing in the organisation. However, a man seems irreplaceable in making the final judgment of the forecasts. Along with the increase in the value of skills related to the judgment of forecasts, the demand for people who will be able to make such judgments, e.g. independent experts, will increase as well.

Currently, such judgments are made by managers of organisations intending to outsource IT. It can be expected that in the near future, employees of companies providing IT outsourcing services (experts) will specialise in conducting such assessments or will outsource this to independent experts.

- Identification of the decision problem and application of the adopted selection criterion

Intending to introduce IT outsourcing in the organisation, the decision-making problem will consist in making a decision regarding its introduction (at the same time determining the scope of IT outsourcing) or a decision to discontinue IT outsourcing. Different selection criteria can be used: economic, organisational, strategic.

- Determining and issuing a decision

Considering the accepted selection criterion, a decision is made to introduce IT outsourcing or its discontinuation.

- Registration of information on the implementation of the decision

If the decision is made to introduce IT outsourcing in the organisation, it is implemented, usually in the form of a project.

The above considerations show that it is possible, purposeful and necessary to apply artificial intelligence in the process of deciding about the introduction of ITO in the organisation. AI can be used to automate making forecasts regarding the development of the situation in the case of introducing ITO in the organisation. The use of artificial intelligence in this decision situation will result in the following consequences:

- Economic effects: a decrease in the costs of making decisions about the introduction of ITOs by partially automating them
- Organisational effects: comprehensive consideration of the decision-making situation will influence better forecasts; reducing the work demand of specialists with appropriate knowledge to make accurate forecasts.

The decision to introduce IT outsourcing may be a tactical or strategic decision. In the initial stages of ITO development, it was primarily a tactical decision,

nowadays it is much more often a strategic decision of an organisation. Decisions of strategic importance in enterprises operating in the dynamic and complex conditions of digital transformation are undertaken in accordance with the guidelines of the Industry 4.0 concept [20], i.e. using modern systems equipped with AI modules.

5. Case study

5.1. Santander Bank UK

In 2008, Santander Bank UK [21] decided to outsource the service of its clients' debit and credit cards to the contractor, Konecta. The company applied a consultative approach to fully understand the bank's goals, its culture and adequately familiarise people with processes, according to the bank's processes and policies. In order to make a smooth transition from internal handling of cards to the use of outsourcing, the following operations were carried out:

- Process analysis and mapping,
- Identification of key operational performance components,
- Analysis of operations, collecting customer feedback,
- Resource forecasting and analysis,
- Meeting at the bank's head office to identify the real needs of the bank and its clients.

The introduction of outsourcing of Santander UK bank card customers has improved the provision of the following services:

- Customer service
- Conflict handling, fraud identification
- Online customer service using secure messages
- Loans and relevant services.

The decision to outsource debit and credit card customer services required that Santander Bank UK implement predictions of possible situations and their assessment. The forecasts and assessments were performed by bank managers. The intention to conduct outsourcing of debit and credit card customer was positively assessed, therefore, the decision was made and implemented for the benefit of the bank and its clients.

5.2. Dell's call centre outsourcing

Dell manufactures and sells personal computers and the operation of its call centre [22] is not a primary activity. Outsourcing of this activity allowed the company to focus on its core business – the production and sales of personal computers to be more competitive on the market. The discussed case concerns the unsuccessful introduction of outsourcing in a call centre in Bangalore, India.

Through direct sales of computers to end-users in the years 1985-2009, Dell's revenues increased tenfold. With the aim to providing better service to a large number of customers and reduce costs, Dell decided to outsource the call centre. The first call centre was established in 2001 in Bangalore, India for customer service from the USA. The second Call Centre was established in 2003 in Hyderabad and the third one was set up in Chandigarh. India has been chosen because of its cheap and qualified workforce. However, Dell encountered some problems in India related to the selection of appropriate employees for its call centre. First, the company had to find appropriate candidates to work in India and teach them Dell culture. The employee should also understand the culture of the country for which they work (call centre served clients from the USA) and which is on the opposite side of the globe. Secondly, there were technological problems, more than half a year the appropriate equipment for the centres was sought and selected. Thirdly, developing solutions that allow qualified employees to work for the company (system of work and remuneration).

Although Dell's market share grew, customer satisfaction fell. Complaints concerned the poor quality of services, communication difficulties (differences in the accent, use of automatic responses), delays in dealing with hardware problems. This is why Dell stopped using the call centre in Bangalore.

The reasons for stopping the use of the call centre in Bangalore can be grouped as follows:

1. Planning and management. Planning is the most difficult phase of outsourcing. The call centre in India was a big project. Dell was developing quickly, and the call centre did not have enough resources to handle a large number of connections. That is why the quality of services performed decreased and did not meet the customers' expectations.
2. Technical skills. The development of technologies has resulted in an increase in the number of Dell products and their technological advancement. However, employees have not been trained in new technologies. This affected customer dissatisfaction with the call centre service.
3. Employees. Call centre needed many qualified employees. The company, however, had difficulty finding the right number of specialists. Dell's payroll policy has also resulted in the departure of a significant number of employees and managers.
4. Cultural differences. Good knowledge of English in India does not mean that the call centre employee will give the US client a clear and unambiguous answer (this is related to American culture). The Hindu tend to prolong the conversation, which affects the ambiguity of the answer.

As a result of the inconsistencies noted, Dell's activities led to their liquidation. Dell continues to use call centre outsourcing as well as outsources other tasks and functions. According to Dell managers, the success of using IT outsourcing is ensured by compliance with the following rules:

- Developing and defining a long-term plan including all processes. This will help increase the efficiency of management, also in the case of company growth.
- Care for technical skills of employees and their progress along with the development of technology.
- Ensuring proper working conditions and remuneration so that they are not easily bought out by another competitive company.
- Culture. Language skills and communication methods should be adequate to the preferences of the target clients.

A negative example of the use of Dell's call centre outsourcing in Bangalore shows that not all possible scenarios were constructed, the forecasts were too optimistic, and their assessment was not done properly. That is why the Dell call centre in Bangalore has been replaced by a call centre located in a different location.

5.3. Insurance company

The insurance company [23] is the third biggest Polish company on the property insurance market, according to share capital. The company's branches are geographically dispersed, which made it difficult to access paper-based documentation. That is why the company decided to centralise the archive and give this function to ArchiDoc. The service provider provided the infrastructure, know-how and human resources necessary to store and share documentation in large quantities. They provided services in the field of receiving, managing and sharing archival documentation. In the first phase, the supplier took over archive resources stored in four locations of the insurance company: in Szczecin, Katowice, Poznań, and Olsztyn. Organising and gathering archival documentation in one place have improved the access to it for employees of the insurer's branches located in different cities. The use of the IT system allowed for quick location of the wanted documents. The service provider applies restrictive security procedures that ensure the highest data protection in accordance with statutory standards.

The success of outsourcing the management of archival records in the insurance company resulted from properly carried out prediction and assessment of forecasts.

6. Conclusions

Introduction of IT outsourcing in the organisation is not an easy process. The aim of the article was to present the course of this process and the possibility of supporting it through the use of artificial intelligence. It was shown that the use of artificial intelligence in these cases is possible, reasonable and beneficial. Artificial intelligence can improve the process of deciding on the introduction of

ITO in the organisation by automating the forecasting of possible situations after the introduction of ITO (development of possible scenarios). The application of artificial intelligence in the situation of making decisions about the introduction of ITO can have consequences of economic (lower costs of making decisions on the introduction of ITO through partial automation) and organisational nature (comprehensive consideration of decision-making situation will bring better forecasts, reduce the need for experts with appropriate knowledge to making accurate forecasts).

Three case studies of enterprises using IT outsourcing in their activities were also presented. These were: Santander Bank UK, in which outsourcing was handed over to the debit and credit card services of the bank's clients, Dell, in which outsourcing concerned a call centre and an insurance company in which the outsourcing covered the management of archive documentation. These companies still use IT outsourcing, although in one of them the use of outsourcing was unsuccessful. The company drew conclusions from the failure and moved the call centre to a different location.

The introduction of IT outsourcing in organisations was initially a tactical decision. In modern enterprises, however, it is more often a strategic decision. Strategic decisions are made using modern systems equipped with AI modules.

The effect of using artificial intelligence in the economy is a decrease in the cost of goods and services that depend on forecasts. As the cost of forecasts decreases, they not only reduce the costs that have always been dependent on prediction – such as inventory management or demand forecasting – but the forecasts will be used to face other problems that in the past were irrelevant for the predictions. The demand for the ethical evaluation of forecasts will increase, which is definitely the domain of people.

Interpreting the development of artificial intelligence in the category of falling prediction costs does not answer every specific question about how this technology will affect the economy. However, there are two important consequences:

1. It will increase the importance of forecasts for the creation of numerous goods and services
2. It will change the value of other input elements, depending on how far they supplement or replace the forecasts.

These changes are approaching. How quickly managers should invest in assessment/judgment capabilities will depend on the rate at which these processes take place. However, it is worth starting activities now. [19]

Already today, AI assistants will transform the relationships between companies and clients. The more AI platforms meet customer expectations, the sooner trust in them will replace brand trust. Marketing will soon become a battlefield for the attention of AI assistants. [24]. Analogical processes should be expected in the functioning of modern enterprises. Artificial intelligence built into modern management systems automates forecasting in strategic decision-making

situations. At the same time, the demand for assessments will increase. Nothing can replace a man in this task. That is why enterprises and managers should invest in the development of skills and skills related to the assessment and judgment of forecasts.

Artificial Intelligence will change IT outsourcing [25]. The five ways in which AI will change ITO are given below:

1. Enhanced automation

AI technology can increase the speed of actions by automating them. Time is a limitation that is especially evident in crisis. Machine learning and deep AI learning reinforces automation. Programmes cannot only perform programmed commands but also learn. Understanding and making decisions constitute the IT functions that could be outsourced so that company employees would perform higher-level job tasks. AI can make judgment-based decisions using unordered input. IT providers that offer AI technology in business models implement solutions that can interpret information automatically, making fewer mistakes than people. Through this, companies can increase efficiency in achieving business goals.

2. More control

The use of AI technology can transfer control processes in an enterprise from a supplier to a buyer. You can estimate the costs of outsourcing IT functions compared to performing these functions for a company when purchasing AI technology.

3. Reduced costs

AI technology can reduce the cost of IT outsourcing due to agility, reliable processing, analysis and comprehensive information. Also, the hidden costs associated with IT outsourcing, such as the time needed for training, can be reduced or eliminated. AI technology is capable of self-learning on tasks, using machine learning techniques. AI does not have to be physically located in one place, compared to a human, which significantly reduces labour costs.

4. Improved contracts and negotiable terms

AI technology may affect the current terms of service and service level agreements. The manner of negotiating contract terms will also change. The cost will not be a lasting competitive advantage. When using AI, however, one should be aware of the ownership of the technology, because ownership agreements can bind the enterprise to a particular supplier.

5. Increased security

The use of IT outsourcing is associated with an increased risk of data and information security. Employees can exploit infrastructure gaps and use the information to act against the company. AI technology reduces this risk. In addition, AI may work with people and experts to predict and identify security breaches. This means greater security for the company.

References

[1] J. Słoniec, "News in the IT outsourcing and trends in its development", *Journal of Positive Management*, vol. 7(4), pp. 3–18, 2017.

[2] J. Słoniec, „Outsourcing IT w dużych organizacjach w Polsce. Modelowanie z wykorzystaniem równań strukturalnych", *Toruń: Wydawnictwo Dom Organizatora*, 2018.

[3] V. Grover, M. J. Cheon, T. C. Teng, "A Descriptive Study on the Outsourcing of Information Systems Functions", *Information & Management*, vol. 27(1), pp. 36, 1994.

[4] K. McLellan, B. Marcolin, P. Beamish, "Financial and Strategic Motivations behind IS Outsourcing", *Journal of Information Technology*, vol. 10(4), pp. 310, 1995.

[5] G. Gupta, H. Gupta, "Outsourcing the IS function. Is it necessary for your organization?" *Information Systems Management*, vol. 9(3), pp. 44, 1992.

[6] Q. Chen, B. Lin, "Global Outsourcing and its Managerial Implications", *Human Systems Management*, vol. 17(2), pp. 110, 1998.

[7] M. D. Hopper, "Rattling SABRE – New Ways to Compete on Information", *Harvard Business Review*, vol. May-June, pp. 118–125, 1990.

[8] R. Heeks, S. Krishna, B. Nicholson, S. Sahay, "Synching or Sinking: Global Software Outsourcing Relationships", *IEEE Software*, vol. 18(2), pp. 54–60, 2001.

[9] N. Marchand, H.-A. Jacobsen, "An Economic Model to Study Dependencies between Independent Software Vendors and Application Service Providers", *Electronic Commerce Research*, vol. 1(3), pp. 315–334, 2001.

[10] P. C. Palvia, "A Dialectic View of Information Systems Outsourcing: Pros and Cons", *Information & Management*, vol. 29(5), pp. 265, 1995.

[11] B. Caldwell, "The New Outsourcing Partnership", *Information Week*, no. 585, pp. 51, 1996.

[12] M. C. Lacity, L. P. Willcocks, "An Empirical Investigation of Information Technology Sourcing Practices: Lessons from Experience", *MIS Quarterly*, vol. 22(3), pp. 363, 1998.

[13] R. B. Myerson, "Basic concepts of Decision Theory, Game theory analysis of conflict." *Cambridge, Massachusetts: Harvard University Press*, 1997.

[14] W. Glasser, "Choice Theory", *New York: Harper Collins Publishers*, 1998.

[15] S. O. Hansson, "Decision Theory: A Brief Introduction", *Stockholm: Royal Institute of Technology (KTH)*, 2005.

[16] D. M. Hausman. (2019, Oct. 01). "Rational Choice Theory", *Stanford Encyclopedia of Philosophy*. [Online]. Available: https://plato.stanford.edu/entries/economics/#RatiChoiTheo

[17] J. Targalski, „Podejmowaniu decyzji", In A. Stabryła, J. Trzcieniecki, (eds.) *Organizacja i zarządzanie*. Kraków: Akademia Ekonomiczna w Krakowie, 1986.

[18] S. Finkenlstein, D. C. Hambrick, A. A. Jr. Cannella, "Strategic Leadership Theory and Research on Executives, Top Management Teams, and Boards", Oxford, New York: Oxford University Press, 2009.

[19] A. Agrawal, J. Gans, A. Goldfarb, "Artificial Intellinence: The Ambiguous Labor Market Impact of Automating Predictio", *Journal of Economic Perspectives*, vol. 33(4), pp. 31–50, 2019.

[20] E. Urbanowska-Sojkin, A. Wienert, „Wykorzystanie systemów IT w informacyjnym wspomaganiu wyborów strategicznych w przedsiębiorstwach działających w różnych sektorach", *Przegląd Organizacji*, no 4/2019, pp. 59, 2019.
[21] Santander Bank UK. (2019, Jun. 01). Available: http://www.gsa-uk.com/files/1093.pdf
[22] A case study on Dell's call centre outsourcing. (2019, Jun. 01). Available: https://www.cnblogs.com/lei1016cn/archive/2011/03/09/1977851.html
[23] Zarządzanie dokumentacją archiwalną dużej instytucji ubezpieczeniowej. (2019, Jun. 01). Available: https://www.archidoc.pl/ubezpieczenia-case-studies, zarzadzanie-dokumentacja-archiwalna-duzej-instytucji-ubezpieczeniowej. html
[24] N. Dawar, "Marketing in the Age of Alexa", *Harvard Business Review*, 2019.
[25] 5 Ways Artificial Intelligence Will Change IT Outsourcing. (2019, Oct. 1). *CIOPages.com Insights*. [Online]. Available: https://www.ciopages.com/5-ways-artificial-intelligence-will-change-it-outsourcing/

Wojciech Urbańczyk[1], *Piotr Buła*[2]

CHANGE MANAGEMENT VERSUS DIGITAL TRANSFORMATION IN THE IT COMPANY FOR OPTIMAL ADAPTATION TO THE NEEDS OF FUTURE TECHNOLOGIES

Keywords: Change Management, Digital Transformation, Future Technologies, Hybrid Solutions, Transition to Modern Technologies

Abstract

The document presents the classic methods of change management against the new methods, which follow from the technological change, the so-called Digital Transformation. The comparison of these two methods revealed similarities as well as contrasts between them. This paper describes the ways to achieve optimal solutions when developing new business models. There is a kind of technological continuity in the IT-industry. Simply put, it is about improving existing systems and adapting them to actual market needs. The combination of past and future in many areas leads to functioning hybrid solutions. In addition to factors such as creativity, innovation, digital potential and the successful transition to modern technologies, the human factor plays a key role in Digital Transformation as well as in change management. To talk about a "sensible" digital transformation, we need patterns that would allow us to build the kind of backbone of the system on which the digital transformation would bloom.

1. Introduction

The data centre and the entire IT infrastructure form the core of today's Enterprise businesses. The technological development and implementation of the latest IT solutions increasingly determine the development and structure of data centres.

High availability and maximum technological efficiency are indispensible 24 hours per day, 365 days a year. Furthermore, for IT to work perfectly, you need more than high-quality products. The substitution of an efficient device cannot solve all problems, regarding e.g. the bandwidth. A professional and organised planning of a data centre is defined through a detailed analysis of an individual's needs. Planning is an essential factor in the concept of new data centres and at expanding projects.

[1] University of Vienna, Faculty of Computer Science, 29 Währinger Str., 1090 Vienna, Austria, w_urban@gmx.at

[2] Cracow University of Economics, Faculty of Economics and International Relations, Department of International Management, 27 Rakowicka Str., 31-530 Kraków, Poland, piotr.bula@uek,krakow.pl

Timeliness then, are paramount at every data centre planning for the entire efficiency of IT.

Planning the architecture from a new data centre is slightly different from moving the existing IT architecture to a new, digital, time-relevant IT construct. When you think about optimising your data centre architecture or adapting it to the expectations that will need to be met in the future, you should not consider the transition as a one-step action. Optimisation of a data centre is an incremental process towards Cloud Computing. Regardless of whether you are planning a new data centre or want to optimise an existing one, the patterns of IT architecture that need to be considered are the same. In developing appropriate methods of applying digital transformation in this article, several questions arise, such as:
If change management is still used as a standard, why do you need digital transformation or digitalisation?
What is the usability of digital transformation at projects that have different dimensions?

The research methods used in the development of this paper were the literature analysis and the implementation of a pilot project at the Federal Data Center. For the purpose of the paper the following definition is used: “To optimally adapt to the needs of future technologies of the IT company like the Federal Data Center and to avoid possible failures of transformation, the exact analysis of the effort for the change management and the digital transformation are essential”. The reflections on the usefulness of using both methods with a focus on these most important features were also discussed. The findings that were gained tiled into further projects and also influenced the reorganisation of certain areas of the Federal Data Center. The lessons learned after successful completion of the operating calendar project, have shown that the digital transformation needs to be done gradually. Some elements and processes such as: involving stakeholders and employees in the transformation process, e-participation, and higher productivity were crucial to the success of the project. The final findings are shown in table 1.

2. Austrian Federal Data Center

Current structures in the organisational and technical areas of Federal Data Center, especially in the public sector, date back to the 1980s. Practice has shown that these structures are outdated, ineffective and usually counterproductive. The need to adapt such structures to the expectations of the IT industry is solely for reasons of energy efficiency and cost savings (e.g. due to historical and political circumstances, most of the "adaptations and changes" made in the public sector are more likely to be cosmetic). The Federal Data Center, like all other data centres, is currently undergoing the transformation phase.

From a data centre investment protection point of view, it is very difficult to predict which technologies will be of interest in the future and which will stand the test of time and provide long-term profitability. The current Federal Data

Center is characterised by a highly complex and complicated structure of IT systems. There are at least a dozen drivers that control the development of the data centre and its infrastructure. Additionally, better control of critical systems, Energy Management, Network Connectivity, Virtualization and Cloud Computing, Service Availability, application stability and reliability are becoming increasingly important.

Such DC structures need to be adapted to the expectations of the IT industry connected with energy efficiency and cost savings. Transformations (especially the Digital Transformation) are necessary because the environment in which the data centres are located is changing – both with respect to the technology and with respect to legal and geopolitical conditions. Legal aspects must be adapted e.g. to the EU requirements [16].

3. Change Management

The classic approach to change management is based on the assumption that organisational shifts are introduced top-down and caused by a central process [6]. This hierarchical and centralised method generates many problems in the psychological field, however, from the digitalisation perspective, they may be useful. Implementation of IT systems, even in the traditional meaning, enforces adjustment to the other systems. Otherwise, sharing data will be problematic, for example, used in external accounting. In the case of ERP systems, it is more visible, because they offer standard features and predefined functions [9]. Therefore, it is necessary to adapt vision and business processes to the overall logic of a chosen system.

Another feature of the classic approach is that the change is episodic and has a gradual trajectory. According to the Lewin's model [11], and other graduals model [5], shifts move an organisation from one state to another. Those models differ in terms of count and distribution of accents in stages, but the idea remains the same – qualitative change seeks to establish a new status quo. The problem of the digital revolution is there is no status quo. According to the Litwin-Burke's model of organisational performance, changes are implied by the environment. External circumstances cause a transformational change which affects mission, strategy, leadership and culture [4]. Systematic nature of change seems to suit the complexity of the digital revolution. Nowadays, more and more firms begin to create their own start-ups instead of looking for them on the market. Through this type of solution, they gain far more creativity and flexibility. Furthermore, shifts developed by internal cells have a better chance of acceptation from regular employees. Despite the differences that are reflected in the approach to Change Management, in all models the tasks resemble management of change. This is confirmed by the widespread acceptance that certain factors are the basic components of all successful changes.

The distinctive factors are:

- development of purpose and vision;
- communication with all affected employees;
- involvement of all affected employees;
- motivation, will, ability and qualification for the change on the management level as well as the employees.

4. Digital Transformation

Digital Transformation applies to all areas of society and the economy in the first place. Digital Transformation opens up new possibilities for creating networks and cooperation of various entities, e.g. exchanging data, and this means initiating processes. In this context, it plays a special role in the Digital Transformation of business models, because business models contain various elements that can be digitally transformed. In innovations of business models, such individual elements of the business model of individual areas as customer, services or the entire business model are subject to change [13]. The Digital Transformation is based on already existing business models. "Digital Transformation (DT) – the use of technology to radically improve performance or reach of enterprises is becoming a hot topic for companies across the globe. Executives in all industries are using digital advances such as analytics, mobility, social media and smart embedded devices – and improving their use of traditional technologies such as ERP – to change customer relationships, internal processes, and value propositions [14]."

PricewaterhouseCoopers (PwC) defines six basic phases for digital transformation (figure 1). The presented phases take into account the different aspects of the digital technology. Defining the strategy: In this phase, the current position of the company is determined, and the business model is designed. Safety and value creation are analysed and evaluated, whereas legal and tax aspects – examined. The first phase aims to understand the impact of digital dynamics on corporate culture and human capital.

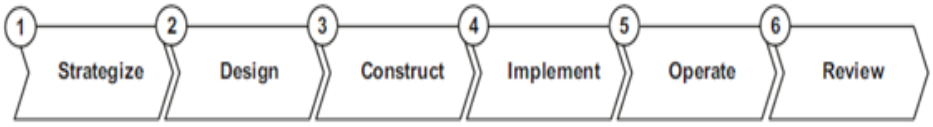

Fig. 1. Approach to PwC 2013. (2013). Digitale Transformation – der größte Wandel seit der industriellen Revolution. PwC, 2013. p 40of the blade with general dimensions

Solutions that can be expected from the Digital Transformation are versatile. The Digital Transformation enables the development of a common platform for Legacy systems and the newest technologies. Old inflexible technologies (which

are one of the most common brakemen in the company's development) are being replaced by new ones. Digital Transformation means faster exchange of information and knowledge not only within the company but also between various industries [12]. Sooner or later, all industries will be drawn into the vortex of Digital Transformation (figure 2).

Fig. 2. Digital Vortex, (2015). How Today's Market Leaders Can Beat Disruptive Competitors at Their Own Game. Global Center for Digital Business Transformation

Changes forced by long-lasting trends such as "job anywhere and anytime" affect the change in the paradigm in the perception of the company's organisational structures, and these are those from which companies benefit more when they are open to innovation [7, 18]. The comparison of these two methods (Change Management and Digital Transformation) shows similarities as well as the contrasts between them. But when it comes to the ability to adapt to future technologies, such as: automation of processes, e-participation or absolute mobility, these are the clear benefits of digital transformation (see table 1).

The digital transformation brings practical advantages to Austria in every area. To confirm this, consider the example of the introduction of digital returns receipts by the judiciary. A return receipt is an official document. It is an unconfirmed consignment with special order or the official delivery of a document, which may only be delivered to the recipient. The hybrid return receipt has been successfully used by the Federal Ministry of Justice for five years. With the introduction of the hybrid returns document, a complex manual process could be automated. The electronic sending of the acknowledgement of receipt has made the process more efficient – *ergo* the digital transformation with a clear cost-benefit calculation. The IT partner for the

integration of the hybrid return slip into the electronic processes of the Federal Ministry of Justice was the Federal Data Center. By eliminating manual reworking and material costs, the judiciary saves around 1 million Euros annually (base 2016) [2].

Tab. 1. Comparison of Change Management and Digital Transformation

	A	B	C
1	**Factors that will affect the shape and functioning of the Federal Data Center in the future**	**Change Mgm.**	**Digital Transform.**
2	Higher productivity	X	X
3	Reduction of administrative effort (introduction of self-service portal)		X
4	Clearly defined duration of the changes of processes in the system	X	
5	Cultural compatibility	X	X
6	Simple in Evaluation of processes		X
7	Faster payback period		X
8	Creation of new products	X	X
9	Involvement of all affected employees	X	X
10	e-participation		X
11	Structures designed independently of the trends		
12	Automation of processes (eg supply chain)		X
13	Agile react to technological changes	X	X
14	Open for the newest changes in systems		X
15	Possibility to implement the old legacy systems in new structures	X	X
16	Effectiveness of communication within a company increases		X
17	Effectiveness of communication between companies and customers increase		X
18	Absolute mobility (time and location independent work)		X
19	Permanent accessibility and localization		X
20	Modeling future system architectures using tools (Software Defined)		X
21	Reduction of complexity (complexity is hard to control manually by human operators)		X
22	Reduction of outsourcing (outsourcing leads to loss of control over IT know-how)	X	
23	Increased fault tolerance and self-organization		X
24	More automation, if the system is too large or to complex to guarantee the safety level		X
25	Have adaptive, self configuring defence mechanism and self healing systems		X
26	Allow reuse of software components		X
27	Less effort to repair errors		X
28	Improves access to all services (use of AI as a basis for eg virtual agent)		X
29	Use of standardized procedures and processes	X	

Source: own study, internal project at Federal Data Center

5. An Example of Digital Business and Operating Calendar at Federal Data Center

For all relevant events in the Federal Data Center, the Business and Operating Calendar is a central calendar for all employees of the Federal Data Center.

The calendar graphically shows all operational changes in the IT landscape of the Federal Data Center. All changes subject to compliance with the change process, including the key data from the affected system to the business IT service and customers, are presented. In addition, all relevant events such as: Maintenance window and the readiness of the production management are registered. The following points are shown in the calendar:

- all activities in the maintenance window. (quarterly maintenance windows, special maintenance windows, and power and emergency tests);
- maintenance windows of the power ranges;
- customer lock-up dates;
- activities to be performed outside of maintenance windows which are subject to compliance with the change management process and which comply with defined criteria.

The calendar is implemented in the mailing system of the Federal Data Center. The Gateway Representation feature gives each Federal Data Center employee read access to the special Calendar Mailbox.

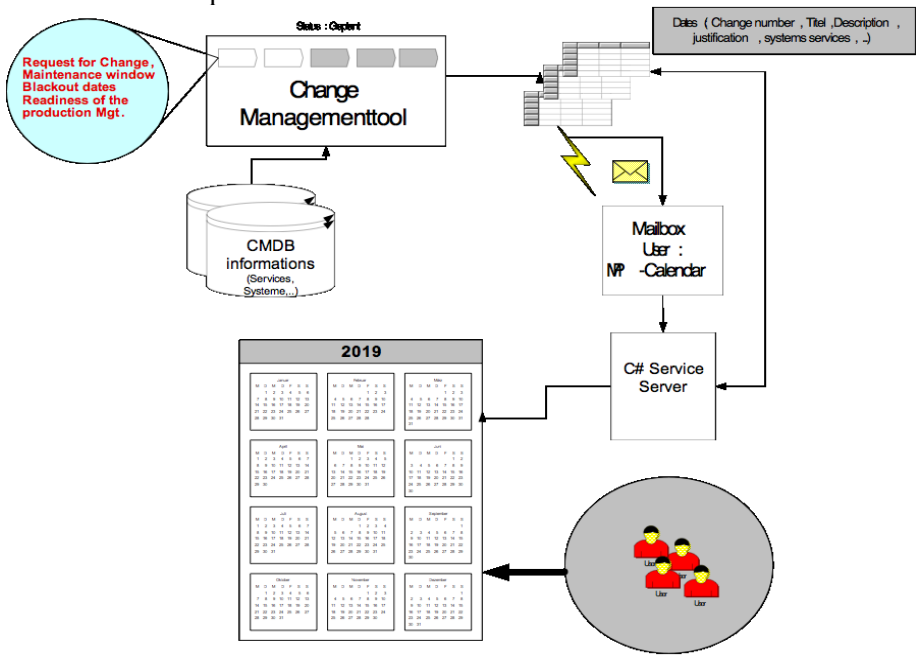

Fig. 3. Business and Operating Calendar at Federal Data Center

Source: own study, an internal project at Federal Data Center

6. Conclusion

Classical change management is dead. The world of today needs a completely new, special combination of mind and skillset to meet the challenges of the future. In general, it is a way to deal with increasingly complex frameworks and conditions, to actively shape the future and prepare oneself and those in their own environments for new challenges. In the last decade, the advancing technical possibilities have determined the trends in the IT industry, for example as evidenced by the study by Cap Gemini [10]. All projects realised in the Digital Transformation environment have a disruptive character. Innovative companies move from existing business models to adjoining areas. As digital technology change plays a major role, digital technologies are becoming the core competence in the future [19].

Digital technologies and their unlimited availability via the mobile Internet, fundamentally change companies. Now you can say that the change becomes digital. From an IT vendor's point of view, this means that Digital Transformation alters customer expectations, increases speed and sets new patterns of collaboration. First of all, the future means "business without borders [8].” Although these changes will shape the future of any company, the most important factor for success in the future still will be a human. Work models such as ROWE (Result Only Work Environment) prevail. Also, for employees, the boundaries between work and leisure are getting blurred more and more. Thanks to the mobile Internet, work loses its traditional place in the office and takes place on the road, from home or even from a holiday home. That is why personal skills are becoming more and more important as factors guaranteeing success [20]. Under the motto "From Fatherland to Partner State," Digital Transformation in Austria focuses on three areas: society, economy and administration, in the hope that Austria will become a pioneer and model for an innovative and citizen-friendly administration in Europe [3].

Analyses of the status of Digital Transformations have shown that they are still business transformations. You need to provide customers with real value and better results for the company – not just for the technological gain. These changes typically affect the customer experience, the digitisation of products and services, the emergence of new business models, and business progress [10]. However, the painful reality is that most transformations fail. Research shows that 70 percent of complex, large-scale change programs fail to reach their stated goals [1]. One could conclude that some methods of change management can be integrated into Digital Transformation.

“Digital Transformation may be considered as a management fashion or as the reincarnation of past IT-enabled change initiatives with new outfits. IT-enabled change resurfaced a few years ago through the business process management movement [15].” It is impossible to test a digital transformation on a living "organism" such as the Federal Data Center. Literature research as well as the

step-by-step implementation of applications are necessary to minimise the risk of digital transformation. The best results have been achieved with a "step by step" method and for sure: every method is good if it leads to success. There is a need for further testing but due to the constraints of this article, it is not possible to analyse all possible solutions. As a possible measure for the future, the tried and tested mechanisms of, for example, TOGAF could come into action. In order to talk about "sensible" digital transformation, you need patterns that will allow you to build a kind of "backbone" into the system on which the digital transformation will be set. Examples of such patterns can be those used to implement new technologies, e.g. resilience patterns [17]. Digital transformation is, after all, nothing more than the implementation of a new technology.

References

[1] M. Bucy, A. Finlayson, G. Kelly, C. Moye, "The 'how' of transformation. McKinsey&Company", 2019, [online]. available: https://www.mckinsey.com/industries/retail/our-insights/the-how-of-transformation.

[2] Bundesrechenzentrum, "Duale Zustellung: vereinfachtes Handling, geringere Kosten", 2019, [online], available: https://www.brz.gv.at/was-wir-tun/services-produkte/e-rechtsverkehr/duale-zustellung-.html.

[3] Bundesrechenzentrum. "Digitalisierung brüngt allen was", 2019, [online], available: https://brz.portal.at/neuigkeiten/innovation/digitalisierung-bringt-allen-was_.html.

[4] W. W. Burke, G. W. Litwin, "A Causal Model Of Organizational Performance And Change", *Journal of Management*, vol. 18(3), pp: 523–545, 1992.

[5] R. By, "Organizational Change Management: A Critical Review", *Journal of Change Management*, vol. 5(4), pp. 369-380, 2005.

[6] J. A. Cannon, R. McGee, "Organizational development and change", London, England: Chartered Institute of Personnel and Development, 2008.

[7] H. Chesbrough, M. Bogers, "Explicating Open Innovation: Clarifying an Emerging Paradigm for Understanding Innovation", 2019, June 21, [online], available: https://poseidon01.ssrn.com/delivery.php?ID=806092&EXT=pdf.

[8] J. Reis, M. Amorim, N. Melão, P. Matos, "Digital Transformation: A Literature Review and Guidelines for Future Research", *Trends and Advances in Information Systems and Technologies*, pp. 412, 2018. https://doi.org/10.1007/978-3-319-77703-0_41.

[9] H. Hoang, "Change management in a modern economy, Modeling approach", Warsaw, Poland: PTM, 2012.

[10] I. Keicher, U. Bohn, T. Anke, C. Crummenerl, B. Gerhard, N. Mergenthal, "Digitale Revolution, Ist Change Management mutig genug für die Zukunft? Capgemini Consulting", 2019, June 12, [online], available: https://www.capgemini.com/consulting-de/wp-content/uploads/sites/32/2017/08/change_management_studie_2012_0.pdf.

[11] K. Lewin, "Field Theory in Social Science", New York: Harper & Row, 1951.

[12] J. Loucks, J. Macaulay, A. Noronha, M. Wade, "Digital Vortex. How Today's Market Leaders Can Beat Disruptive Competitors at Their Own Game. International Institute for Management Development", 2019, May 28, [online], available: http://digitalvortex.imd.org/wp-content/uploads/2016/06/Digital-Vortex-Excerpt.pdf.
[13] D. Schallmo, "Kompendium Geschäftsmodell-Innovation – Grundlagen, aktuelle Ansätze und Fallbeispiele zur Erfolgreichen Geschäftsmodell-Innovation. Vorgehensmodell der Geschäftsmodell-Innovation - bestehende Ansätze, Phasen, Aktivitäten und Ergebnise", Wiesbaden: Springer Fachmedien, pp. 51–74, 2014.
[14] G. Westerman, C. Calméjane, D. Bonnet, P. Ferraris, A. McAfee, "Digital Transformation: A Roadmap For Billion Dollar Organisations, Findings From Phase 1 Of The Digital Transformation Study", Conducted By The MIT Center For Digital Business And Capgemini Consulting, 2019, March 06 [online]. available: https://www.capgemini.com/wpcontent/uploads/ 2017/07/Digital_Transformation __A_Road-Map_for_Billion-Dollar_Organizations.pdf.
[15] J. Reis, M. Amorim, N. Melão, P. Matos, "Digital Transformation: A Literature Review and Guidelines for Future Research", *Trends and Advances in Information Systems and Technologies*, pp. 419, 2018, https://doi.org/10.1007/978-3-319-77703-0_41.
[16] EUR-Lex, Access to European Union Law, "KOMISJA EUROPEJSKA. (06. 2018). "Document 52018PC0434. Wniosek, ROZPORZADZENIE PARLAMENTU EUROPEJSKIEGO I RADY ustanawiające program „Cyfrowa Europa" na lata 2021–2027, COM/2018/434 final - 2018/0227 (COD)", 2019, September 21, [online]. available: https://eur-lex.europa.eu/legal-content/PL/TXT/?uri=CELEX%3A52018PC0434.
[17] W. Urbanczyk, J. Werewka, "Enterprise Architecture Approach to Resilience of Government Data Centre Infrastructure", *In Information Systems Architecture and Technology: Proceedings of 39th International Conference on Information Systems Architecture and Technology–ISAT 2018*. Springer International Publishing, 2018.
[18] C. M. Olszak, "Strategia Cyfrowa Wspolczesnej Organizacji", *Studia Ekonomiczne, Zeszyty Naukowe Uniwersytetu Ekonomicznego w Katowicach*, vol. 232, 2015.
[19] P. Adamczewski, "Ku dojrzalosci organizacji inteligentnych", *Studia i Prace, Kolegium Zarzadzania i Finansow*, vol. 161, pp. 72, 2018.
[20] J. Reis, M. Amorim, N. Melão, P. Matos, "Digital Transformation: A Literature Review and Guidelines for Future Research", *Trends and Advances in Information Systems and Technologies*, pp. 418, 2018. https://doi.org/10.1007/978-3-319-77703-0_41.

Michał Uliczka[1], *Ireneusz Smykla*[2]

A COMPARATIVE ANALYSIS OF METHODS USED FOR THE DETERMINATION OF AIRCRAFT AERODYNAMIC CHARACTERISTICS

Keywords: Em-10 "Bielik", analysis, simulation, aerodynamic characteristics, performance

Abstract

This paper presents three methods of determining aerodynamic characteristics and compares the results on the example of the EM-10 "BIELIK" aircraft. The choice of the aircraft is not accidental. It is distinguished by an airframe of the so-called non-linear aerodynamics of flow, which results from using a leading-edge extension. The exploited methods of determining aerody-namic characteristics were as follows: aerospace engineering formulas, computer simulation of the airflow around the project created in CAD programme and examining the prototype in a wind tunnel. Finally, the authors compared the obtained results and determined the effectiveness of the first two methods in relation to the third one, whose results prove to be closest to real values. The following have been compared: lift and drag graphs, depending upon the angles of attack and the aircraft polar.

1. Introduction

When beginning a design of a new aircraft, for a previously assumed performance, it is essential to decide on an appropriate aerofoil, which should be adequate to the future scope of tasks. The foundation for all further calculations is a wing polar curve, which can be obtained by selecting a previously defined and calculated aerofoil, or by calculating it single-handedly. Despite its tremendous impact on the polar curve of the entire aircraft, the impact of other elements of the airframe cannot be disregarded. Differences between the wing polar curve and the polar curve of the whole plane show that a skilful design of the fuselage, stabilisers, canopy, inlet, undercarriage may prove equally important. Therefore, in order to effectively design an aircraft, it is necessary to accurately forecast the aircraft polar curve at an early stage of its design, which will determine the shape of all airframe parts [8].

A determination of an aircraft polar curve can be made with different methods:

a) the method using aerospace engineering formulas based on data to describe the used aerofoil, wing parameters and other airframe parts. This method uses

[1] Polish Air Force University, Faculty of Aviation, 35 Dywizjonu 303 Str., 08-521 Dęblin, Poland, ml.uliczka@gmail.com

[2] Polish Air Force University, Faculty of Aviation, 35 Dywizjonu 303 Str., 08-521 Dęblin, Poland, i.smykla@law.mil.pl

two-stage calculations, first by starting with computations of the wing polar curve, and then by calculating the polar curve of the whole aircraft [7].

b) the method which exploits testing in a wind tunnel. The examined model is built in a given scale, and then undergoes testing. The results are converted appropriately so as to obtain values corresponding to an airframe of real dimensions.

c) the method which uses computer simulation in a programme intended to conduct parametric 3D modelling (CAD 3D), which allows designing solid models as well as sheet metal, welded constructions, moulds, surface models. The program should have a fully integrated package to simulate the flow of liquids and gases in real conditions and an effective analysis of the impact of fluid flow (heat exchange or the impact of forces) [6].

The first method is based on making calculations after entering a great deal of geometrical data (describing the size of airframe components) into appropriate formulas. In addition, graphs are used to determine certain parameters. The data are stored in the form of tables. This method assumes certain simplifications (to reduce the sophistication level of calculations), leading to inaccurate findings, especially at larger angles of attack. Despite its inaccuracies, the method of engineering calculations gives a possibility to make quite a precise and quick analysis of the examined airframe [9].

The second method is performed on the basis of appropriate technical equipment, such as the above-mentioned wind tunnel, with an adequate financial expenditure. Thus, it is primarily used by aircraft facilities that are capable of allocating sufficient resources for this purpose. This method is being increasingly superseded by the third method that uses computer simulation, due to the fact that its accuracy and computing power are constantly growing. It also allows making a flow simulation and an imagery of forces, as well as performance of an aircraft during a flight.

The aim of this article is to compare the efficiency of all the above-mentioned methods for the determination of the aircraft polar curve, on the example of EM-10 “Bielik”, with distinctive non-linear aerodynamics caused by the leading-edge extension [1].

1. EM-10 “Bielik” aircraft characteristics

The concept of EM-10 “Bielik” dates back to the late 1990s. In order to meet demand of executing a large number of flights by military pilots undergoing training, and at the same time to avoid a huge increase in the training costs, the aerospace facility, currently named Margański & Mysłowski Aircraft Company, began to develop a concept of a flying simulator. Their main intention was to create a simple and light (also economical) airplane, which does not carry any weapons, and which facilitates fighter combat training with simulation. The bulk of the installations, together with cockpit layout, was used from the TS-11 “Iskra”.

Due to the use of parts from the other aircraft, their large number may have been used and obtained free of charge or at a minimum price. The aircraft was completed, mounted on a trailer and transported to Mielec (Poland) to perform a test flight on June 4, 2003. After a month, a second one-hour flight was executed, during which the "Bielik" climbed to 3,000 m. After these attempts, a demonstration flight for the military was planned. Its main aim was to convince military commanders to introduce the aircraft into the training for military pilots. Unfortunately, before the scheduled date of the flight, it already became obvious that the Air Force would not purchase "Bielik". Consequently, a third flight did not take place [2].

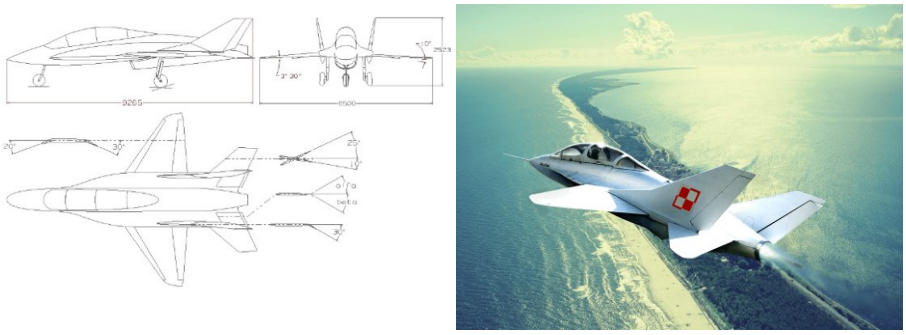

Fig. 1. Orthographic projections of EM-10 (left) [3], graphics depicting EM-10 during a flight (right) [4]

EM-10 "Bielik" has got an airframe which structure is built of carbon/epoxy composite. The fuselage is made from stressed skin, of a sandwich-type structure, which cross-section is oval in shape, extended by additional leading-edge root extensions on both sides. The front part consists of a tandem-seat cockpit, a front fuel tank, equipment compartments located in the nose, in the leading-edge root extensions and the front undercarriage. The rear part houses the main fuel tanks, an engine compartment, equipment compartments, an aerodynamic brake and the main undercarriage. The wing is tripartite. It has flaps on both, the leading edge and the trailing edge. The part which is near the fuselage constitutes the so-called leading-edge root extension, which is the structural part of the very fuselage. It is trapezoidal, anhedral and an angle of incidence is equal to zero. The aerofoil, likewise, all flight control surfaces, is symmetrical. Its thickness constitutes 6% along the entire wingspan. The rudder is two-part and has mass balancing. The rudders are swivelled individually and only outwards. The elevons have mass and aerodynamic balancing. On their trailing edges, there are balancing flaps. The airbrake is mounted on the upper part of the fuselage. It is a plate, pivotable using a hydraulic cylinder. The air inlet is single, located under the fuselage and located in such a manner that the boundary layer does not reach it, either. In EM-10 "Bielik", there is one CJ610-6 engine manufactured by General Electric Co., USA. It is single-shaft, turbojet, with an eight-stage axial compressor, a changeable setup of pre-stator blades coupled directly, a two-stage axial

turbine and regulated bleed air in-between compressor stages. It has got an annular combustion chamber and the compression ratio of 6.8:1 [2].

2. Determining the characteristics of EM-10 “Bielik”

3.1. Analysis of aerodynamic characteristics using aerospace engineering formulas

The engineering method is based on making a number of calculations after entering a great deal of geometrical data (describing the size of airframe components) into appropriate formulas. The method uses two-stage calculations, first by starting with computations of the wing polar curve, and then by calculating the polar curve of the entire aircraft. Obviously, the calculated polar curve is burdened with error (as a result of assumptions made to simplify the computations). The higher angle of attack, the larger are the errors due to the non-linear characteristics; as, for example, an increase in lift by increasing an angle of attack. For small angles of attack, the errors are relatively small, and the results faithfully represent the behaviour of the aircraft in the air and its performance [10]. The figure shows a measurement of the aircraft dimensions in the vertical projection for carrying out necessary calculations.

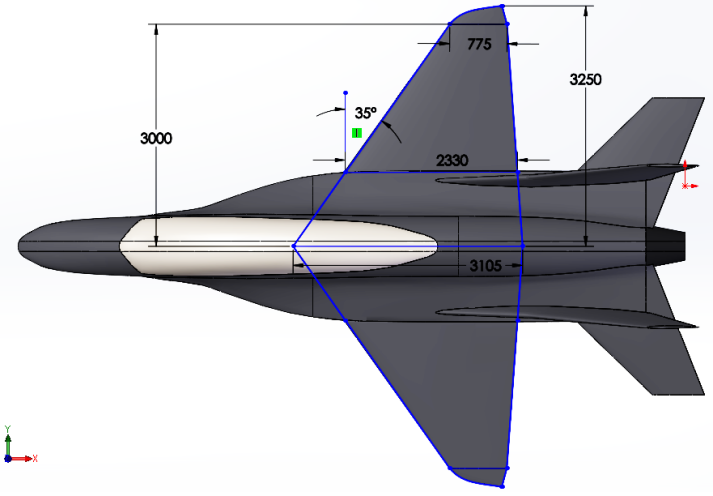

Fig. 2. Measurement of EM-10 dimensions in a vertical projection [1]

On completion of the calculations, the authors obtained findings which are depicted in graphs of the lift coefficient and of the drag coefficient, which vary depending on the angle of attack. On the basis of these two graphs, the authors determined the polar graph of the aircraft Cz(Cx).

3.2. Analysis of aerodynamic characteristics using SolidWorks software package

Creating a model in the SolidWorks environment was conducted on the basis of technical drawings of the aircraft (available in the Temporary Flight Manual) and additionally supported by the view of a prototype constructed by aircraft facilities in the then version of the UniGraphix programme. After creating the model, it was necessary to make the simulation. This was connected with setting up multiple configurations so as to test any angle of attack in the interval between (-40) to 40 degrees with a 1° leap. It was also necessary to set up all the flow conditions, detailed grid parameters forming the area of calculations, determining other quantities which were necessary to carry them out.

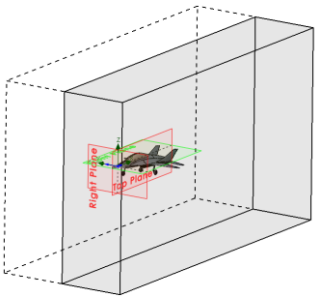

Fig. 3a. Aircraft model made in SolidWorks software package [1]; Fig. 3b. Space for calculating a flow [1]

Prior to the calculations, the authors determined the objectives of the simulation: lift, drag force, lift and drag coefficients. The calculations were divided and conducted by fourteen computers in order to obtain the test results in a relatively short period of time. Due to very accurate calculations, (computational grid consisting of over 1.5 million points), the simulation lasted over thirty hours. At the end of the simulation and after collecting the results of over 88 GB, it was possible to create tables and graphs of aerodynamic characteristics of the aircraft.

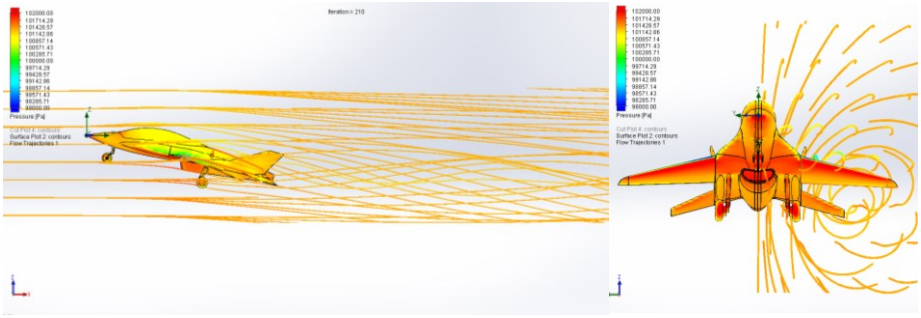

Fig. 4a. Side view of airstreams [1]; Fig. 4b. Front view of airstreams [1]

3.3. Analysis of aerodynamic characteristics using a wind tunnel

At the design stage, the aircraft was tested with models in an appropriate scale, fixed in the wind tunnel on the premises of Warsaw University of Technology. Owing to the courtesy of Krzysztof Kubryński, Ph.D., a world-renowned aerodynamics expert who designed modern aerodynamics of the "Bielik", it became possible to obtain aerodynamic characteristics which were determined using a wind tunnel. After establishing an e-mail contact, Kubryński shared the results of his research in the form of polar graphs and a lift coefficient, depending on the angle of attack. Using the resulting graphs, it was possible to determine the missing graph of the drag force coefficient, dependent upon the angle of attack.

Fig. 5. Models used for testing in the wind tunnel [5]

3. Comparison of results and summary

The graphs below show the test results obtained using the three methods used for determining aircraft aerodynamic characteristics.

The aerodynamics of EM-10 "Bielik" is completely different from most aircraft. The lift force operates on a completely different principle. This is also true for the drag force. The emerging momentum behaves differently. These properties result from detaching the airstream on the wing. Consequences of such a detachment are tremendous. There is the so-called non-linear aerodynamics, in which the lift force is created by vortices causing high under pressure, and the aerodynamic characteristics differ significantly – the lift force increases non-linearly and at higher angles of attack, due to the destruction of vortices, there is a decline in the lift force. The main problem of designing this type of aircraft is the fact that the phenomenon of destroying vortices is largely dependent on the airframe geometry in an unpredictable manner. For this reason, the fundamental

problem is the computational analysis of the properties of this aircraft based on typical engineering methods, as confirmed by the above-mentioned results – engineering formulas in this case prove to be completely useless, since aerodynamic characteristics depend upon a vast number of elements, ranging from wing parameters, shape of the leading-edge root extension, entire fuselage layout, flight controls, etc. They are all interdependent in a non-linear manner, making them unpredictable. While a classic aircraft can be designed by means of computational methods, the design of this type of aircraft seems to be impossible as it is necessary to perform a large amount of research in a wind tunnel and through trial and error construct all the elements.

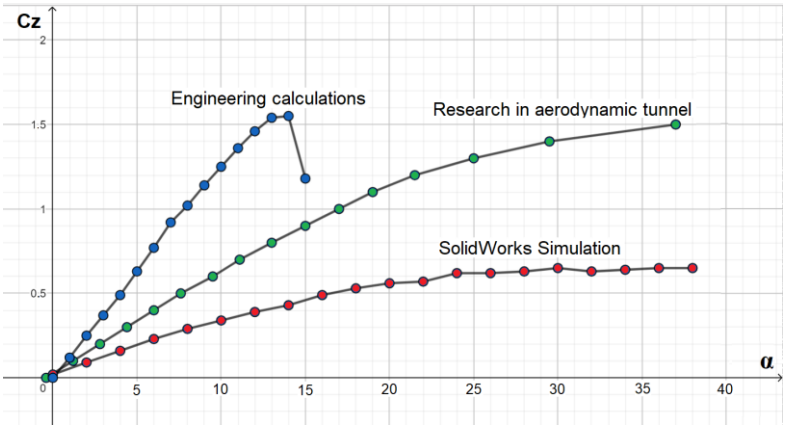

Fig. 6. Cz(α) graphs determined by means of different methods [11]

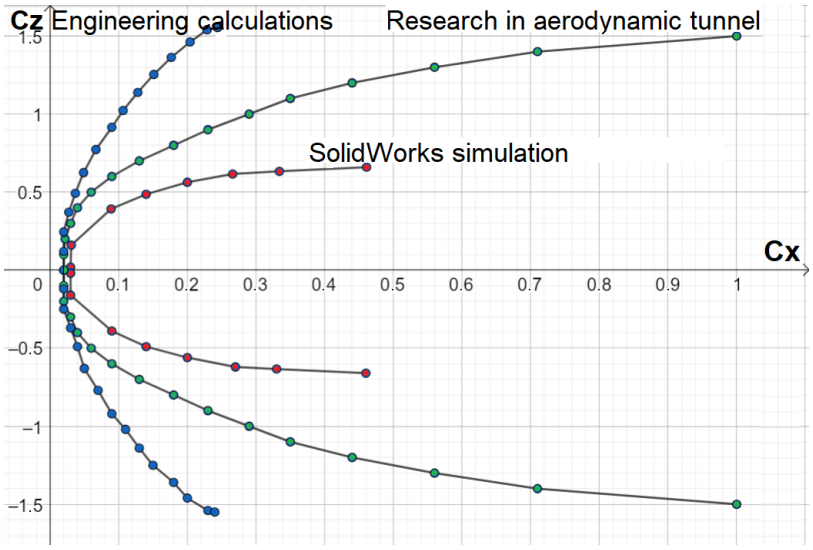

Fig. 7. Polar curves graphs determined by means of different methods [11]

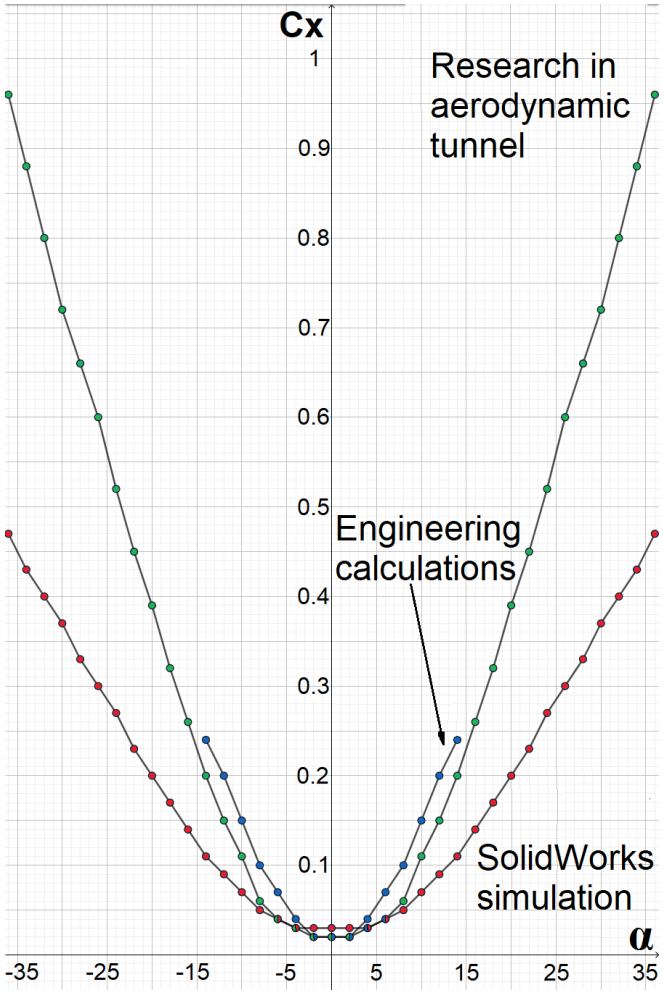

Fig. 8. Cx(α) graphs determined by means of different methods [11]

4. Conclusions

a) The calculations conducted by means of aerospace engineering to determine aerodynamic characteristics confirm their shortcomings. Even though the maximum value of the lift coefficient is approximately the same, the course of changes of this coefficient, along with a change of the angle of attack, is different. In accordance with the computational method, the aircraft is stalled when the angle of attack is slightly higher than 14°, whereas in reality the angle must be increased up to 40° so as to cause such stalling. Due to such a discrepancy, calculations with regard to the length of take-off and landing are incorrect.

b) The results of computer simulation in the SolidWorks environment differ from those obtained by calculations. Their course is more similar to real characteristics (in both characteristics, the change tendencies are similar, and stall occurs in the vicinity of the angle of attack value equal to 40°), however, the values of both the lift and drag coefficient are too small, more than twofold.

c) Despite a wide range of applications of aerospace engineering formulas for aerodynamic characteristics or for computer simulations in CAD programmes, it is important to take into consideration the fact that an analysis of different aircraft may produce different results that are far from reality, as illustrated by EM-10 "Bielik" examination.

d) At the stage of designing an aircraft, it is recommended to check aerodynamic characteristics by means of various methods in order to reduce the errors of the obtained findings and to increase the efficiency of changes in an airframe structure.

References

[1] M. Uliczka, „Analiza charakterystyk aerodynamicznych i osiągów samolotu EM-10 "BIELIK", Dęblin 2019.

[2] Glassowka - Recording of aviation supporters of 16 May 2015.

[3] Temporary EM-10 „BIELIK" flight manual.

[4] https://i0.wp.com/simulation.org.pl/site/wp-content/uploads/2014/01/em-10-02.png, accessed on 15.07.2018.

[5] Photograph received from EM-10 „Bielik" aircraft constructor - P. Krzysztof Kubryński.

[6] Dassault Systems SolidWorks Corporation, "An Introduction to Flow Analysis Applications with SolidWorks Flow Simulation", Student Guide, Concord 2010.

[7] W. Fiszdon, "Mechanika Lotu", *PWN*, Warszawa, 1961.

[8] M. Sadraey, "Aircraft Performance Analysis", *VDM*, Verlag 2009.

[9] A. Abłamowicz, W. Nowakowski, "Podstawy aerodynamiki i mechaniki lotu", Warszawa, 1980.

[10] B. W. McCormick, "Aerodynamics, Aeronautics and Flight Mechanics", *Wiley, New York*, 1979.

[11] Graphics made in the GEOGEBRA software programme.

[12] P. Jackson, "Jane's All The World's Aircraft 2004-2005", *Jane's Information Group*; Subsequent edition, 2004.

[13] B. W. McCormik, "Aeronautics, Aerodynamics, and flight mechanics", Whiley, 1994.

[14] J. Roskam, "Airplane Aerodynamics and Performance", *DARcorporatio*n, Revised edition, 2016.

[15] P. J. Swatton, "Aircraft Performance Theory for Pilots", *Blackwell Publishing company*, 2000.

[16] F. Hale, "Introduction to aircraft performance, selection and design", *John Wiley & So*ns, 1984.

[17] M. Eshelby, "Aircraft Performance, Theory and Practice", *Elsevie*r, 2000.

[18] JAA ATPL BOOK 06 - Oxford Aviation Jeppesen - Mass Balance and Performance.
[19] A. Filippone, “Flight Performance of Fixed and Rotary Wing Aircraft”, *American Institute of Aeronautics & Ast*, 2006.
[20] T. H. G. Megson, “Aircraft structures for engineering students”, *Elsevier Ltd*, 2013.

Miami Mohammed[1,2]

FEM ANALYSIS OF TWO-CORE PHOTONIC CRYSTAL FIBRE COUPLING CHARACTERISTICS

Keywords: Photonic crystal fiber, Effective refractive index, coupling length, coupling characteristics, finite element method

Abstract

Coupling characteristics of two-core photonic crystal fiber are analyzed using COMSOL MULTIPHYSICS software that is depended on the finite element method. The effective mode indexes and the electric field distributions, coupling length for different geometrical designs are evaluated. The results show the coupling length dependence the wavelengths to realize significantly short coupling lengths of two-core photonic crystal fiber in um at the telecom wavelength 1.55 um and 1.31 um compared with the traditional fiber coupler. The geometrical parameters of the PCF play an important role in the dependence of the mode characteristics between cores of PCF coupler, such as the hole diameter, hole pitch, air-filling fraction and, core separation. Increasing the core separation leads to a drastic reduction in the coupling strength between the cores of photonic crystal fiber or may lead to suppression of the coupling between the cores of photonic crystal fiber. Our proposed is an excellent device for coupler and power splitter, multiplex and de-multiplex applications.

1. Introduction

The Photonic Crystal Fibers (PCFs) is a high-flexibility design varying in the geometrical parameters, such as the hole diameter, hole pitch, and the core separation [1, 2]. They are made up of a set of air holes that run along the fibre length [3, 4]. Due to the differences in the geometrical design PCFs have different light-guiding mechanism, which either guide light by total internal reflection (MTIR) between the core and the cladding region, or by photonic bandgap (MPBG) [5–8]. PCFs have attracted a considerable amount of attention recently because of their unique properties that are non-existent in classical optical fibres [5, 6, 8], such as endlessly single-mode operation, high birefringence, high nonlinearity [3, 9, 10], effective-core-area at the single-mode region, and anomalous dispersion at visible and near-infrared wavelengths [5, 6]. The recent developments revealed a design of the PCF with two cores or multiple cores when high coupling is needed this design provides improvement in the size and performance of the fibre for widely researched and different applications [7, 9,

[1] Institute of Applied Physics, University of Muenster, Corrensstr. 2\4, 48149 Muenster, Germany

[2] Department of Physics, College of Science, University of Al-Mustansiriyah, Baghdad, Iraq, m_moha05@uni-muenster.de

11], such as a directional coupler [11–13], coupling and switching [14, 15], study of the coupling characteristic of dual-core PCF for applications as Multiplexer-demultiplexer [5, 8], polarized splitter PCF [16, 17] and for reduction in coupling, by introducing non-uniformity in core size of dual-core PCF [18-20]. Photonic crystal fibre (PCFs) coupler consists of two identical cores of PCF, and the two cores are placed close to each other with cores separation, the light guided via one of two cores, so that can exchange energy with each other by the excitation of the evanescent part of the fundamental modes of each guide during the propagation [6, 12]. These evanescent modes depended on the wavelength, result from different energy exchanges depending on the wavelength used [12].

In this paper, coupling properties of a two-core PCF coupler are evaluated using COMSOL MULTIPHYSICS software based on finite element method (FEM). The performance of this design is tested in order to predict the coupling characteristics of two-core PCF coupler dependence one of the geometrical parameters of this structure, such as the separation of cores. Through the geometrical designes of the two-core PCF coupler structure, we can obtain coupling lengths of (μm), i.e. much shorter in traditional optical fibre couplers of hundreds or tens of (mm). This parameter affects the coupling between cores, and in some times increasing in the core separation between two cores leads to the suppression of the coupling between cores. The design these structures; may be applicable in a wider range of applications in optical communication, e.g. as coupler, polarizer splitter.

1.1. Design methodology

The coupling in photonic crystal fibre (PCFs) can be modelled by two identical cores that are placed close to one another (coupling Mode). Energy transmission can occur between the two cores through the coupling in their evanescent fields [3, 12]. A two-core PCF structure, as shown in Fig. 1. The structural parameters are the hole pitch Λ=4 μm, hole diameter d=1.16 μm, the air-filling fraction is d/Λ=0.29, and core separation D=3 μm at the wavelength λ=1.55 μm, respectively. The refractive index of the core n_{co}=1.45 is slightly larger than the refractive index of the cladding n_{clad}=1.4, modelled for light guiding by total internal reflection mechanism (MTIR) between the core and the cladding region. Figure1, shows the PCF coupler obtained by means of COMSOL MULTIPHYSICS software based FEM with a perfectly matched layer (PML) as a boundary. FEM allows dividing the cross-section of two-core PCFs into finite small elements by using FEM triangular mesh generator tool and selecting the analysis study mode.

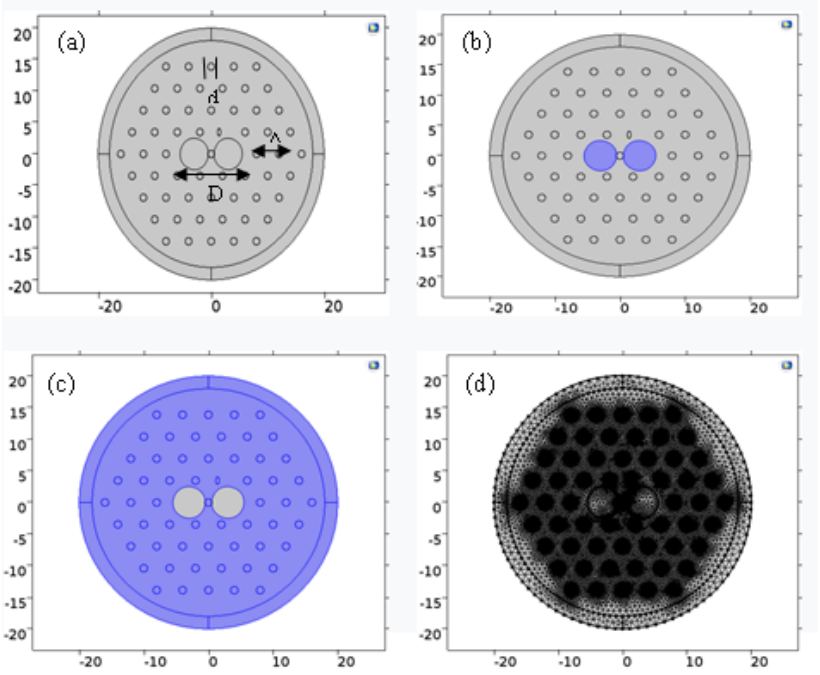

Fig. 1. Cross-section of two-core PCF coupler, the geometry of PCF design characterized by the structure parameters, such as the core diameter=5 µm, the hole pitch Λ=4 µm, hole diameter d=1.16 µm, the air-filling fraction d/Λ=0.29, and cores separation D=3 µm, at the wavelength λ=1.55 µm, respectively (a). Insert cladding material (b), Insert core material (c), triangular FEM mesh (d)

FEM is capable of performing supermode analysis of the two-core PCF and directly solve the Maxwell equations to obtain an approximate value of the effective refractive indexes, and subsequently to find the coupling length of two-core PCF [6, 7]. According to the supermode theory that depends on mode coupling, there are four modes with different propagation constants either two modes propagate with the same phase called even (symmetric) modes or two modes propagate with a different phase called odd (anti-symmetric) modes along x-and y-polarization fields [3, 9]. The coupling length (L_c) can be described as the single power is exchanged between two cores; as a result, the weak overlap of the adjacent electric field. A part of the light is confined into one core, then transfer to the other core after propagation distance called coupling length. As a result of the difference in propagation constants of even and odd modes and their refractive indexes are shown in equation (1). The coupling length is determined as bellow [3, 5, 8, 12]:

$$L_c = \frac{\pi}{\beta_{even} - \beta_{odd}} = \frac{\lambda}{2(n_{even} - n_{odd})} \tag{1}$$

The coupling length is affected mainly by the core diameter of the coupler, cores separation, and the wavelength [6]. The coupling coefficient relates to coupling length as in equation (2) follow below:

$$\kappa = \frac{\pi}{2L_c} \tag{2}$$

1.2. Simulation results and discussion

The numerical results show the coupling of two-core PCF at the wavelengths λ=1.55 μm and 1.31μm, as shown in figures 2, 3, 4, and 5 along the x-/y- polarized field. The effective mode indexes along the x-/y- polarized field are the same value for even and odd modes 1.4382 and 1.4375 and for the 1.55 μm. The effective mode indexes for even and odd modes also take the same value along the x-/y- polarized field for the wavelength 1.31μm are 1.4409 and 1.4406. Then, the difference in the effective refractive index for even and odd modes are 0.0007 and 0.0003, and coupling lengths are L_c =1,107 μm and 2166 μm for the wavelength 1.55μm and 1.31μm, respectively. Resulting, it is possible to design two-core or even multicore PCF coupler with the coupling lengths of (μm) much shorter than the traditional optical fiber couplers that are designed with the coupling lengths of (mm). Therefore, it is possible to achieve very short coupling lengths depending on the PCF's design, which could be useful for multiplexer-demultiplexer MUX-DEMUX applications in terms of short coupling lengths.

Difference between the effective refractive indexes of the even and odd modes along the x-/y- polarization field for PCF coupler is so small at the short wavelength, although this difference starts to increase at the long wavelength, as shown in figure.6 (a). Variation coupling length with wavelength for two-core PCF couplers for modes along x- /y- polarization field, as shown in figure.6 (b), this demonstrates that the coupling length decreases with an increase of the wavelength. At short wavelengths, the coupling length takes a large value at the short wavelengths and begins to pointedly decrease at the longer wavelengths, because the difference between the effective refractive index of the even and odd modes along x-/y- polarization field at the short wavelengths is lower than the longer wavelengths, and then this is relatively increased with increased the wavelength. The cause of the sudden decrease in the coupling length in the short wavelengths can be attributed to the material dispersion of silica glass, which plays an important role in evaluating the difference between the effective refractive index of the even and odd modes.

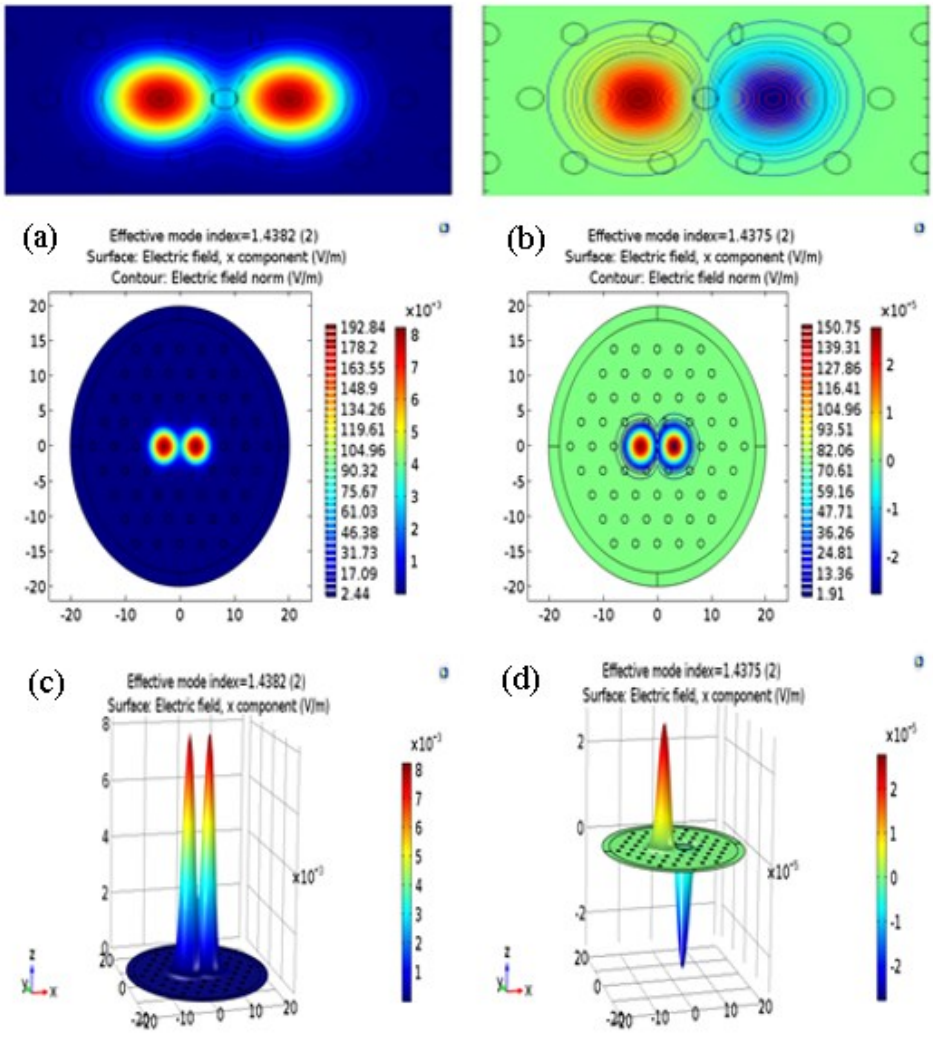

Fig. 2. A cross–section of two–core PCF represents the even supermodes in (a) and odd supermodes in (b) of the electric field distributions along the x-polarization field in (a and b). The field intensity represented in the contour scale of the electric field norm E of the boundary mode and Ex, respectively. The profile of the electric field for even and odd supermodes along the x-polarization field in (c and d) at wavelength 1. 55 µm

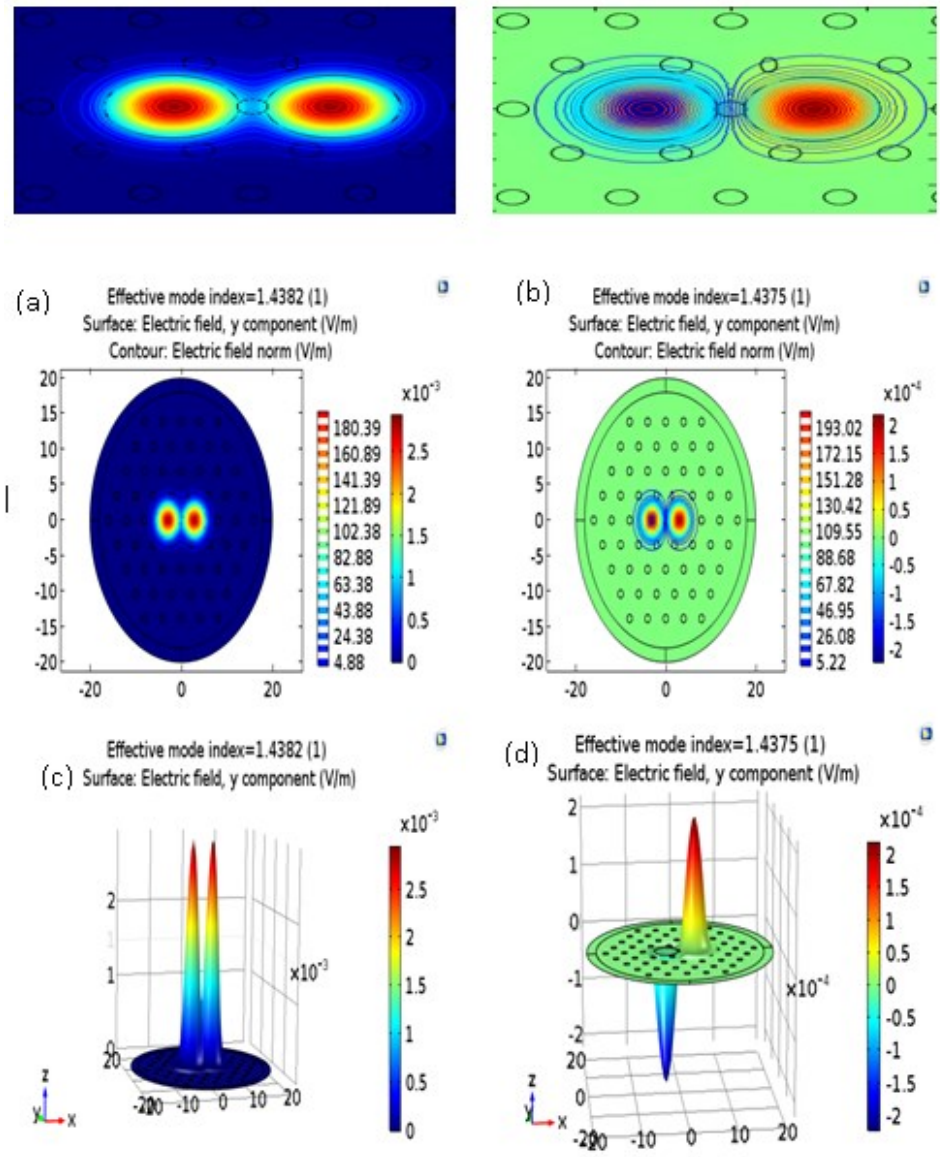

Fig. 3. A cross–section of two–core PCF represents the even supermodes in (a) and odd supermodes in (b) of the electric field distributions along the y-polarization field in (a and b). The field intensity represented in the contour scale of the electric field norm E of the boundary mode and Ey, respectively. The profile of the electric field for even and odd supermodes along the y-polarization field in (c and d) at wavelength 1. 55 µm

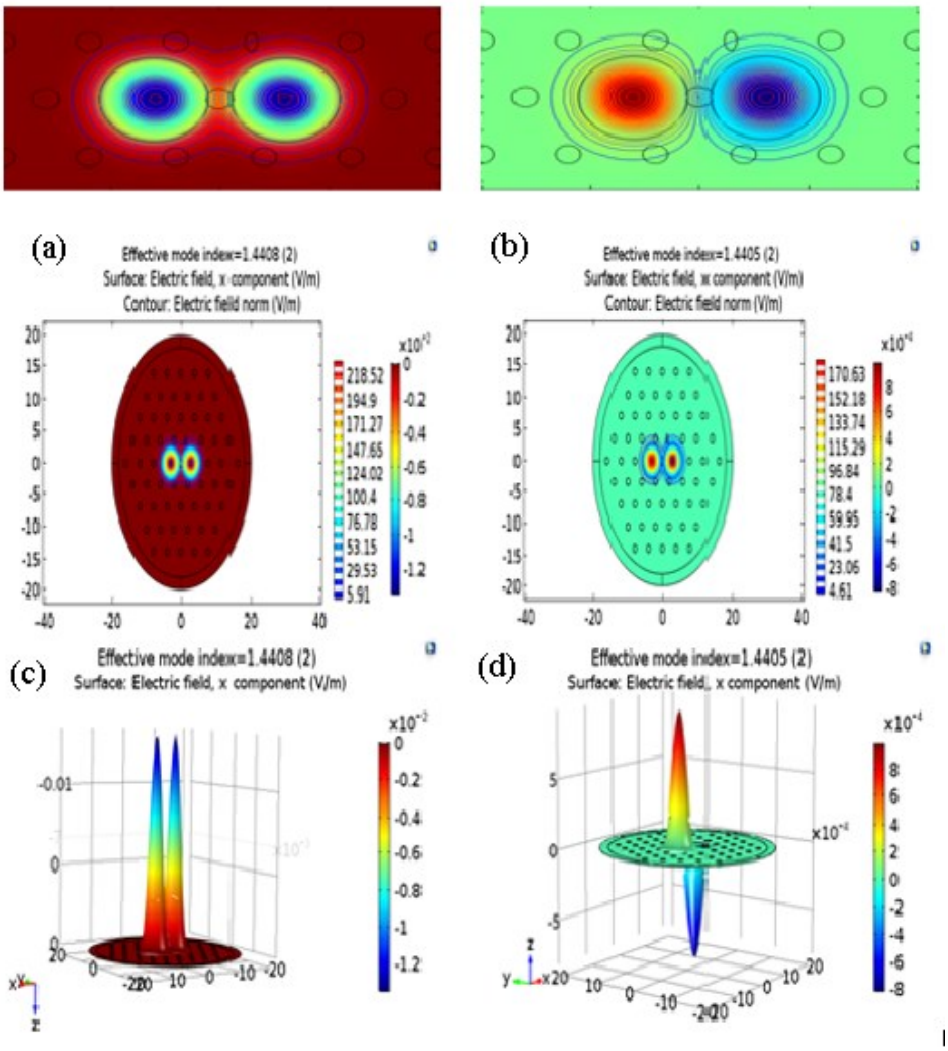

Fig. 4. A cross-section of two-core PCF represents the even supermodes in (a) and odd supermodes in (b) of the electric field distributions along the x-polarization field in (a and b). The field intensity represented in the contour scale of the electric field norm E of the boundary mode and Ex, respectively. The profile of the electric field for even and odd supermodes along the x-polarization field in (c and d) at wavelength 1. 31 µm

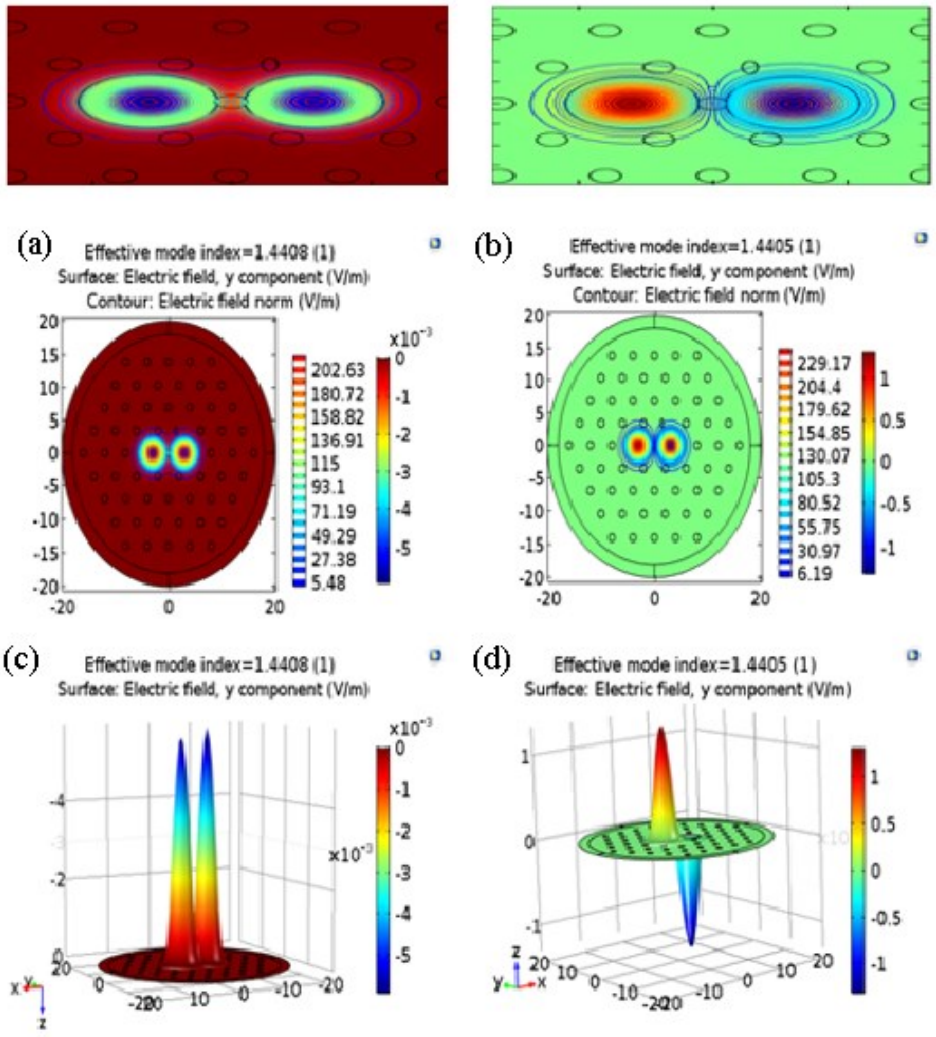

Fig. 5. A cross-section of two-core PCF represents the even supermodes in (a) and odd supermodes in (b) of the electric field distributions along the y-polarization field in (a and b). The field intensity represented in the contour scale of the electric field norm E of the boundary mode and Ey, respectively. The profile of the electric field for even and odd supermodes along the y-polarization field in (c and d) at wavelength 1. 31 µm

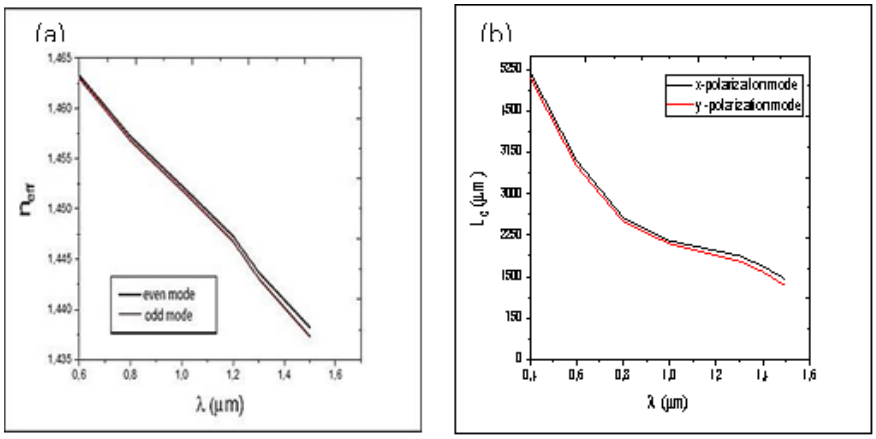

Fig. 6. Show the difference between the effective refractive indexes of the even and odd modes along the x-/ y polarization modes for PCF coupler with wavelength (a). Variation coupling length with wavelength for two-core PCF couplers for even mode along x-/ y-polarization field (b).

1.3. Effect of the geometrical parameters of the two-core PCF on the coupling length

In order to investigate the influences of the geometric structural parameters of two-core PCF on the coupling length. We simulated changes in the structural parameters of the PCF coupler, such as the hole diameter d, hole pitch Λ and, D the core separation between two-core PCF coupler. We wanted to see what the outcome would be if these parameters were changed; how can be the change in the effective refractive index n_{eff} then the change in the coupling length L_c occurs.

1.3.1. Effect of the change in hole diameter (d) of the two-core PCF

The numerical results, we found that the coupling length L_c increases as the hole diameter increases, as shown in figure 7. Resulting in a decrease in the difference between even and odd modes when the hole diameter increases, as shown in by increasing the hole diameter d, the core separation between cores of coupler PCF is decreased at fixed the value of (d/Λ).

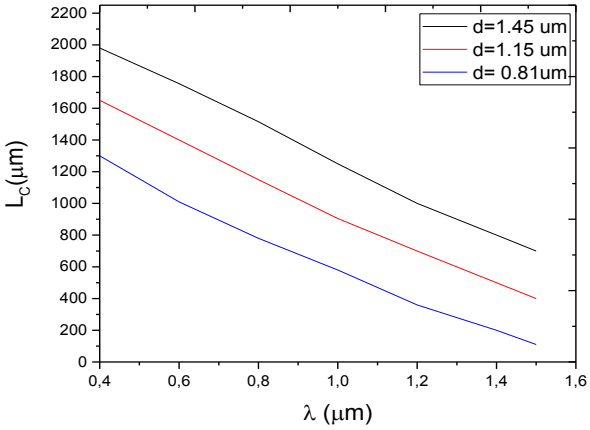

Fig 7. Variation coupling length with wavelength for different hole diameter and with hole pitch Λ =4.60 μm.

1.3.2. Effect of the change in hole pitch of the two-core PCF

The numerical results, we found that the coupling length L_c significantly decreases with an increase in hole diameter for different hole pitch (Λ), and this corresponds to an increase of the core radius. Design PCF coupler with a large hole diameter is more likely to decoupling because the mode is confined to one of the cores. Therefore, the coupling length decreases with the hole diameter increasing. On the other hand, the coupling length directly increases with increasing the hole pitch, and it takes a maximum value at hole pitch 5.60 μm. By reducing the hole pitch to 3.60 μm, we found the coupling length also decreases, as shown in figure 8.

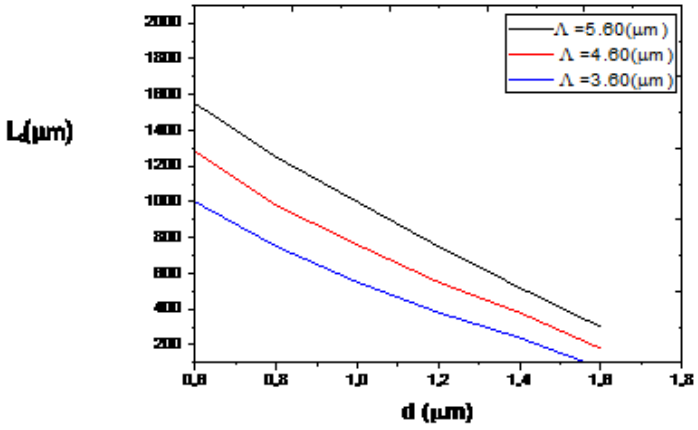

Fig. 8. Variation in the coupling length with the hole diameter d and with different hole pitch Λ =3.60 μm, 4.60 μm, 5.60 μm.

1.3.3. Effect of the change in air filling fraction of the two-core PCF

The numerical results, we found that the coupling length L_c increases with increasing of the hole pitch. Λ or with decreasing air–filling fraction d/Λ, as shown in figure 9, show that the coupling length becomes less than 1000 μm at increasing the value of air–filling fraction d/Λ to greater than 0.4 and the structure become multimode, while decrease the value of air–filling fraction d/Λ to less than 0.4 into the endlessly single-mode regime, a single-mode will be realized. Therefore, changes in d/Λ of two-core PCF appear coupling lengths extremely low, and the mode field area becomes larger.

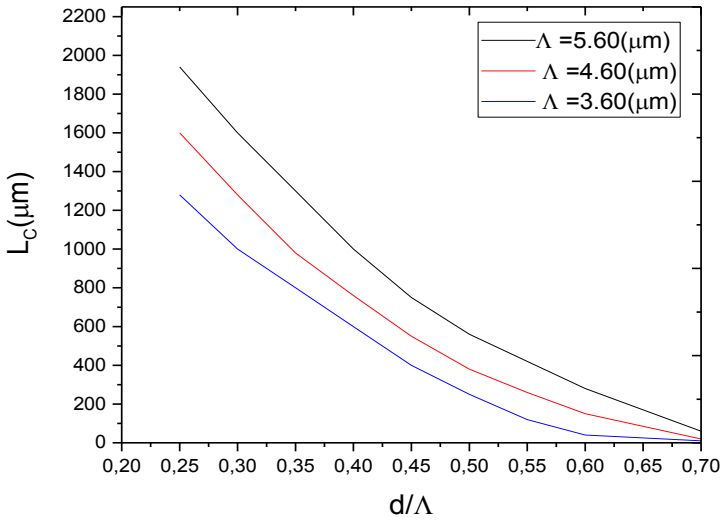

Fig. 9. Variation in the coupling length with the air–filling fraction d/Λ and with different hole pitch Λ =3.60 μm, 4.60 μm, 5.60 μm.

1.4. Effect of the core separation of the two-core PCF on the coupling length

We changed the core separation between the two cores of the PCF coupler with pitch Λ=4 μm and air–filling fraction d/Λ=0.29, in order to investigate the influence the core separation on the coupling strength between the cores and then on the coupling length, the simulation results were performed at a wavelength 1.55 μm, as shown in figure 10, shows that the coupling strength between the two-core PCF coupler is strong at small cores separation and reduce or suppression this strength at the large core separation. Therefore, the core separation is played an important role in determining the coupling strength between cores of PCF coupler, and then this effect on the coupling length. Increasing in the core separation between the cores of PCF coupler from 2 μm to 4.5 μm, We find from the results of the characteristics of coupling change with the change of cores separation, where the strength of the coupling is great between the two-core coupled at small

distances, such as 2 µm with a decrease in the length of the coupling, the coupling length is (203.94 µm). While the increase in the core separation such as 4.5 µm, 5 µm and 5.5 µm, we find the strength of coupling gradually decreases and the coupling length increased to (7750 µm), Increasing in the core separation to 5 µm and 5.5 µm leads to the coupling suppression the strength of coupling between the coupled cores of PCF as shown in figure 3, show how to vary the coupling length with different core separation from 2 µm to 5.5 µm at the wavelength 1.55 µm shown as in (j). These results give us possibly for designing coupling lengths short or large of two-core PCF coupler to the decrease or increase of the rate of data transmitted in close or in far distance telecommunication.

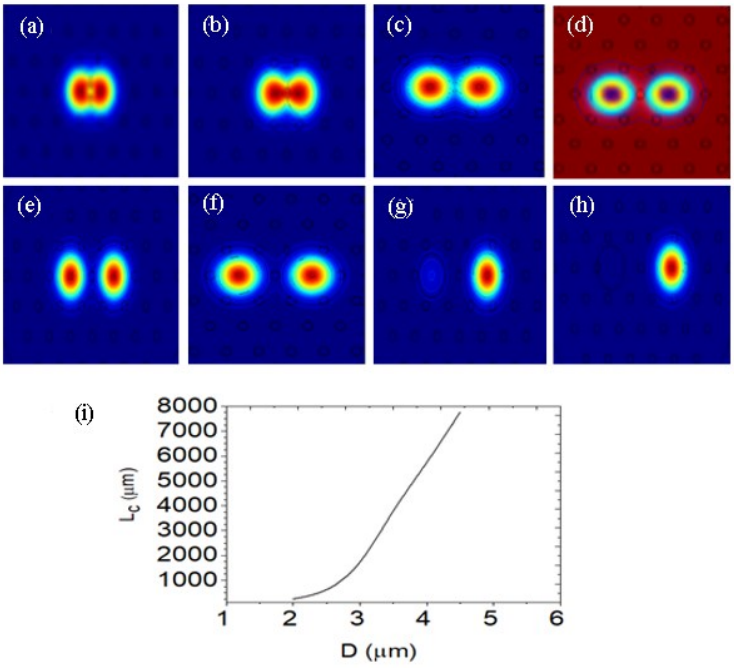

Fig. 10. Effect the core separation of two-core PCF on the coupling length, (a) the core separation D change to 2 µm (a), 2.5 µm (b), 3 µm (c), 3.5 µm (d), 4 µm (e), 4.5 µm (f), 5 µm (g), 5.5 µm (h). We find from the results of the characteristics of coupling change with the change of cores separation, where the strength of the coupling is great between the two-core coupled at small distances such as 2 µm with a decrease in the length of the coupling. While the increase in the core separation such as 5 or 5 µm and 5.5 µm. We find the strength of coupling gradually decreases until the coupling becomes suppression between the two-core coupled, in (j), variation in coupling length with different cores separation from 2µm to 5.5 µm at the wavelength 1.55 µm.

2. Conclusions

Coupling characteristics of a two-core PCF have been numerically analyzed with different designs using COMSOL MULTIPHYSICS software-FEM. The study aimed to show it is possible to design two-core PCF coupler with different wavelengths, such as 1.55μm and 1.31μm in order to realize short coupling lengths in (μm), such as 1,107 μm for the wavelength 1.55 μm and 2166 μm for the wavelength 1.55 μm are much shorter than the traditional optical fiber couplers that have designed with the coupling lengths in several tens of (mm). We also found from the numerical results that the coupling characteristics of two-core PCF coupler are effected by changing the geometrical parameters of PCF coupler, such as the hole diameter, hole pitch, air–filling fraction d/Λ, these characteristics of two-core or even multi-cores PCF coupler, have potential in several applications such as the multiplexer-demultiplexing for wavelength division mode system (WDM), coupler and polarized splitter. Increasing the core separation between two cores to a significant reduction in the coupling strength between the coupled cores leads to the coupling suppression between them. These results give us possibly for designing coupling lengths short or large of two-core PCF coupler to the decrease or increase of the rate of data transmitted in close or in far distance telecommunication.

Acknowledgments

This work was partially supported by the Republic of Iraq Ministry of High Education& Scientific Research scholarship (MoHESR Grant No. 16408). And also author acknowledges the University of Muenster-department of physics, Germany, to support.

References

[1] K. L. Reichenbach , C. Xu, „*Independent core propagation in two-core photonic crystal fibers resulting from structural nonuniformities*“, *J. Opt. Express*, vol. 13(25), 10336- 10348, 2005.

[2] P. S. Maji, P. R. Chaudhuri, "*Near-elliptic Core Triangular-lattice and Square-lattice PCFs: A Comparison of Birefringence, Cut-off and GVD Characteristics Towards Fiber Device Application", Journal of the Optical Society of Korea*, vol. (3), pp. 207–216, 2014.

[3] X. Yu, M. Liu, Y. Chung, M. Yan, P. Shum, "*Coupling coefficient of two-core microstructured optical fiber", Optics Communications*, 260, pp. 164–169, 2006. 2006.

[4] A. S. Dhakar, Y. K. Katiyar, "*Highly negative dispersion in honeycomb photonic crystal fiber of borosilicate material with circular", International Journal of Engineering, Management & Sciences IJEMS -1*, pp. 10336–10348, 2014.

[5] K. Saitoh, Y. Sato, M. Koshiba, *"Coupling characteristics of dual-core photonic crystal fiber couplers", J. Optics Express*, vol. 11(24), pp. 3188–3195, 2003.

[6] P. K. Rohini, A. S. Raja, D. S. Sunda, *"Modeling of twin core liquid filled photonic crystal fiber coupler with elliptical air holes", International Journal of Engineering, Management & Sciences IJARTET*, vol. II, pp. 2394–3785, 2015, http://www.ijartet.com.
[7] C. Guan, L. Yuan , J. Shi, *"Supermode analysis of multicore photonic crystal fibers", J. Optics Communications*, vol. 283(13), 2686-2689, 2010.
[8] K. R. Khan, X. Wu T, *"Finite element modeling of dual-core photonic crystal fiber" J. Applied Computational Electromagnetics Society ACES*, March 2008.
[9] H. He, L. Wang , *J. Optik*, vol. 142, pp. 5941–5944, 2013.
[10] H. Wang,, X. Yan, S. Li S, G. An, X. Zhang , J. Sensors, vol. 16, 1655, 2016.
[11] N. Mothe, P. D. Bin, *"Numerical analysis of directional coupling in dual-core microstructured optical fibers", J. Optics Express*, vol. 17, pp. 15778–15789, 2009.
[12] D. Mohammed, C. Mohammed, *"Coupling mode of dual-core micro structured fibers",* 2005, https://arxiv.org/abs/1504.02705.
[13] T. Uthayakumar,, R. V. Raja, K. Porsezian, P. Grelu, *"Analytical formulation of supermodes in multicore fibers with hexagonally distributed cores", J. IEEE Photonics* , 7, pp. 1–11, 2015.
[14] I. Veichev, Toulouse Inpro. *Conf. on Lasers and Electro-Optics* J. Opt. Soc. Am., 2004-CTuV1.
[15] T. Uthayakumar, R. V. J. Raja, K. Porsezian, P. Grelu, *"Impact of structural asymmetry on the efficiency of triple-core photonic crystal fiber for all-optical logic operation", Journal of the Optical Society of America B*, 32(9), pp. 1920–1929, 2015.
[16] M. Y. Chen, B. Sun,Y. K. Zhang, X. Fu X, *"Design of broadband polarization splitter based on partial coupling in square-lattice photonic-crystal fiber", J. Applied Optics,* vol. 49(16), pp. 3042–3048, 2010.
[17] K. Wen, J. Y. Wang , *J. Quant. Electro*., 25, pp. 505–508, 2008.
[18] M. Parto, M. Amen, Miri M-ALI, R. Amezcua, G. LI, D. N. Christodoulides, *J. Optics Letters*, 41, 1917-1920, 2016.
[19] L. Szostklewicz, M. Napierala, A. Ziolowicz, A. N. Pytel, T. Tenderenda, T. Nasilowski, *„Cross talk analysis in multicore optical fibers by supermode theory", J. Optics Letters*, 41(16), pp. 3759–3762, 2016.
[20] K. L. Reichenbach, C. Xu, *„Numerical analysis of light propagation in image fibers or coherent fiber bundles", J. Optics Express,* vol 15(5), pp. 2151–2165, 2007.

Tomasz Łusiak[1], Andrej Novak[2], Martin Bugaj[3]

NUMERICAL ANALYSIS AND EXPERIMENTAL STUDIES OF AIRCRAFT WING MODELS

Keywords: simulation analysis, wing, aerofoil, CFD

Abstract

The aim of the study could be achieved by analysing measurements taken on any aerofoil, but in order to increase its usefulness, the study was carried out on the wings of an existing model of a gyroplane. In this way, the results will not only be used to determine the characteristics of the aerospace profile itself, but also to compare the aerodynamic parameters of the wing with and without interference resistance. The tested profile is a flat-convex low speed profile. Trapezoidal contour wing with low elongation, because it comes from the model of a gyroplane, It is therefore an additional element in the process of generating the load-bearing capacity. The wing has no elevation but is characterized by a slight aerodynamic dislocation.

1. Introduction

Aerodynamic testing of an aerofoil is a very complex process, consisting of several stages. On each of them, there may appear errors that will more or less disrupt the obtained results [1]. These errors may result from test methodology, model making technology, measurement errors or ordinary human errors [20]. On the basis of the experience gained during the above mentioned tests, it can be concluded that their accuracy is affected by:

- 3D printing technology,
- care during the machining of the model,
- selection of sizes of the tested model for the wind tunnel being at your disposal,
- selection of mounting to the model dimensions; stiffness is very important, but also alignment of the holder, e.g. perpendicular to the base of the model,
- accuracy of the position of the model in the tunnel at zero angle of attack,
- precise setting of the desired flow velocities and meticulous recording of the displayed values,

[1] Polish Air Force University, Faculty of Aviation, 35 Dywizjonu 303 Str., 08-521 Dęblin, Poland, t.lusiak@law.mil.pl
[2] University of Zilina, Department of Air Transport, Univerzitná 8215/1, 010 26 Žilina, Slovakia, andrej.novak@fpedas.uniza.sk
[3] University of Zilina, Department of Air Transport, Univerzitná 8215/1, 010 26 Žilina, Slovakia, martin.bugaj@fpedas.uniza.sk

- carefulness in all calculations, checking that the formulae entered in the formulae and values are right and in place,
- proper configuration of all settings in the flow simulation program, including the chosen test accuracy [2].

The aim of conducted tests is to verify to what extent measurements of wind parameters of an object carried out in a wind tunnel and using a computer simulation, namely the SolidWorks module: Flow Simulation, differ from each other. In order to obtain reliable results, models used for experiments must have the same shape and roughness of the surface, which in combination with the same flow velocity will allow to maintain a similar Reynolds number [3]. The conditions of the test medium are also important. Since any values can be set in the computer simulation, they will be adjusted to those of the wind tunnel test:

- air temperature: 26˚C (299.15 K),
- air pressure: 1012 hPa,
- air density: 1,178512 kg/m^2.

The flow analysis was carried out in the range of angles of attack from -6 to 23 degrees. The research was carried out on two models reduced by four times and five times compared to the original dimensions of the wing [4]. The need to make a model reduced five times appeared during the examination of a larger model, because its size and weight and the way it was mounted in the tunnel did not guarantee the stability of the model, which was visible at higher flow velocities and angles of attack (vibrations and oscillations of the model) [5]. This could have affected the measured values of the forces and prevented them from being measured within the assumed range of attack angles (the mount could not hold the model in its base). These problems were eliminated during the examination of a smaller model. The paper will also compare the results of both models, which will allow us to determine the impact of selecting a model for the wind tunnel that is available [6].

2. Methodology

The numerical profile tests were carried out using the SolidWorks Flow Simulation module [8]. Before the flow simulation can be started, a number of important data must be entered and the test scenario properly configured and prepared (figure 1). The basis is to select the type of flow (internal, internal, and external). In the case of the study of aerofoils, this will have an external impact [7]. Software makes it possible to enter data concerning heat conduction, radiation or the influence of gravity.

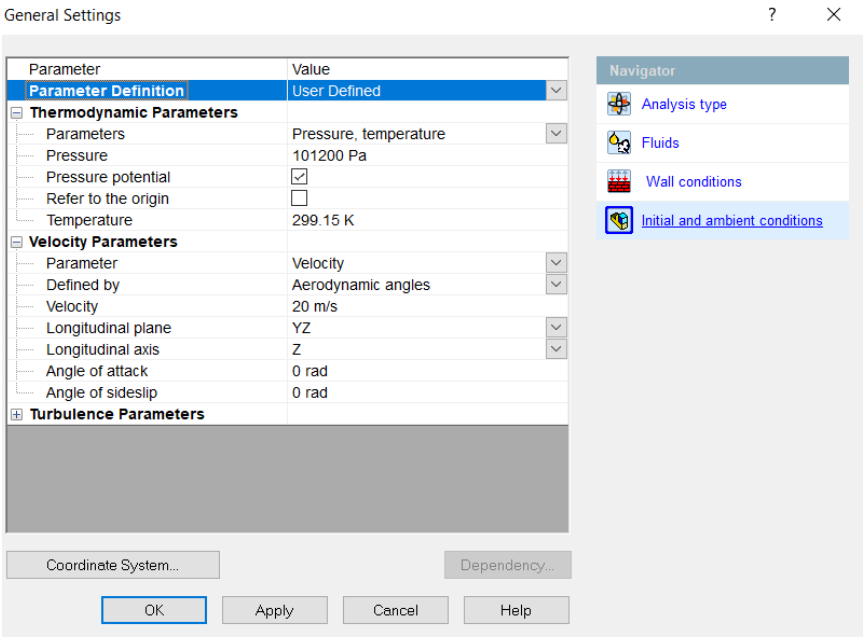

Fig. 1. Panel for basic settings of the test to be carried out

Next, the type of gas or liquid flowing around the model is selected from the program database (in this case it is, of course, atmospheric air). The surface roughness setting also influences the test results [10]. No precise roughness measurements were made on the models, but on the basis of typical values obtained during finishing its value was determined to be about 0.5 micrometre; thus, such a value was introduced into the project. The final step in the basic settings was to determine the initial conditions [9]. These include, for example, thermodynamic parameters (pressure, density, air temperature), flow parameters (velocity, angle of attack, angle of attack, plane and longitudinal axis) or turbulence parameters.

3. Research object

Next step was to determine the so-called computing space around the tested model, within which the calculations will be performed (Fig. 2). Too large area will result in increased time needed to calculate the results, too narrow may not allow for a thorough examination of all phenomena or will reduce accuracy and credibility of the results obtained [12]. The program should specify the values of which parameters we want to know and whether these values are to be global or concern, for example, a specific point, a specific area or whether they are to be calculated from the introduced equation [11]. Options include static, dynamic or total pressure, flow velocity and forces generated in a given axis (minimum,

average or maximum values of these parameters), liquid temperature and density, turbulence data or force moments.

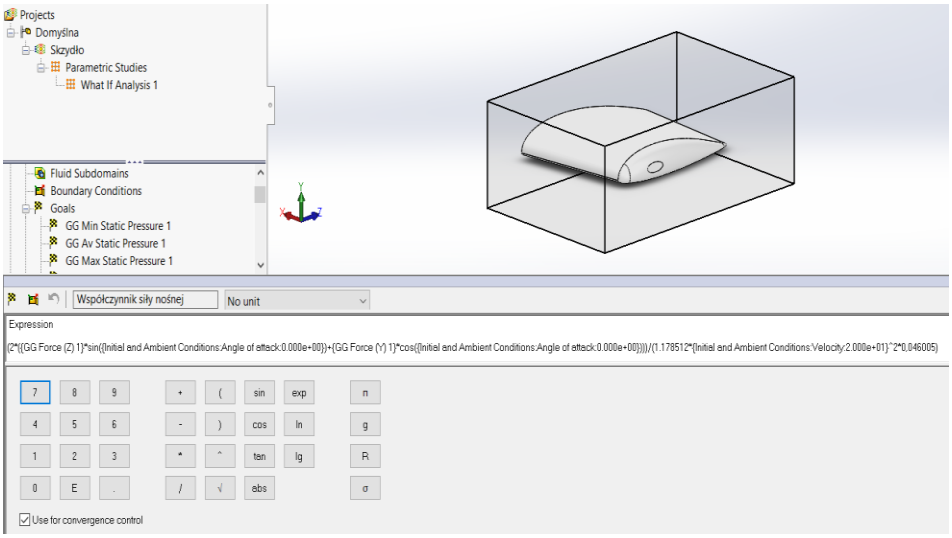

Fig. 2. Entrance to a calculation task. Visible defined calculation

Among many options in this project, it is necessary to know values of forces in Y and Z axes corresponding to the bearing forces (lift, drag), which will be necessary to introduce into the equations used to calculate the Cz and Cx coefficients (figure 2). Transformation of the formulae for the load-bearing forces has given the formula for the coefficients of these forces:

$$C_{z(x)} = \frac{2F_{z(x)}}{\rho V^2 S} \quad \text{(X.Y)}$$

Forces will be calculated by software; the density value has been entered based on the temperature and air pressure values as follows $\rho = \frac{p}{RT}$ (where R is an individual gas constant of 287,5 J/kgK for dry air), the flow velocity is set, and the surface is manually entered on the basis of model measurement [13]. Since the angle of attack will vary with respect to the coordinate axes, it is necessary to introduce trigonometric relationships into the formula, which will give values of forces in correlation to the direction of the incoming air stream. Ultimately, the formula for lift and drag coefficients will take the following form:

$$C_z = \frac{2(F_z cos\alpha + F_x sin\alpha)}{\rho V^2 S} \qquad C_x = \frac{2(F_z sin\alpha + F_x cos\alpha)}{\rho V^2 S} \quad (1.1)$$

A very important element, when performing computer simulations of streams, is the definition of the so-called Mesh grid (figure 3). It discredits the surface of the tested model using the finite element method (a surface system approximating the

original shape is created), which allows to carry out simulations and calculations [14]. Of course, the denser the grid, the more accurate results should be obtained, but this may significantly extend duration of calculation.

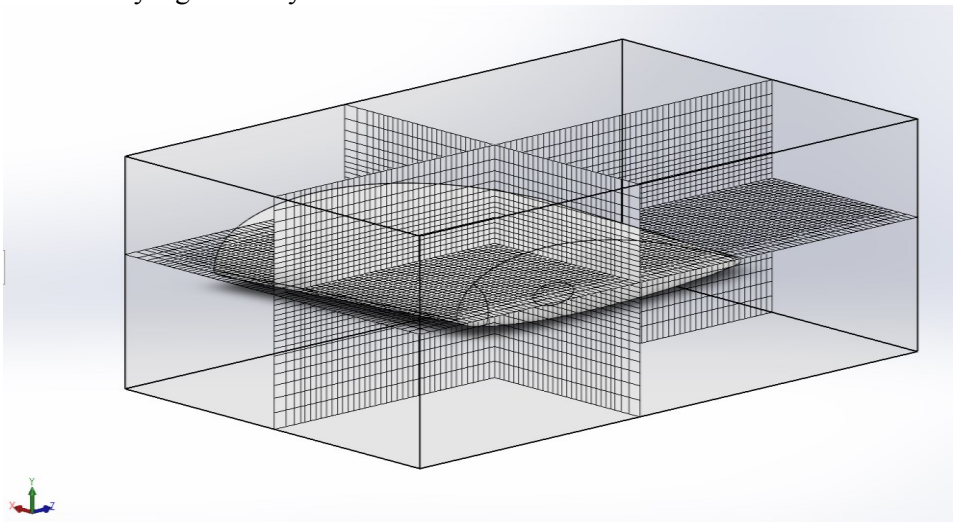

Fig. 3. Model after discretisation

4. Testing a wing model in a wind tunnel

The tests were carried out on the HM 170 Open wind tunnel test stand of G.U.N.T. Hamburg (figure 4). The tested object was placed in a working chamber on a rod connected at the base with an electronic sensor measuring two components of acting forces [15]. Data on forces, flow velocity, moments, angle of attack or pressure distribution can be collected and analysed on a PC.

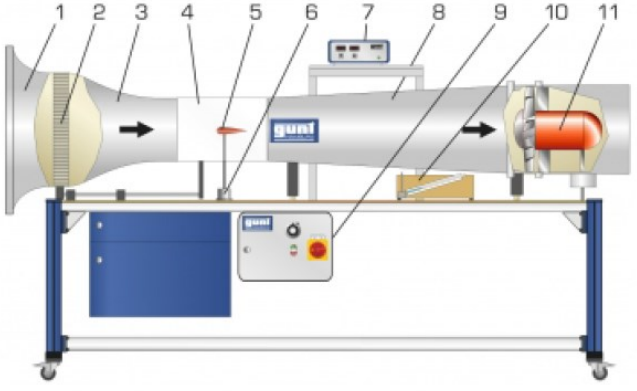

Fig. 4. Structure diagram HM 170. 1) inlet; 2) flow regulator; 3) nozzle; 4) measuring section; 5) tested object; 6) force meter; 7) display; 8) diffuser; 9) switch box; 10) pressure gauge; 11) axial fan

The Wind Tunnel technical data:

- dimensions of the measuring section: (W/H) 292x292x420mm;
- flow velocity: 3.1-28m/s;
- power consumption: 2,2kW;
- range of force measurement: ±18N;
- attack angle: ±180˚.

The model prepared for the test was of sufficient size in comparison to the fastening rod and its diameter, so the test began with the proper preparation of the fastening of the model. The aerofoil was prepared to allow the bar to be inserted throughout the entire wingspan. In addition, the part of the rod attaching the model to the tunnel seat was reinforced with an aluminium sleeve, which significantly increased rigidity and stability of the entire installation [16]. After the model was mounted in the working part of the tunnel, the zero rake angle was set and the force meter was calibrated, tests could have been started. With a use of the flow regulator, speed of the flowing air was increased, which was indicated by the manometer [18].

When the target value was reached, aerodynamics forces were read and written down. The attack angle was then adjusted by means of a graduated scale placed at the base of the model on the load cell (figure 5). In this way, force values for the intended rake angles were measured consistently. The procedure for other air velocities was analogous.

Fig. 5. The model is mounted in a workstation. Platform with a scale of attack angles and a device for reading the values of generated bearing and resistance forces

5. Result of research

The numerical analyses cover complex issues of correlation between particular groups of analyses [17]. Flow Simulation allows to use many options for measuring and visualising the above mentioned parameters, such as gradient representation of pressure values in a given cross-section or on a given surface or animation of the trajectory of the flow of particles around an object (figure 6), but their use is not necessary in this work.

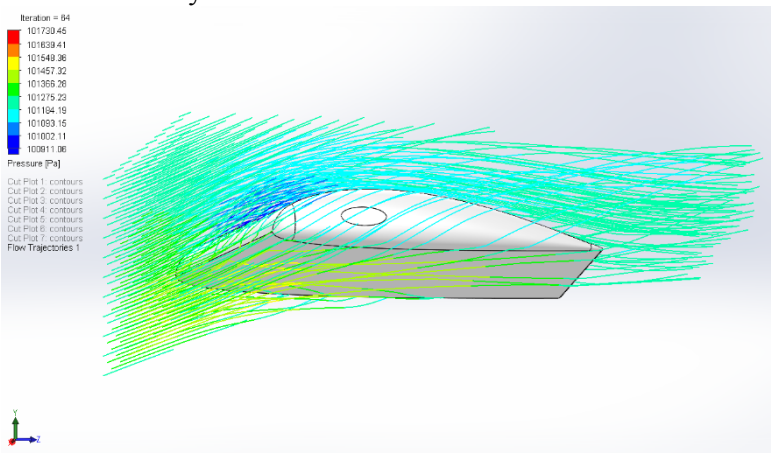

Fig. 6. Visualisation of particle trajectory around the model with gradient pressure distribution

The easiest way to carry out the intended research is to create a parametric study with a specific test scenario in Flow Simulation, which determines the range of changes in the angle of attack and velocity of flow [19]. Obtained results are exported to Excel file, where they can be processed and analysed.

Tab. 1. Values of forces and coefficients obtained during the test of a larger wind tunnel model for individual approach angles and flow velocities

α	15m/s				18m/s				20m/s			
	Fz	Fx	Cz	Cx	Fz	Fx	Cz	Cx	Fz	Fx	Cz	Cx
-6	-0,49	0,3	-0,080	0,049								
-4	0,08	0,2	0,013	0,033	-0,23	0,29	-0,026	0,033	0,1	0,38	0,009	0,035
-2	0,28	0,19	0,046	0,031	0,38	0,27	0,043	0,031	0,81	0,41	0,075	0,038
0	0,62	0,2	0,102	0,033	0,81	0,28	0,092	0,032	1,16	0,33	0,107	0,030
2	0,97	0,22	0,159	0,036	1,41	0,32	0,161	0,036	1,69	0,37	0,156	0,034
4	1,4	0,27	0,230	0,044	2,05	0,38	0,233	0,043	2,48	0,44	0,229	0,041
6	1,9	0,35	0,312	0,057	2,79	0,5	0,318	0,057	3,48	0,61	0,321	0,056
8	2,37	0,45	0,389	0,074	3,6	0,67	0,410	0,076	4,42	0,82	0,408	0,076

10	2,8	0,57	0,459	0,093	4,34	0,87	0,494	0,099	5,27	1,04	0,486	0,096
12	3,37	0,72	0,553	0,118	5,22	1,15	0,594	0,131	6,17	1,33	0,569	0,123
14	3,86	0,9	0,633	0,148	5,87	1,38	0,668	0,157	7,22	1,68	0,666	0,155
16	4,39	1,1	0,720	0,180	6,67	1,68	0,759	0,191	7,84	2,7	0,723	0,249
18	4,95	1,36	0,812	0,223	7,55	2,07	0,860	0,236	7,33	2,55	0,676	0,235
19	5,53	1,62	0,907	0,266	7,83	2,27	0,891	0,258				
20	5,56	1,63	0,912	0,267	7,61	2,45	0,866	0,279				
21	5,77	1,76	0,946	0,289	7,4	2,54	0,843	0,289				
22	6,02	1,9	0,987	0,312	7,2	2,65	0,820	0,302				
23	6,26	2,02	1,026	0,331								

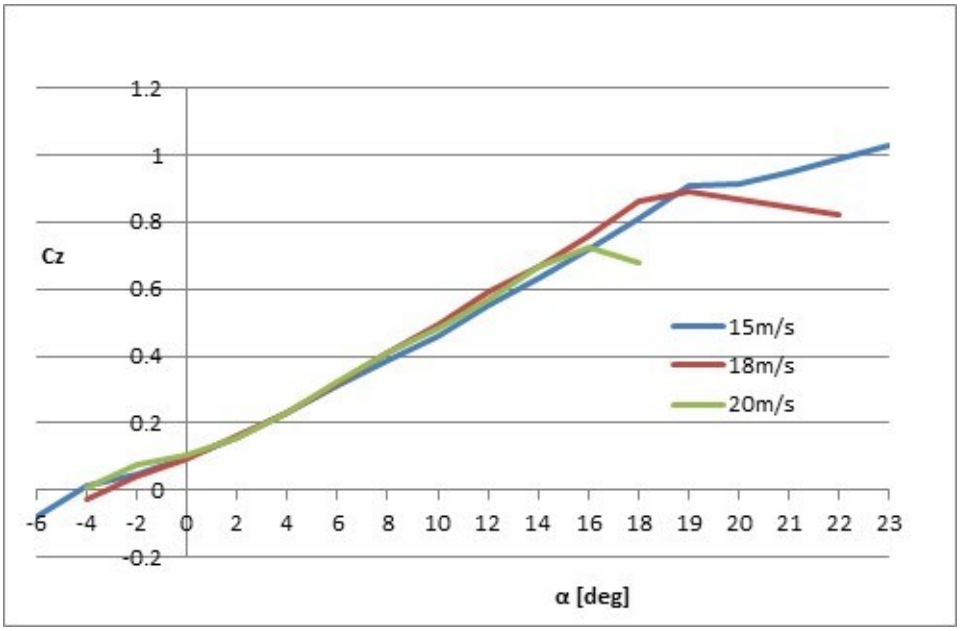

Fig. 7. Coefficient of bearing force as a function of the angle of attack for individual flow velocities

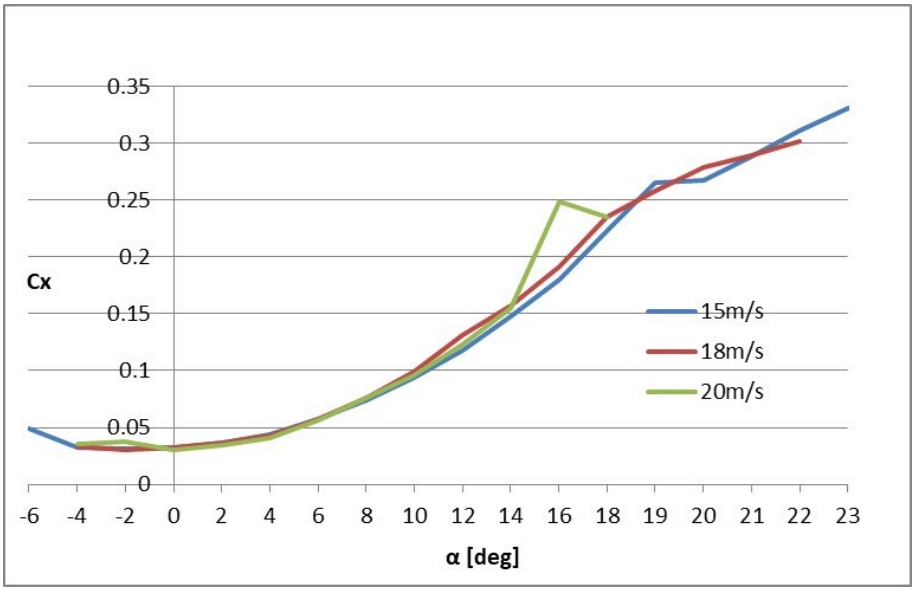

Fig. 8. Resistance force coefficient as a function of the angle of attack for individual flow velocities

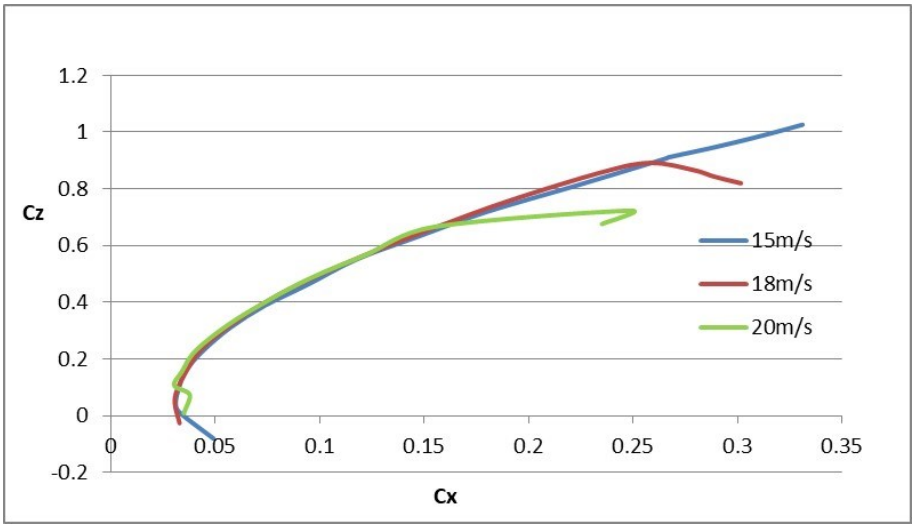

Fig. 9. Polar profile for individual flow velocities

The courses in figure 7, for the angle of attack to about 14 degrees were overlapping but then had started to show bigger differences, caused probably by the mentioned vibrations, bending of the mount and turbulent airflow. It is also possible to notice a decrease in the value of Cz above the angle of 16° at the speed of 20 m/s and above 19° for 18 m/s, which indicates that the critical angle has

been reached. The second diagram also shows similar waveforms with no major differences in the values of across the entire range of attack angles. The exception is a flow rate of 20 m/s for an angle of 16° and 18°, because the value of the resistance force coefficient should not decrease with the increase of the angle of attack [8]. This situation is probably the result of the model's oscillation under the influence of large forces acting on it. The third diagram confirms the significant influence of vibrations on the character of the waveforms. While for lower speeds the characteristics overlap, for V=20m/s they start to very early.

Tab. 2. Flow Simulation model test force and coefficient values for individual rake angles and flow velocities

α	15m/s				18m/s				20m/s			
	Fz	Fx	Cz	Cx	Fz	Fx	Cz	Cx	Fz	Fx	Cz	Cx
-6	0,30	0,38	0,043	0,057	-0,03	0,37	-0,008	0,042	-0,02	0,45	-0,006	0,041
-4	0,41	0,33	0,063	0,049	0,33	0,35	0,035	0,037	0,40	0,42	0,034	0,036
-2	0,56	0,27	0,090	0,041	0,66	0,33	0,073	0,035	0,81	0,40	0,073	0,035
0	0,55	0,20	0,090	0,032	0,78	0,28	0,089	0,031	0,95	0,34	0,087	0,031
2	0,82	0,21	0,136	0,039	1,18	0,28	0,135	0,037	1,46	0,35	0,136	0,037
4	1,20	0,22	0,198	0,050	1,61	0,27	0,185	0,043	2,00	0,33	0,186	0,043
6	1,50	0,18	0,248	0,054	2,10	0,25	0,241	0,053	2,60	0,30	0,242	0,053
8	1,82	0,15	0,299	0,066	2,68	0,22	0,305	0,067	3,31	0,27	0,306	0,067
10	2,49	0,14	0,406	0,093	3,11	0,21	0,353	0,085	4,14	0,22	0,379	0,086
12	2,93	0,10	0,473	0,116	4,06	0,15	0,456	0,113	4,94	0,18	0,449	0,111
14	3,38	0,06	0,540	0,144	4,71	0,06	0,522	0,137	5,55	0,19	0,501	0,141
16	3,87	0,00	0,610	0,176	5,23	0,04	0,574	0,169	6,53	0,08	0,581	0,173
18	4,61	-0,08	0,715	0,222	6,09	0,11	0,664	0,226	7,36	0,22	0,652	0,229
19	4,89	-0,09	0,754	0,247	6,41	0,09	0,693	0,247	8,83	-0,32	0,760	0,237
20	5,11	-0,14	0,780	0,266	7,17	-0,11	0,762	0,267	9,40	-0,39	0,802	0,263
21	5,23	-0,09	0,795	0,293	7,50	-0,06	0,795	0,300	9,97	-0,41	0,845	0,294
22	5,16	-0,06	0,781	0,307	7,66	0,03	0,810	0,330	10,53	-0,48	0,884	0,323
23	6,27	-0,24	0,931	0,366	8,55	-0,22	0,886	0,357	11,05	-0,41	0,924	0,364

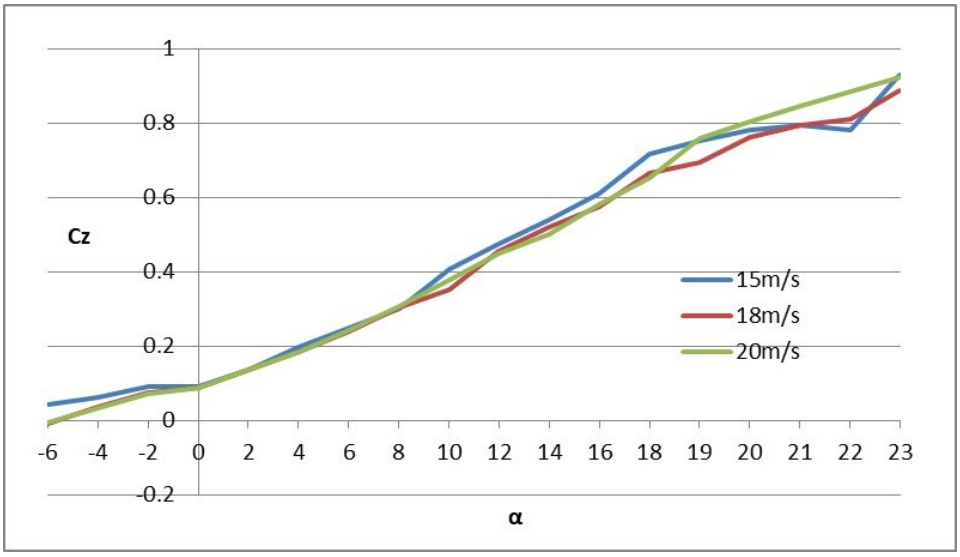

Fig. 10. Coefficient of bearing force as a function of the angle of attack for individual flow velocities

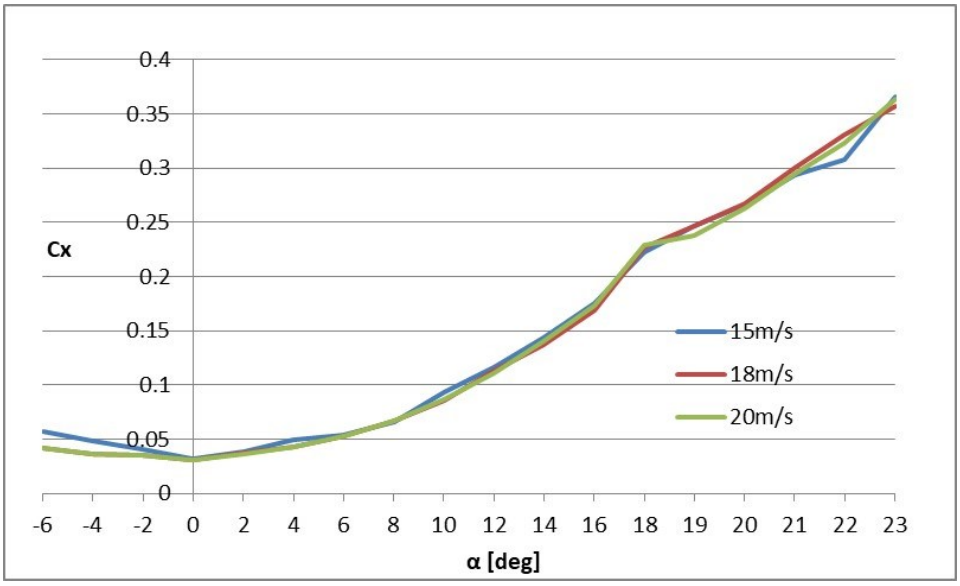

Fig. 11. Resistance force coefficient as a function of the angle of attack for individual flow velocities

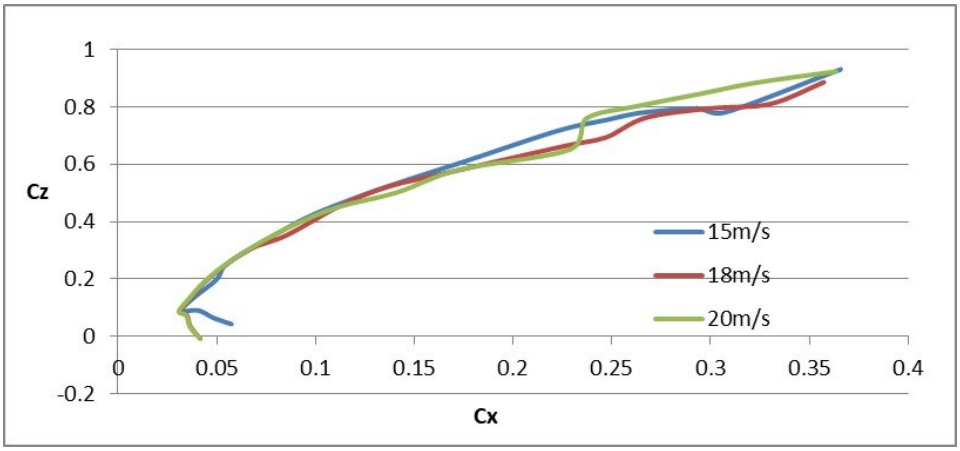

Fig. 12. Polar profile for individual flow velocities

Analysing figures 10, 11 and 12, a very good coverage of all the runs can be observed, especially at small angles of attack and on the second one. The computer simulation eliminated imperfections of the actual mounting, which makes characteristics more similar to each other, as it should theoretically be. Of course, there are differences around the angle of 18–19°, which are more pronounced in the Cz(α) graph, but this is more likely to be a result of the turbulent stream that is defined and included in Flow Simulation, and errors caused by the low density of the Mesh grid.

6. Conclusions

Aerofoil aerodynamic testing is a very complex process, consisting of several stages. On each of them there may appear errors that will more or less disrupt the obtained results. These errors may result from test methodology, model making technology, measurement errors or ordinary human errors. On the basis of the experience gained in carrying out the above mentioned tests, it can be concluded that their accuracy is affected by:

- 3D printing technology,
- care during the machining of the model,
- selection of sizes of the tested model for the wind tunnel being at your disposal,
- selection of mounting to the model dimensions; stiffness is very important, but also alignment of the holder, e.g. perpendicular to the base of the model,
- accuracy of the position of the model in the tunnel so that the zero angle of attack is actually a zero angle of attack,

- precise setting of the desired flow velocities and meticulous recording of the displayed values,
- carefulness in all calculations, checking that the formulae entered in the formulae and values are right and in place,
- proper configuration of all settings in the flow simulation program, including the chosen test accuracy.

Comparison of model wind tunnel and Flow Simulation test results show figure 13, figure 14 and figure 15 combine characteristics for different test methods.

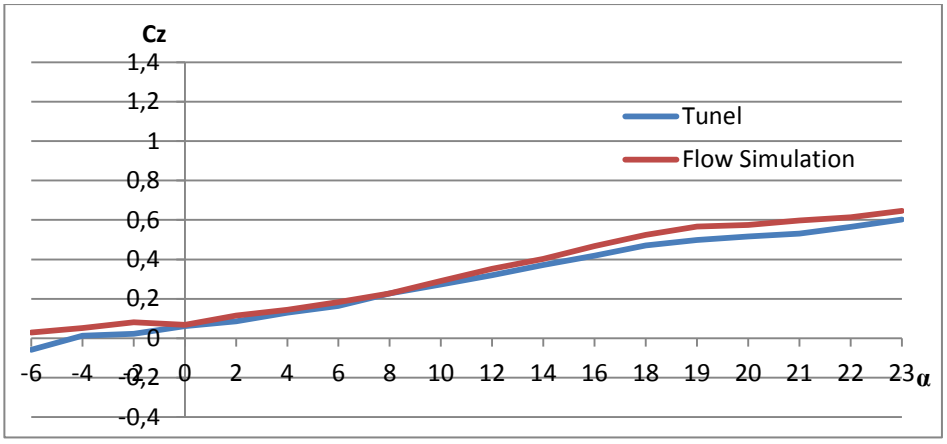

Fig. 13. Coefficient of bearing force as a function of the angle of attack (Wind tunnel, Flow Simulation)

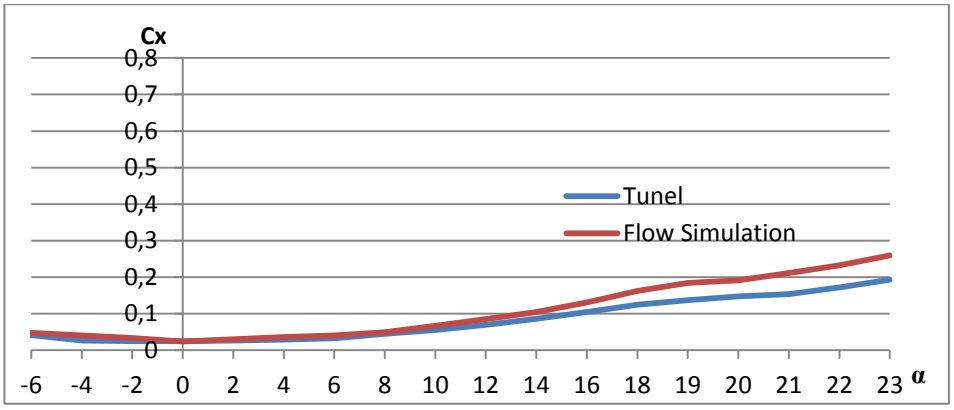

Fig. 14. Resistance force coefficient as a function of the angle of attack (Wind tunnel, Flow Simulation)

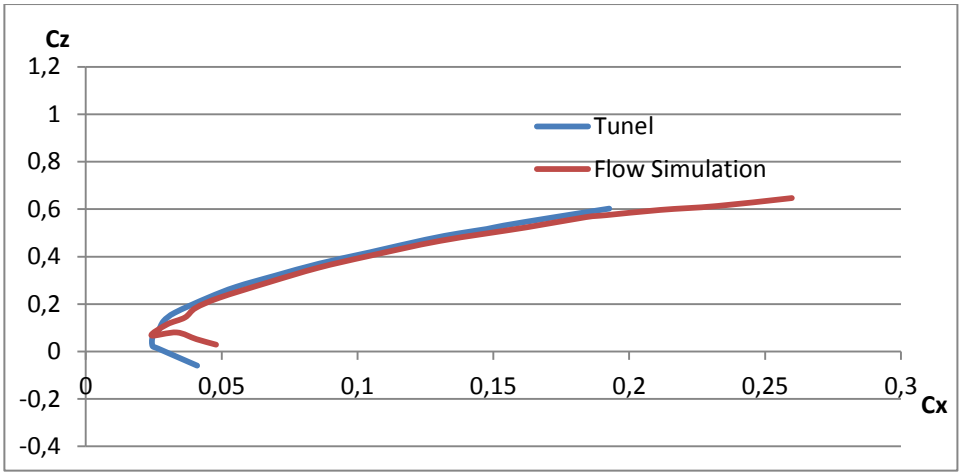

Fig. 15. Polar profile for individual flow velocities (Wind tunnel, Flow Simulation)

Verification of the obtained results allows to conclude that the computer-generated data are repeatable, because the similar course and error rate were characterised by the characteristics of a larger model. Generally, the diagrams overlap, but on chart 19 for flow velocity of 15 m/s between 16th and 19th degree of the angle of attack, a calculation error appeared apparently. It can therefore already be concluded that more trust and reliability should be placed in the results obtained in the wind tunnel. All characteristics show only minor deviations between wind tunnel and Flow Simulation results.

At an approach angle of 23°, the difference between the drag coefficient and all flow velocities is approximately 0.05. It is therefore difficult to determine which method of testing introduces distortion in Cx values. The wind tunnel test did not observe that the mounting rod rested against the working chamber casing, which could reduce the measured drag. In addition, if this were the case, the difference in Cx should be greater for higher flow velocities, but the opposite is observed. The influence of various types of turbulence would also intensify when the flow velocity is increased. Perhaps, roughness of the surface of the model differs from the one introduced into the simulation and the effect of this effect is more visible during the measurement of the drag than the lift force.

Acknowledgements

This work has been financed by the Polish National Centre for Research and Development under the POIR program. Grant Agreement No. POIR.01.01.01-00-0827/15-00.

References

[1] M. Brzeziński, "Production organization and control", *Design of production systems and production control process (in Polish).* Warszawa: Placet, 2002.

[2] M. Brzostek, "*Drukowanie 3D w praktyce", Juni* 9, 2018, www.pclab.pl.

[3] A. Clough, M. Ainley, S. Hunt, "Preliminary Impact Assessment on the Safety of Communications for Unmanned Aircraft Systems", 2009, retrieved from https://www.easa.europa.eu.

[4] Z. Czyż, T. Łusiak, P. Karpiński, J. Czarnigowski, "Numerical investigation of the gyroplane longitudinal static stability for the selected stabilizer angles", *Journal of Physics: Conference Series*, vol. 1101(1). 2018, https://doi.org/10.1088/1742-6596/1101/1/012003.

[5] Z. Czyż, K. Siadkowska, R. Sochaczewski, "CFD Analysis of Charge Exchange in an Aircraft Opposed-Piston Diesel Engine. *MATEC Web of Conferences*, vol. 252, 04002, 2019, https://doi.org/10.1051/matecconf/201925204002.

[6] G.U.N.T. Gerätebau GmbH, *HM 170 Open wind tunnel. July* 16, 2018 https://www.gunt.de/images/datasheet/769/HM-170-Open-wind-tunnel-gunt-769-pdf_1_en-GB.pdf.

[7] S. Holoda, P. Pecho, M. Janovec, M. Bugaj, "Modification in Structural Design of L-13 "blanik" Aircraft's Wing to Obtain Airworthiness", *Procedia Engineering,* vol. 192, 2017, pp. 330–335, DOI: 10.1016/j.proeng.2017.06.057

[8] A. Krzysiak, "Tunnel corrections to the results of profile model tests in wind tunnels", Warszawa: Instytut Lotnictwa, 2016.

[9] J. H. S. Fincham, M. I. Friswell, M. I., "Aerodynamic optimisation of a camber morphing aerofoil", *Aerospace Science and Technology*, vol. 43, pp. 245–255, 2015, https://doi.org/10.1016/j.ast.2015.02.023.

[10] G. D. Goh, S. Agarwala, G. L. Goh, V. Dikshit, S. L. Sing, W. Y. Yeong, "Additive manufacturing in unmanned aerial vehicles (UAVs): Challenges and potential", *Aerospace Science and Technology*, vol. 63, pp. 140–151, 2017, https://doi.org/10.1016/j.ast.2016.12.019.

[11] M. Greaves, F. Elasha, J. Worskett, D. Mba, H. Rashid, R. Keong, "Vibration Health or Alternative Monitoring Technologies for Helicopters", 2012, retrieved from https://www.easa.europa.eu.

[12] D. Joshi, "Commercial Unmanned Aerial Vehicle (UAV). Market Analysis – Industry trends, companies and what you should know", *Business Insider*, 2017, retrieved from http://www.businessinsider.com/commercial-uav-market-analysis-2017-8.

[13] M. Mazur, J. McMillan, "Global Market for Commercial Applications of Drone Technology Valued at over $127 bn", 2016, retrieved from https://press.pwc.com.

[14] D. Mba, S. Place, H. Rashid, R. Keong, "Research Project EASA.2011/5 HELMGOP - Helicopter main gearbox loss of oil performance optimisation", 2012, retrieved from https://www.easa.europa.eu.

[15] R. Morek, "CAx – introduction", Juni 9, 2018, http://procestechnologiczny. com.pl/cax -wprowadzenie.

[16] P. Sarkar, R. Raczynski, (2017). Recent Progress in Flow Control for Practical Flows. In P. Doerffer, G. N. Barakos, & M. M. Luczak (Eds.), Springer, pp. 126–135, https://doi.org/10.1007/978-3-319-50568-8.
[17] Skrzypietz, B. T. (2012). Unmanned Aircraft Systems for Civilian Missions. *Brandenburg Institute for Cociety and Security Policy Paper*, (1), pp. 1–28. Retrieved from http://www.bigs-potsdam.org.
[18] Skultety, F., Badanik, B., Bartos, M., Kandera, B. (2018). Design of Controllable Unmanned Rescue Parachute Wing Transportation Research Procedia, vol. 35, 2018, pp. 220–229, DOI: 10.1016/j.trpro.2018.12.026.
[19] Sedlackova, A.N., Kurdel, P., Mrekaj, B. (2017). Synthesis criterion of ergatic base complex with focus on its reliability, INFORMATICS 2017 , vol. 2018-January, 27 March 2018, pp. 318–321, DOI: 10.1109/INFORMATICS.2017.8327267.
[20] Zheng, W., Yan, J., Chen, X., Xu, S., & Li, Y. (2018). Technology and engineering application of cross area HVDC interconnection system high-precision simulation modeling based on ADPSS. *Global Energy Interconnection*, vol. 1(5), pp. 627–635. https://doi.org/10.14171/j.2096-5117.gei.2018.05.012tyl Literatura.

Tymoteusz Lindner[1], Daniel Wyrwał[2], Tomasz Kapłon[3]

POSITIONING OF THE ROBOTIC ARM USING REINFORCEMENT LEARNING POLICY GRADIENT ALGORITHM

Keywords: robotic arm, reinforcement learning, policy gradient, positioning

Abstract

Autonomous learning is one of the hallmarks of human behaviour and ability to self-learning will be crucial in order to achieve true autonomy in advanced machines. Smart robots will be a core in the Industry 4.0. A key characteristic of a smart system is its ability to learn. Robots can learn complex task like walking, cleaning house or simple task, such as reaching a particular position. Reinforcement learning algorithms enable learning using experience obtained in the process of machine learning. It allows the agent learn to act in different ways depending on the situation in which the agent found itself in the environment. In this paper authors present a research on accuracy of positioning of robotic arm gripper using policy gradient (PG) algorithm Deep Deterministic Policy Gradient (DDPG) combined with Hindsight Experience Replay (HER). The agent (robotic arm) is trained in virtual environment using physics engine. The robot learns from observation: cartesian position of robotic arm gripper, cartesian velocity of robotic arm gripper, joint's angles and joint's velocity. The task of the robot is to reach the specific position as quickly and as accurately as possible. Model trained in virtual environment is deployed in physical robotic arm. The accuracy of positioning is compared with PID control algorithm.

1. Introduction

Reinforcement learning has been shown to be an effective framework for solving complex control problems. In simulated domains, agents have been trained to perform a diverse set of challenging tasks [4], [8], [12] and highly dynamic motor skills [6], [9], [15], [16].

Unfortunately, many of the capabilities demonstrated by simulated agents have often not been realised by their physical counterparts. For tasks such as gripping, shifting, fitting one item to another, walking, running it is not easy to implement an agent trained in simulation in the real environment. There is a problem of accurate modelling of the environment, observation and variable parameters, such as mass, damping, friction etc. Camera observation, friction, suppression etc. are

[1] Poznan University of Technology, Piotrowo Street 3, Poznan 60-965, Poland, tymoteusz.lindner@put.poznan.pl
[2] Poznan University of Technology, Piotrowo Street 3, Poznan 60-965, Poland, daniel.wyrwal@put.poznan.pl
[3] Poznan University of Technology, Piotrowo Street 3, Poznan 60-965, Poland, tomasz.z.kaplon@doctorate.put.poznan.pl

difficult to represent in simulation as a number. There have been various techniques to address these types of problems such as Domain Randomization [14] [17], Domain Adaptation [3], RCAN [7].

In the 2016 study [2], the authors developed an algorithm on a simulated planar 6-DOF with a discrete action-set and showed that all the points reached by the manipulator have average accuracy of 0.0056 m (±0.002). The algorithm was found to be repeatable. The authors implemented the concept on the Baxter robotic arm to generate solutions up to 0.008 m. The authors of another study [11] used a closed-loop controller on a 3D soft-arm to position the end effector to reach a ball. In the research by Giorelli et al. [5] used a Jacobian-based approach to reach an average tip accuracy of 6% of the total manipulator length. These traditional methods are limited by modelling assumptions, computational expense, and most importantly, precision that needs to be further reduced for technological advancements in soft robotics. Learning mechanisms [13] provide a more promising approach by encoding correlations between sensorimotor data through internal models [20]. Imitation learning was applied to a high-dimensional soft manipulator by the authors of the work on STIFF-FLOP surgical robot [10]. However, this implies that the robot can only be as good as the provided information. The interaction with the environment through exploration is essential for a robot to learn optimal behaviour [18] [19].

The authors who presented the results from the research on the implementation of Reinforcement Learning algorithms for the robotic arm, focused on whether the agent was successful. In this paper, the focus is shifted to how the robotic arm was successful and what the positioning accuracy was. Despite being trained exclusively in simulation, the algorithm is able to maintain a similar level of performance when deployed on a physical robot, reliably moving to the target location with random initial configuration.

2. Background

2.1. Reinforcement Learning

The main aspects of Reinforcement Learning are the agent and the environment. The agent is a robotic arm and the environment is the world that the agent is surrounded by. At every step of interaction, the agent gets an observation of the state ($s \in S$) of the world and subsequently decides to perform an action ($a \in A$). The environment changes when the agent acts on it. The agent perceives a reward ($r \in R$) from the environment, a number that tells it how good or bad the current world state is. The goal of the agent is to maximise its cumulative reward, called return. The agent learns the policy $\pi(s)$ (strategy) by interacting with the environment, through trial and error. Reinforcement learning methods are ways, that the agent can learn behaviours to achieve its goal. A view of a simplified agent-environment interaction loop is shown in figure 1.

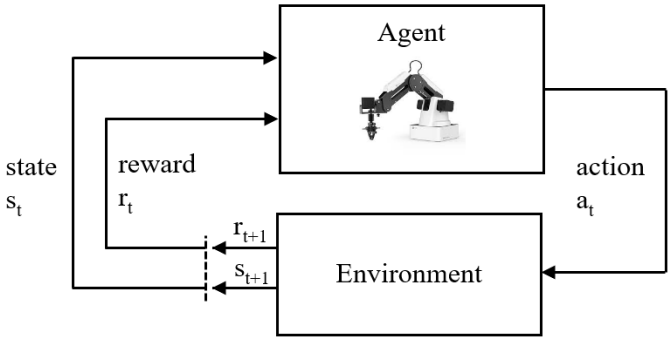

Fig. 1. Agent-environment interaction loop

2.2. Algorithm

Deep Deterministic Policy Gradients (DDPG) combined with Hindsight Experience Replay (HER) were used in the learning process. These two algorithms are briefly outlined below.

DDPG [8] is a model-free Reinforcement Learning algorithm for continuous action spaces. DDPG contains two neural networks: a target policy (also called an actor) $\pi(s)$ and an action-value function approximator (called the critic) $Q(s,a)$. The task of the critic is to approximate the actor's action-value function Q^{π}. Episodes are generated using a behavioural policy which is a noisy version of the target policy:

$$\pi_b(s) = \pi(s) + N(0, 1) \tag{1}$$

The critic is trained based on targets y_t which are computed using actions outputted by the actor:

$$y_t = r_t + \gamma Q(s_{t+1}, \pi(s_{t+1})) \tag{2}$$

The actor is trained with mini-batch gradient descent on the loss:

$$L_a = -E_s Q(s, \pi(s)) \tag{3}$$

where s is sampled from the replay buffer. The gradient L_a with regard to actor parameters can be computed by backpropagation through the combined critic and actor networks.

Hindsight Experience Replay [1] is a buffer of past experiences for learning from failures. The Authors of HER suggest the following strategy: suppose agent performs an episode of trying to reach the target state g from initial state s_0, but fails to do so and ends up in some state s' at the end of the episode. The trajectory is cached into replay buffer:

$$\{(s_0, g, a_0, r_0, s_1), (s_1, g, a_1, r_1, s_2), \ldots, (s_n, g, a_n, r_n, s')\} \quad (4)$$

The idea in HER is to imagine that goal has actually been in state s_n all along, and the agent has reached the goal successfully and got the positive reward. In addition, the following trajectory is cached:

$$\{(s_0, s', a_0, r_0, s_1), (s_1, s', a_1, r_1, s_2), \ldots, (s_n, s', a_n, r_n, s')\} \quad (5)$$

This trajectory is the imagined one and is motivated by the human ability to learn useful things from failed attempts. The reward received at the final step of the episode is now a positive reward gained from reaching the imagined goal. This approach allows the agent to gradually improve the policy and obtain the goal much more quickly.

3. Robotic system

The robotic system consists of two parts: hardware and software. The hardware consists of a robotic arm and a computer. The virtual environment that allows to simulate a virtual robotic arm and the algorithm used to learn complete the task is implemented on the computer. The configuration of the computer is as follows: OS is Ubuntu 18.04, CPU is Intel Core i7-8700K and GPU is GeForce GTX 1060.

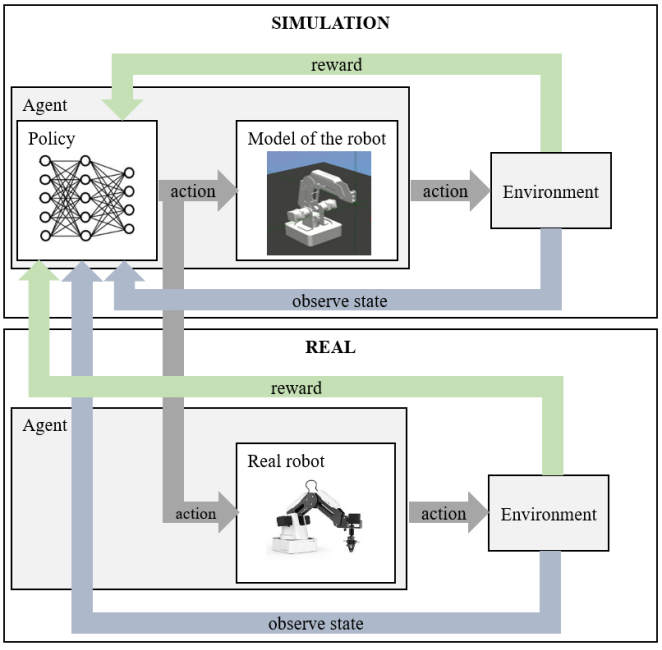

Fig. 2. Scheme of the system

The agent is a 4-DOF robotic arm Dobot Magician, shown in figure 3. This robot's repeatability precision reaches 0.2 mm, which is the maximum error that can occur. In addition, the robot has a lightweight body enough to be placed on the desktop. The joint structure of the robotic arm is shown in figure 3. Maximum payload of the robotic arm is 500g. The working range of four-degree joints are $[-90^0, 90^0]$, $[0^0, 85^0]$, $[-10^0, 95^0]$, and $[90^0, -90^0]$, respectively. In the presented model, the J4 joint was removed due to its lack of influence on positioning. The robotic arm has three channels for the communication with the computer, WIFI, USB and Bluetooth. In this work, the robotic arm communicates with the computer using the USB connection.

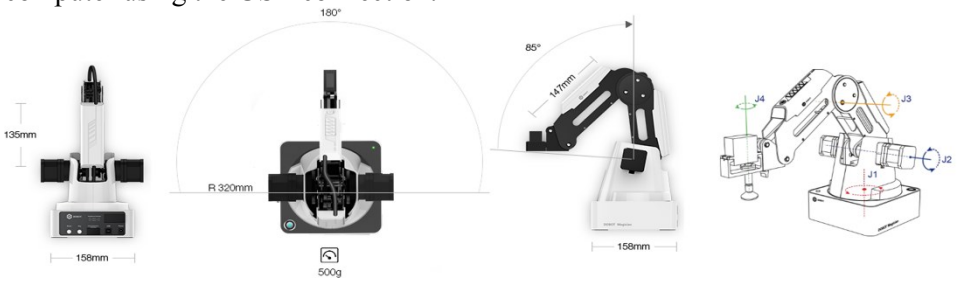

Fig. 3. Dobot Magician

Source: https://www.dobot.cc/dobot-magician/product-overview.html, Dobot Magician User Guide v1.7.0

The agent was trained in a virtual environment to learn the optimal policy ensuring the completion of the task. After training the optimal policy in simulation was tested on a virtual model of the robot and the physical robot, whose simplified scheme is shown in figure 2.

4. Experimental Investigation

4.1. Experiment description

The task of the robot was to reach the target position as quickly and as accurately as possible. The robot was moving without any payload. During the training robot started each episode from the same position. During the training the target position was sampled from the uniform distribution in the 3D space box (coordinates x_g, y_g, z_g). The maximum number of steps for each episode was 100. An episode ended after reaching the maximum number of steps or when the robot reached a sufficiently close position to the target. The distance threshold success d_{th} was set to 0.5mm.

The agent's observations were: gripper position (x, y, z), linear velocity gripper (v_x, v_y, v_z), joint's angles ($j1, j2, j3$), linear velocity joint's angles (v_{j1}, v_{j2}, v_{j3}),

target position (x_g, y_g, z_g). Altogether, there were 12 observations and the executed action was a 3-dimensional gripper movement (Δx, Δy, Δz).

Three different reward functions were put to test, which are described in section 4.2. The positioning accuracy of Reinforcement Learning algorithm was compared with the PID controller, briefly described in section 4.3.

The authors carried out the tests in the virtual environment on the model of the robot and on the physical one. The results were compared for the same target position. It was g_x = 0.04199m, g_y = 0.26923m, g_z = 0.15352m. There are also presented average results for randomly sampled target positions.

4.2. Reward functions

Three reward functions were tested:

- sparse,
- dense,
- dense trajectory.

The first reward function is binary. The agent obtains a reward of 0 if the object is at the target location (within a tolerance of 0.5mm) and −1 otherwise.

The second reward function takes into account the achieved position a and the target position g. The reward is calculated based on the Euclidean distance between point a and point g from the formula:

$$r_d = -\sqrt{(a_x\text{-}g_x)^2+(a_y\text{-}g_y)^2+(a_z\text{-}g_z)^2} \tag{6}$$

The third reward is an extension of the second reward. It also takes into account the trajectory on which the agent moves. The reward is calculated from the formula:

$$r_{dtr} = -\sqrt{(a_x\text{-}g_x)^2+(a_y\text{-}g_y)^2+(a_z\text{-}g_z)^2} - d\cdot w \tag{7}$$

where d is the distance between the achieved position a and the point that lies on the ideal trajectory based on the initial position s and target position g. The distance d is calculated from the formula:

$$d = \frac{|\vec{sg}\times\vec{sa}|}{|\vec{sg}|} \tag{8}$$

Coefficient w is weight coefficient, which describes the extent to which the distance d is relevant for calculating the reward $r_{dtr.}$

4.3. PID algorithm description

For each axis there is a separate, independent PID controller. The controller's input is the gripper position (x, y, z) and the controller's output is the gripper movement (Δx, Δy, Δz). PID's coefficients were: $K_P = 3$, $K_I = 0.5$. $K_D = 10$. The scheme of the controller is shown in figure 4.

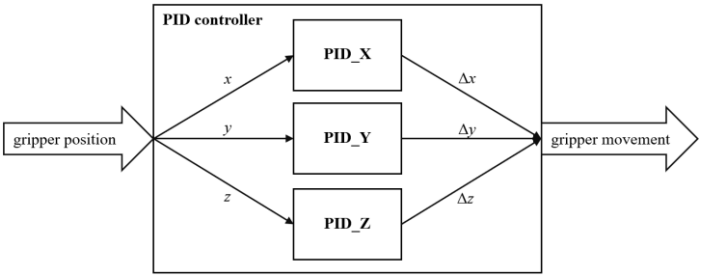

Fig 4. Scheme of the PID controller

4.4. Simulation results

The trajectory on which the robot's gripper moved is shown in figure 5. The algorithm with sparse reward achieves the goal fastest of all reward functions (the smallest number of steps). At the end of the movement, there are oscillations of the robot's gripper that disqualify this reward function. The trajectory is gently bent. For the tested target position (g_x = 0.04199m, g_y = 0.26923m, g_z = 0.15352m), the error e is 1.49mm. Error e is calculated from the formula:

$$e = \sqrt{x^2+y^2+z^2} \tag{9}$$

The algorithm with dense reward reduces oscillations, makes the robot's move more smoothly, but it takes more time to attain the target position. The trajectory as in the case of the previous reward function is gently bent. For different target position, the trajectory is slightly different. For tested target point, the error e is 0.71mm. For dense and sparse reward functions, it is difficult to predict exactly what trajectory the robot will follow.

The problem of moving on a specific trajectory was solved in the algorithm with the dense trajectory reward function. For coefficient $w = 2$, the trajectory was much more optimal and closer to the ideal trajectory created based on start position s and target position g, however, the end position was not sufficiently near the target position. The average distance d between the achieved position and ideal trajectory was 1.25mm. For coefficient $w = 20$, the trajectory on which the robot's gripper moved was almost a straight line. The average distance d between the achieved position and ideal trajectory was 0.51 mm. For this type of reward, the gripper's end position is the closest to the tested target position of all tested reward functions.

All results are collected in table 1, which gives data on the gripper's end position, the difference between gripper's end position and the target position, error *e* and the number of steps (actions) required to attain the end position.

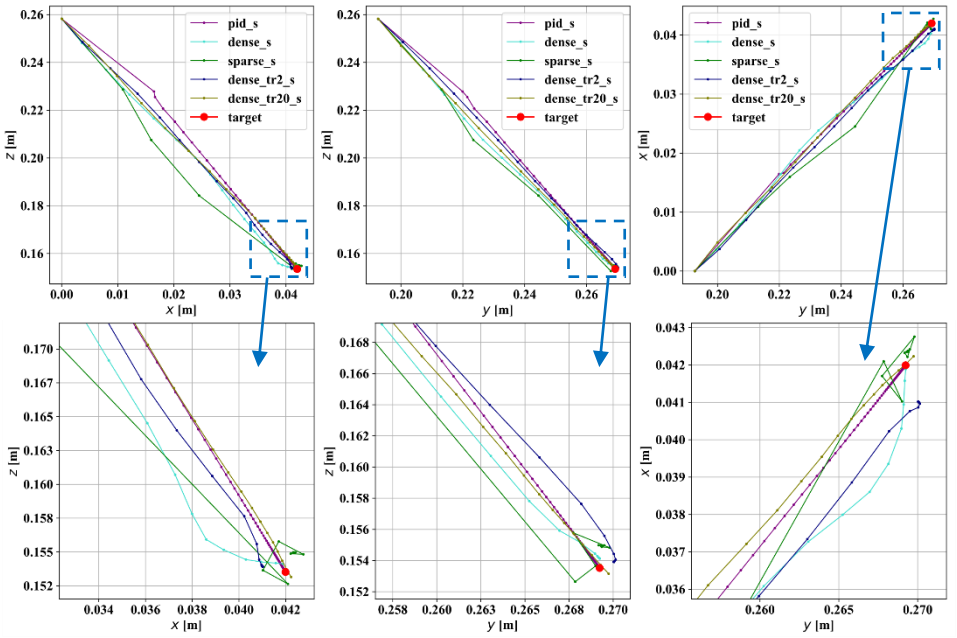

Fig. 5. Simulation results for target position: g_x = 0.04199m, g_y = 0.26923m, g_z = 0.15352m

Tab. 1. Simulation results for target position: gx = 0.04199 m, gy = 0.26923 m, gz = 0.15352 m

alg./reward fun.	end position - *x, y, z* [m]	difference - *x, y, z* [mm]	***e*** **[mm]**	steps
PID	0.04198, 0.26921, 0.15357	0.01, 0.03, -0.04	**0.05**	100/ 61*
sparse	0.04237, 0.26937, 0.15496	-0.37, -0.14, 0.43	**1.49**	18
dense	0.04189, 0.26924, 0.15423	0.11, -0.01, -0.70	**0.71**	28
dense tr *w*=2	0.04102, 0.27004, 0.15392	0.97, -0.81, -0.39	**1.33**	29
dense tr *w*=20	0.04223, 0.26974, 0.15315	-0.24, -0.51, 0.37	**0.67**	39

*due to integral term in the PID controller, the robot's gripper was still moving to minimise the error (until the maximum number of steps for the episode is reached – 100). The second number indicates the number of steps after which the gripper reached the position 0.5 mm from the target position.

4.5. Results of deployment of the physical robot

The trajectory on which the robot's gripper moved is shown in figure 6. The algorithm with sparse reward had huge oscillations comparing to simulation results. For some target positions, the robot falls in undefined oscillations. The robot's gripper moved around target position until the end of the episode.

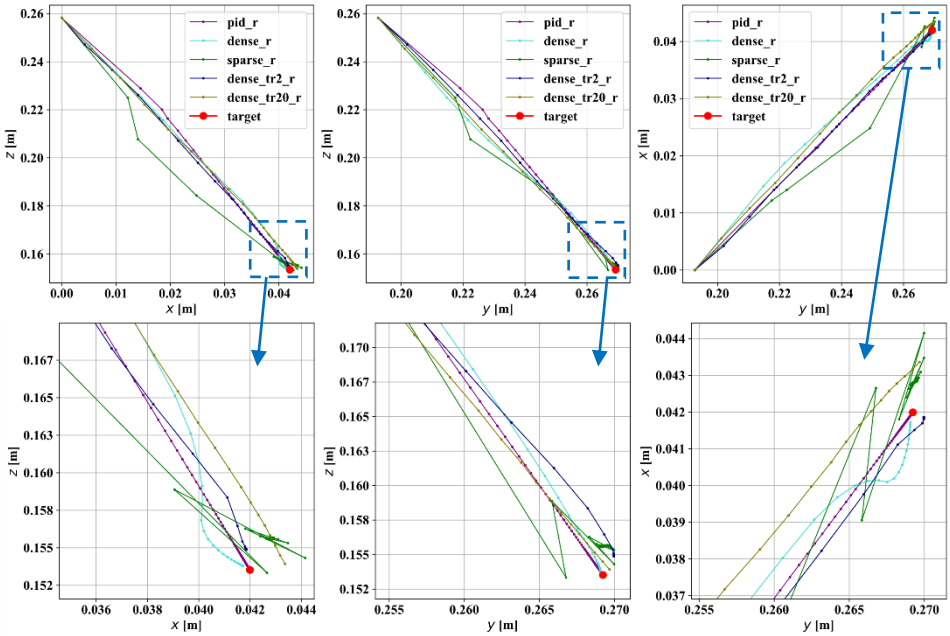

Fig. 6. Results of deployment on a physical robot for target position: g_x = 0.04199m, g_y = 0.26923m, g_z = 0.15352m

The algorithm with dense reward makes the robot move more smoothly, but the trajectory is slightly bent. Error e is 0.41 mm, which is the best result for this particular target position. The algorithm with dense trajectory reward function solves the problem of bent trajectory. For coefficient w = 2, the average distance d between the achieved position and ideal trajectory was 1.38 mm. For coefficient w = 20, the average distance d was 1.27 mm.

All results for target position: g_x = 0.04199 m, g_y = 0.26923 m, g_z = 0.15352 m are collected in table 2, which contains information about the gripper's end position, the difference between the gripper's end position and the target position, error e and the number of steps (actions) required to attain the end position.

Tab. 2. Results of deployment on a physical robot for target position: gx = 0.04199 m, gy = 0.26923 m, gz = 0.15352 m

alg./reward fun.	end position: *x, y, z* [m]	difference: *x, y, z* [mm]	***e*** **[mm]**	steps
PID	0.04198, 0.26921, 0.15356	0.01, 0.03, -0.04	**0.05**	100/ 63*
sparse	0.04282, 0.26938, 0.15564	-0.82, -0.15, -2.11	**2.27**	21
dense	0.04173, 0.26907, 0.15378	0.26, 0.16, -0.26	**0.41**	31
dense tr *w*=2	0.04186, 0.26996, 0.15489	0.14, -0.73, -1.36	**1.55**	32
dense tr *w*=20	0.04337, 0.26968, 0.15393	-1.37, -0.45, -0.40	**1.50**	40
*due to integral term in the PID controller, the robot's gripper was still moving to minimise the error (until the maximum number of steps for the episode is reached – 100). The second number indicates after what number of steps the gripper reached the position 0.5 mm from the target position (target).				

4.6. Comparison of simulation and deployment of the physical robot

The three tested types of reward functions (sparse, dense, dense trajectory $w = 20$) employed in the simulation and the physical robot are compared in figure 7. For dense reward and dense trajectory reward, the results for simulation and deployment on a physical robot are comparable. Transfer of learned agent from simulation to real object gives similar accuracy of positioning. Unwanted oscillations appearing in the algorithm with sparse reward function, should be rejected.

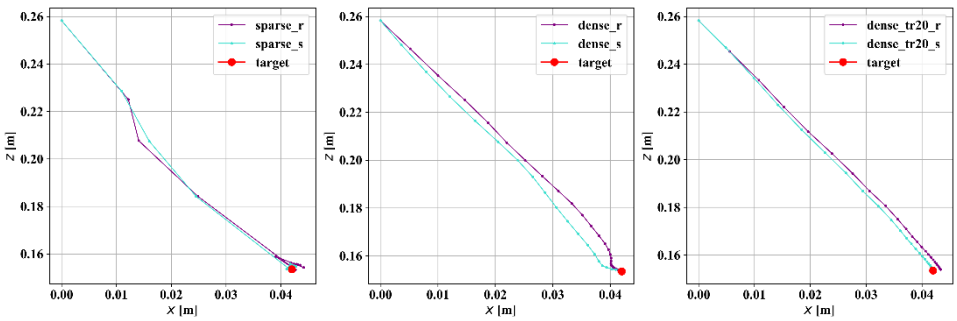

Fig. 7. Comparison of the results for simulation and deployment of the physical robot

Table 3 shows the average error *e* and the average number of steps the agent had to execute to attain the randomly sampled target positions. Referring to table 3, it can be stated that the best positioning accuracy, both for simulation and deployment on the physical robot has an algorithm with dense trajectory reward with coefficient $w = 20$. Deployment on the physical robot can be considered as successful because difference compared to simulation is about 0.5 mm.

Tab. 3. Average error and number of steps

sim/physical	reward function	avg. e ± std [mm]	avg. steps ± std
simulation	sparse	**1.137**±0.518	19±1
	dense	**2.177**±1.575	29±2
	dense tr w=2	**1.762**±1.293	29±2
	dense tr w=20	**1.044**±0.625	39±2
physical	sparse	**6.757**±7.855	73±37
	dense	**2.224**±1.952	31±2
	dense tr w=2	**1.939**±1.703	32±2
	dense tr w=20	**1.552**±1.481	39±2

5. Conclusions

The robot controlled by Reinforcement Learning algorithms has an advantage over the classic control methods. The robot develops its own strategies of action based on the collected experience, gaining a certain degree of autonomy. Thanks to generalisation it can adapt to slight changes occurring in the environment, which is what the classic control methods experience the problem with.

For the tested reward functions, the best accuracy and reliability was shown by the algorithm with dense trajectory reward function. Although it does not reach the target in the smallest number of steps. In the simulation, the algorithm had a positioning accuracy of 1.044 mm (±0.625), whereas in deployment on a physical robot – 1.552 mm (±1.481). The authors of the study referenced at the beginning of this paper [2] reached accuracy 5.6 mm (±2.0) in simulation and 8 mm for a physical robot.

In the future, the authors plan to test the accuracy of positioning for the robot that has to avoid obstacles and move along a specific, more complicated trajectory.

Acknowledgement

The work presented in this paper was funded from 02/22/SBAD/1505.

References

[1] M. Andrychowicz et al., “Hindsight Experience Replay”, *arXiv:1707.01495 [cs]*, Jul. 2017.

[2] Y. Ansari, E. Falotico, Y. Mollard, B. Busch, M. Cianchetti, and C. Laschi, “A Multiagent Reinforcement Learning approach for inverse kinematics of high dimensional manipulators with precision positioning”, *in 2016 6th IEEE International Conference on Biomedical Robotics and Biomechatronics (BioRob)*, pp. 457–463, 2016.

[3] L. Duan, D. Xu, and I. W. Tsang, “Learning with Augmented Features for Heterogeneous Domain Adaptation”, pp. 8.
[4] Y. Duan, X. Chen, R. Houthooft, J. Schulman, and P. Abbeel, “Benchmarking Deep Reinforcement Learning for Continuous Control”, *arXiv:1604.06778 [cs]*, Apr. 2016.
[5] M. Giorelli, F. Renda, M. Calisti, A. Arienti, G. Ferri, and C. Laschi, “A two dimensional inverse kinetics model of a cable driven manipulator inspired by the octopus arm”, *in 2012 IEEE International Conference on Robotics and Automation*, pp. 3819–3824, 2012.
[6] N. Heess et al., “Emergence of Locomotion Behaviours in Rich Environments”, *arXiv:1707.02286 [cs]*, Jul. 2017.
[7] S. James et al., “Sim-to-Real via Sim-to-Sim: Data-efficient Robotic Grasping via Randomized-to-Canonical Adaptation Networks”, *arXiv:1812.07252 [cs],* Dec. 2018.
[8] T. P. Lillicrap et al., “Continuous control with deep reinforcement learning”, *arXiv:1509.02971 [cs, stat]*, Sep. 2015.
[9] L. Liu and J. Hodgins, “Learning to Schedule Control Fragments for Physics-Based Characters Using Deep Q-Learning”, *ACM Transactions on Graphics*, vol. 36(3), pp. 1–14, Jun. 2017.
[10] M. S. Malekzadeh, S. Calinon, D. Bruno, and D. G. Caldwell, “Learning by imitation with the STIFF-FLOP surgical robot: a biomimetic approach inspired by octopus movements”, Robotics and Biomimetics, vol. 1, pp. 1–15, 2014.
[11] A. D. Marchese and D. Rus, “Design, kinematics, and control of a soft spatial fluidic elastomer manipulator”, *I. J. Robotics Res*., vol. 35, pp. 840–869, 2016.
[12] V. Mnih et al., “Human-level control through deep reinforcement learning”, *Nature*, vol. 518 (7540), pp. 529–533, Feb. 2015.
[13] D. Nguyen-Tuong and J. Peters, “Model learning for robot control: a survey”, *Cogn Process*, vol. 12 (4), pp. 319–340, Nov. 2011.
[14] X. B. Peng, M. Andrychowicz, W. Zaremba, and P. Abbeel, “Sim-to-Real Transfer of Robotic Control with Dynamics Randomization”, *2018 IEEE International Conference on Robotics and Automation (ICRA)*, pp. 1–8, May 2018.
[15] X. B. Peng, G. Berseth, and M. van de Panne, “Terrain-adaptive locomotion skills using deep reinforcement learning”, *ACM Transactions on Graphics*, vol. 35 (4), pp. 1–12, Jul. 2016.
[16] X. B. Peng, G. Berseth, K. Yin, and M. Van De Panne, “DeepLoco: dynamic locomotion skills using hierarchical deep reinforcement learning”, *ACM Transactions on Graphics*, vol. 36 (4), pp. 1–13, Jul. 2017.
[17] J. Tobin, R. Fong, A. Ray, J. Schneider, W. Zaremba, and P. Abbeel, “Domain Randomization for Transferring Deep Neural Networks from Simulation to the Real World”, *arXiv:1703.06907 [cs],* Mar. 2017.
[18] L. Vannucci, N. Cauli, E. Falotico, A. Bernardino, and C. Laschi, “Adaptive visual pursuit involving eye-head coordination and prediction of the target motion”, *in Proceedings of the 14th IEEE-RAS International Conference on Humanoid Robots (Humanoids)*, Madrid, Spain, pp. 541–546, 2014.
[19] L. Vannucci, E. Falotico, N. Di Lecce, P. Dario, and C. Laschi, “Integrating Feedback and Predictive Control in a Bio-Inspired Model of Visual Pursuit Implemented on a Humanoid Robot”, *in Biomimetic and Biohybrid Systems*, pp. 256–267, 2015.
[20] D. M. Wolpert, R. C. Miall, and M. Kawato, “Internal models in the cerebellum”, *Trends Cogn. Sci. (Regul. Ed.),* vol. 2 (9), pp. 338–347, Sep. 1998.

Jarosław Chmiel[1], *Lech Dorobczyński*[2]

DIGITAL PROCESSING OF ELECTROCHEMICAL SIGNALS GENERATED IN CONDITIONS OF CAVITATION IN LIQUIDS

Keywords: Statistical analysis of signals, median filtration, cavitation, electrochemistry, hydrogen adsorption

Abstract

A method of analysis of long time series containing a quasi-periodic signal disturbed by random components is presented. The measurement data contained electrical and pressure signals, recorded at high sampling rates during electrochemical tests in a cavitation cloud on the vibratory rig. Statistical analysis of signals, recorded in digital form allowed to separate of signal variations onto following components:

- Component of long period containing constant values, being consequence of applied potential difference, quasi-static variations caused by thermal drift, variations in liquid composition and its conductivity and variations of period are at least 10 time longer, than period of basic wave caused by macroscopic pulsation of cavitation cloud;
- Component of frequency corresponding to basic frequency of liquid oscillation;
- Component of short period (with duration time below 12 μs), associated with cavitation phenomenon in liquid.

Signal processing was carried out with use of adaptive median filter under the terms synchronous sampling with sampling rate not lower than 50 – 100 times more than basic frequency of sampled signal i.e. 1 – 2 MHz.

1. Introduction

The phenomenon of cavitation is connected with gradients of pressure formed in a liquid and is a consequence of turbulent flow or high power vibrations induced by an external factor. The nature of cavitation and methods of its examination have been described in numerous publications, e.g. [1 -5]. Cavitation erosion is a process of material damage that accompanies the dynamic pulse influence of liquid on material surface. Imploding gas or vapour bubbles which first form in areas of low pressure act in the form of microjets or impact waves in cavitation cloud (figure 1) [2]. When a liquid exerts physical and chemical influence on a material, there occur mechanical masking effects of cavitation erosion nature caused by chemical and electrochemical

[1] Maritime University of Szczecin, Wały Chrobrego 1, 70-501 Szczecin, Poland, j.chmiel@am.szczecin.pl

[2] Maritime University of Szczecin, Wały Chrobrego 1, 70-501 Szczecin, Poland, l.dorobczynski@am.szczecin.pl

phenomena. In this connection, the process of cavitation erosion is sometimes classified as a specific form of corrosion, which seems unjustified [5 – 12].

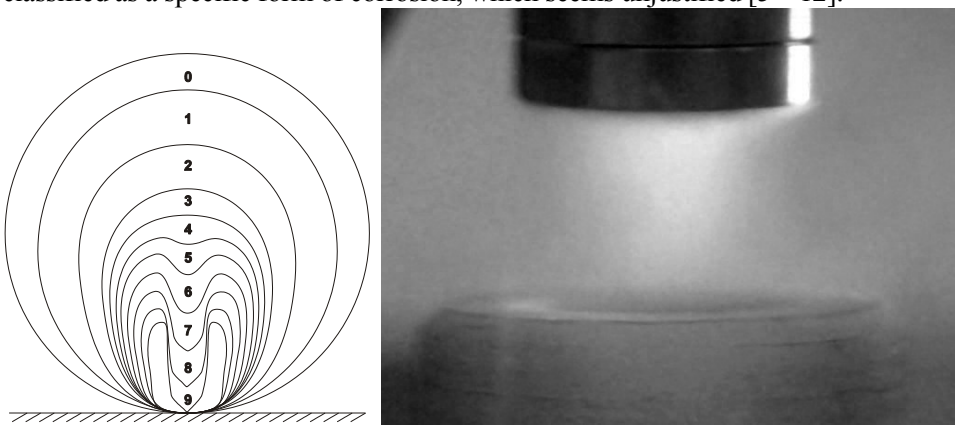

Fig. 1. A scheme of implosion of a cavitation bubble [2] and cavitation cloud observed under the exciter on a vibratory rig

Conventional methods of signal processing used during electrochemical research in the presence of cavitation are as follows:

- classic band filtration carried out with the use of analogue circuits in a measuring channel or using digital filters designed on the basis of analogue prototypes, therefore it is an on-line type of filtration,
- digital filtration implemented in the off-line mode, consisting of FFT, removal of unwanted components of the spectrum and IFFT [13, 14].

During research performed in conditions specific for the vibration facility with a fixed specimen, differences were found between mass losses of corrosive nature estimated by using Faraday's law (after current signal filtration) and determined by spectrophotometric analysis of water after the process. Properties of the mentioned differences, depending on the power density of cavitational load, gave indications that low-pass filtration methods might be a source of errors.

2. Laboratory stand and research conditions

The laboratory stand (figure 2) permitted to change the power density of cavitational load from 0 to 1000 kW/m2 by variation of amplitude oscillation of the exciter or by changing the gap between the exciter and a specimen [15]. The laboratory stand consisted of:

1. Ultrasonic processor Sonics VCX-500 with frequency of 20 kHz and amplitude up to 124 μm.
2. Elpan EP-20a analogue potentiostat, with bandwidth up to 100 kHz, equipped with an amplifier with voltage outputs: Uw-ref (voltage between working and

reference electrodes), as well as U(i) – voltage of value proportional to the current value.

3. Three-electrode work cells, with volume of 2 dm^3,
- working stationary electrode: Armco type iron (in the first stage), in the second stage of investigation it was replaced by the mentioned below piezoelectric converter, wherein the sensors membrane was used as a working electrode;
- counter electrode of TiAl6V4 alloy, used as an oscillator horn tip;
- reference electrode AgCl Eurosensor type EAgClU-302.

4. Cooling system based on a Polyscience 9512 refrigerating circulator.
5. Measuring and control system containing
- pressure/charge converter Kistler 603B, connected to a charge-coupled preamplifier Brüel & Kjaer 2635 with inner low- and high-pass filters with cut-off frequencies of 100 kHz and 0.2 Hz, respectively;
- PC computer with MS Windows XP operating system and Intel Core 2 Duo processor;
- sequential A/D converter Advantech PCI-1716 under control of MeasX DasyLab 9.0 software as master controller of experimental device;
- four-channel parallel A/D converter Advantech PCI-1714 with specialised software for data acquisition up to 10 MHz per channel, used as time magnifying glass, providing the main measurement data stream;
- support two-channel digital oscilloscope with bandwidth up to 100 MHz.

The research conditions were as follows:
- working liquids: NaCl solution in deionised water 30 g/dm^3, deionised water with conductivity <0,1μS/m and tap water;
- applied temperature: 293 +/- 1 K;
- size of the gap between the oscillator and the sensor membrane: 5 mm;
- Electrochemical conditions: open circuit potential (OCP), forced anode and cathode polarisation: +/- 1V;
- amplitude (peak-to-peak) ranged from 25 to 124 μm and respectively power density showed in table 1 [15].

Tab. 1. Dependencies amplitude – power density [15]

amplitude (μm)	20	50	75	100	124
power density (kW /m^2)	0.24	5.4	22.6	55.9	102

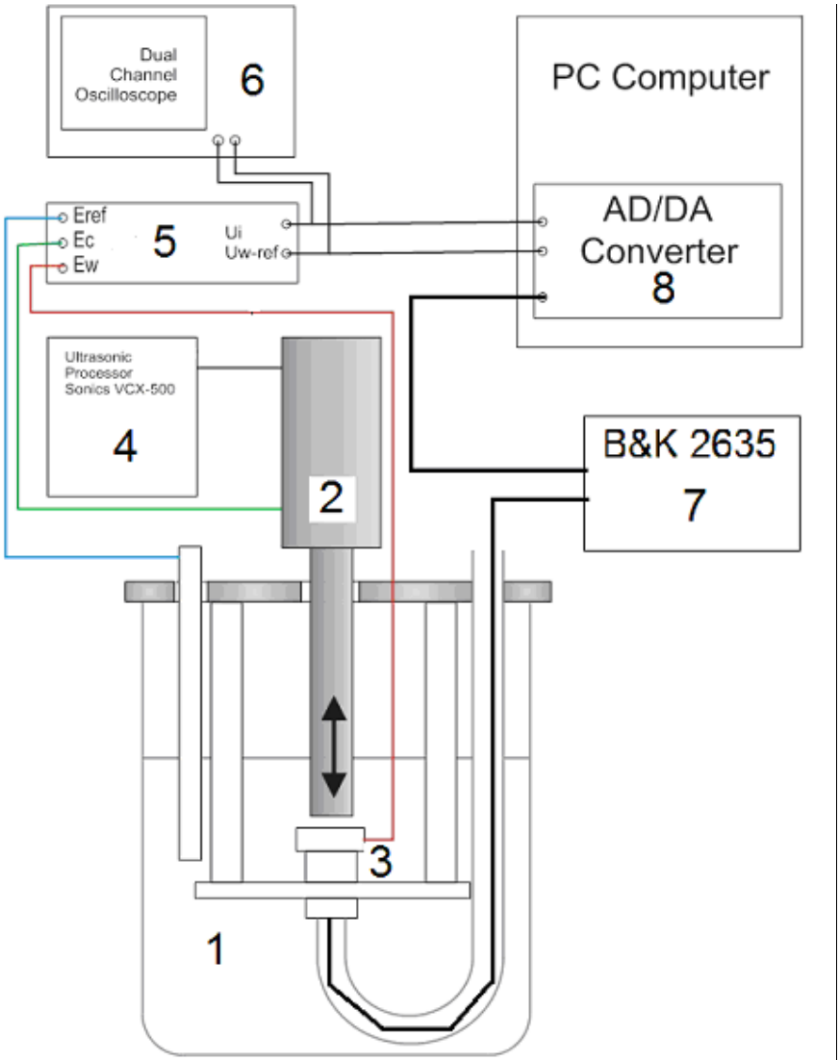

Fig. 2. Layout of the laboratory stand. Legend: 1. Work cell, 2. Ultrasonic oscillator, 3. Specimen holder with specimen or with pressure sensor 4. Ultrasonic processor Sonics VCX-500, 5. Potentiostat Elpan EP-20a, 6. Dual-channel oscilloscope, 7. Charge coupled preamplifier Brüel & Kjaer type 2635, 8. A/D converter Advantech PCI-1714

3. Signal recording and analysis

The collected data sets were recorded by means of the A/D Advantech PCI-1714 converter with 12-bit resolution and sampling frequency of 1 MHz. The applied sampling frequency allowed to obtain synchronous sampling up to 50 samples per period of oscillations, assuming the periodic nature of measured

signals. Due to limited software compatibility, the main data stream was recorded in text files, with accuracy to 5 decimal places, 0.01 mV for the 1V range, which was also adjusted to the 12-bit resolution of the converter.

The obtained data files, size from 5 to 10 MB, are two main classes of signals stored in the form of a four-column array and were subjected to numerical analysis off-line. These classes are:

- electrochemical signals obtained from the Uw-ref and U(i) potentiostat outputs;
- pressure signal acting on the membrane surface of the piezoelectric transducer.

During electrochemical measurements in vibratory cavitation conditions, oscillations of potential and anode current, disturbing periodical nature of measured signals were observed on the oscilloscope screen (figure3).

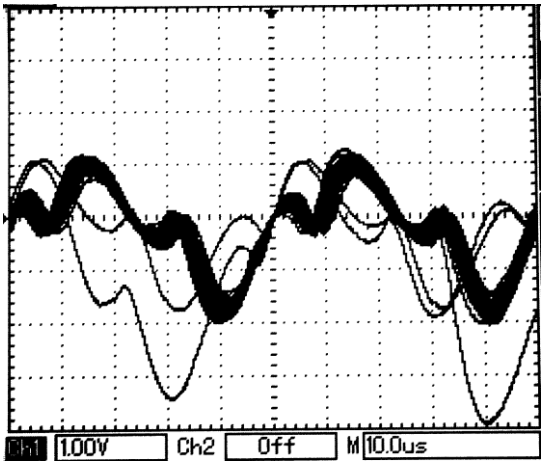

Fig. 3. Typical raw signals of anode circuit current in the presence of cavitation. Amplification of current – potential converter: 10 mA/V, time base 100 µs, duration time of oscillogram recording: 2 s

Together with mentioned disturbances, acoustic effects typical for cavitational phenomena were observed. Preliminary analysis of recorded electrochemical signals allowed to state that they were superposition of:

- constant or slowly varying component (with time constant of several minutes), related with a bias potential of the working electrode, and corresponding to the value of anode current in static conditions (steady state) without cavitation and variations of period are at least 10 time longer than period of basic wave caused by macroscopic pulsation of cavitation cloud;
- periodic component with a frequency of 20 kHz, corresponding to liquid oscillation in the gap between the electrodes and forced by oscillator, herein called the fundamental wave,

- fast varying component of a complex structure with a dominating aperiodic term; characterised by irregular distortions of the fundamental wave, where duration time of the distorting pulse can be estimated as one-fourth of the fundamental wave period, i.e. 12 μs.

3.1. Signal processing methods

During the experiment, in order to identify properties of particular components, three variants of measured signals processing were implemented:

- classic low-, high- and band-pass filters, applied in the analogue part of measuring system in order to suppress slow-varying and periodic components in real time;
- digital off-line signal processing using the sequence: FFT- removal of unwanted components of spectrum – IFFT;
- digital filtration, aimed at spectrum sectors, with particular consideration of median filter.

Efficiency of analogue filtration was found to be unsatisfactory due to random variation and aperiodicity of the distorting impulses. In multiple cases, together with the suppression of periodical signal, also fast-variable aperiodic pulses were attenuated.

Filtration combined with spectral analysis gives satisfactory results when the disturbance term is periodic. In the analysed case, aperiodicity of disturbances implied problems with the choice of effective masks intended to eliminate selected harmonic components, which is implied by properties of global FFT-based filters, operating on data sets of great size (multiplicity). Global selection of masks often leads to elimination of disturbances together with significant components of the fundamental wave.

Median filtration of the one-dimensional signal is performed by finding the value of median in a relatively narrow time window of a given width, determined as 2M-1 samples, where M denotes the filter range (figure 4.A). The advantage of such filters is high efficiency in detection and suppression of disturbances of random nature. The negative feature is significant delay of signal, impeding the use of such filter in on-line mode [13].

In the studied case a median filter was applied, based on set of samples taken in successive periods, and corresponding to the same phase angle of undisturbed fundamental wave (figure 4.B) .

Recorded Uw-ref and U(i) signals were subjected to median filtration with filters of 2nd to 6th order. It was found that:

- filters of 3rd and 4th order have small selectivity in comparison with higher order filters,
- filters of 4th and 5th order have significant enhancement of selectivity and fidelity of signal reconstruction,

- increasing the filter order (over 6th) causes risk of losing sampling synchronism (e.g. due to generator frequency drift) and generation of artifacts at the ends of time-domain window and introduce greater delays.

For reasons mentioned above, the filter of 4th order was chosen as optimal.

3.2. Analysis of electrochemical signals

The fundamental wave was extracted from the raw signal (figure 5A) by means of the 4th order median filter (figure 5.B). The difference between the reconstructed fundamental wave and the raw signal is defined as a disturbance signal (figure5.c).

Similar properties were observed for Uw-ref and U(i) signals. The disturbance signal consists of:

- main pulses in some cases aperiodic, with amplitude range comparable with the fundamental wave amplitude, and duration time of about 10 μs. The pulse sign has a random character;
- pulses preceding the main pulse are of a significantly smaller amplitude and duration time of 3 μs;
- pulses following the main pulse have a shape of significantly damped oscillations with a period of 10 to 12 μs.

Due to the physical nature of the phenomenon and geometrical features of the cell, the current impulses may have multiple characteristics:

1. movement of the positive charge package to the surface of the auxiliary electrode (positive – up);
2. movement of the negative charge package in the direction of the auxiliary electrode (negative – up);
3. movement of the positive charge package in the direction of the working electrode (positive –down);
4. movement of the negative charge package in the direction of the working electrode (negative – down).

The first and fourth classes give a positive current signal, whereas the second and third a negative current signal, respectively (figure 5 C).

In relation to the model of concentration of positive charges on the particle-liquid and bubble-liquid interface, the 3rd class of charge movement, i.e. the positive charge package movement towards the working electrode surface, was considered to be the most important.

The first and fourth classes give a positive current signal, whereas the second and third a negative current signal, respectively (figure 5 C).

In relation to the model of concentration of positive charges on the particle-liquid and bubble-liquid interface, the 3rd class of charge movement, i.e. the positive charge package movement towards the working electrode surface, was considered to be the most important.

A.

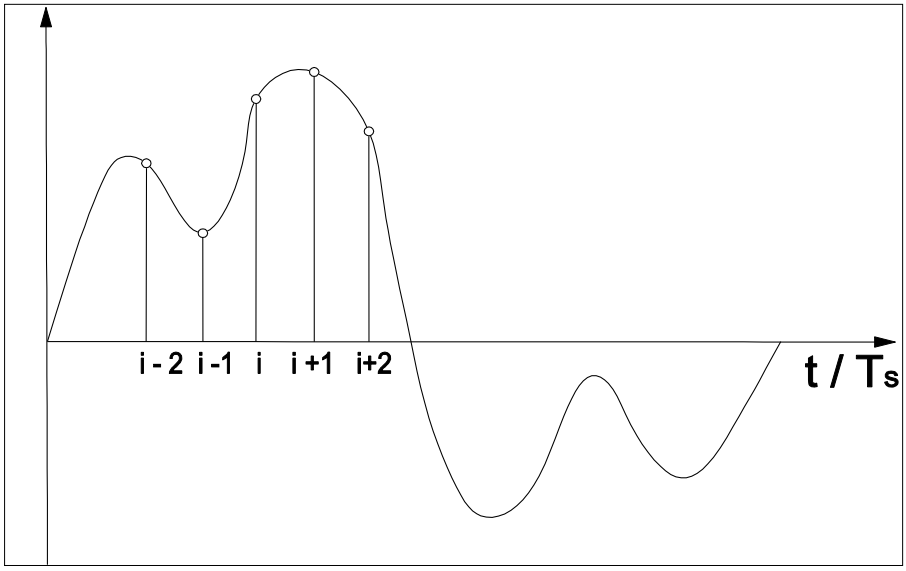

B.

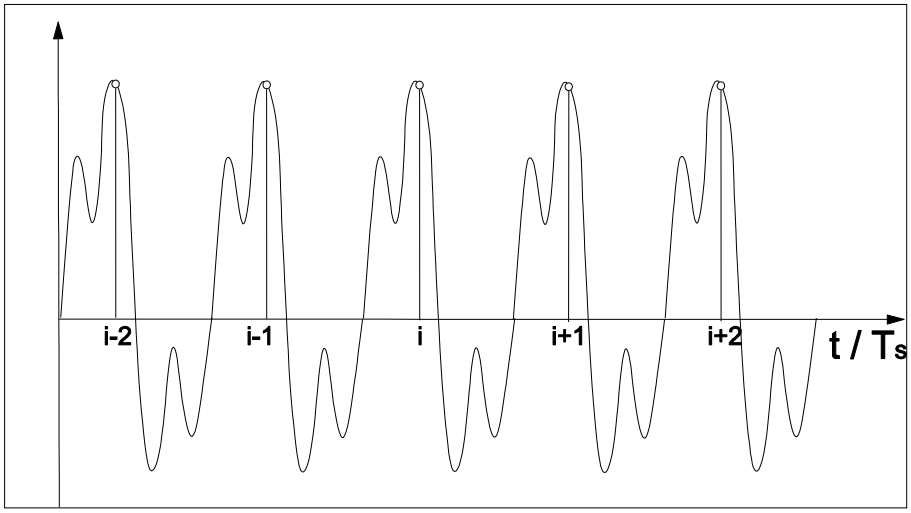

Fig. 4. Third-order filter if = f (i), A. General case of third-order filter, when Ts denotes sampling time, B. Third-order filter for periodic signals

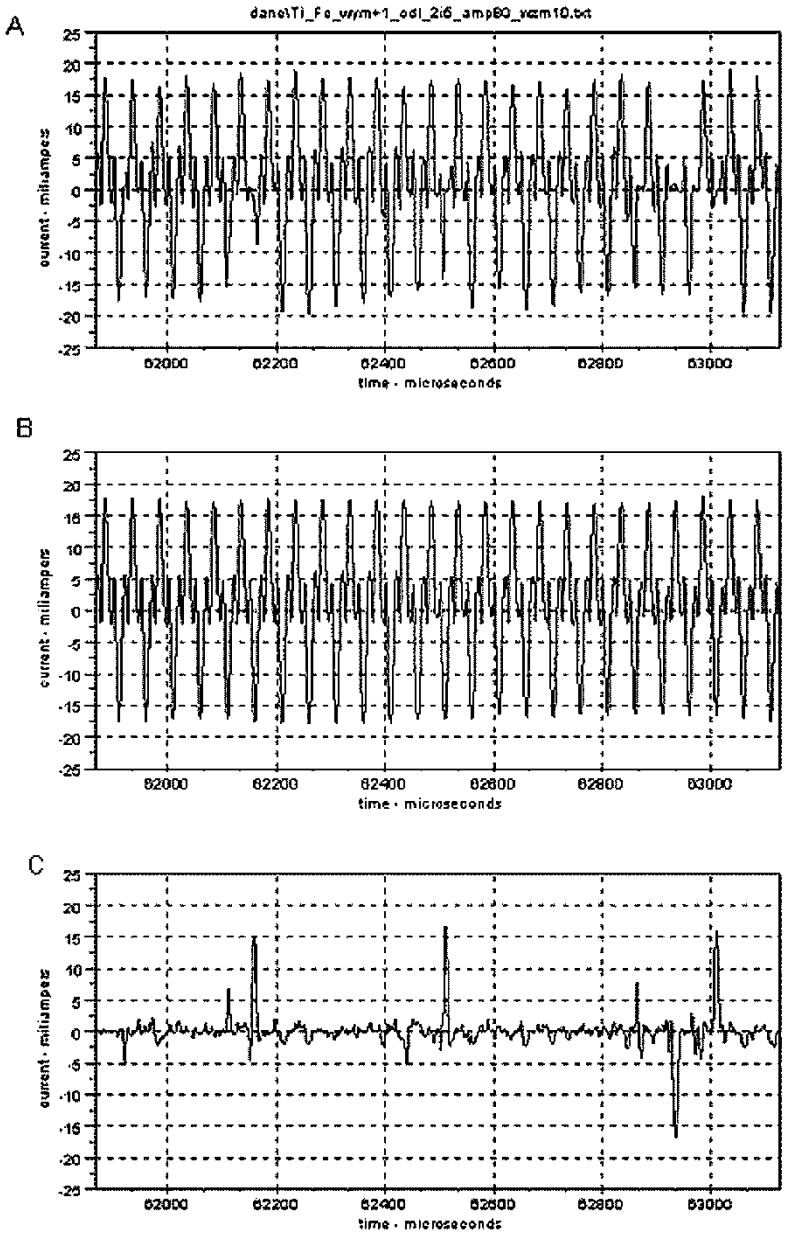

Fig. 5. Examples of recorded and computed waveforms of Uw-ref potential variations (generated in Scilab environment). From top to bottom: A. raw signal, B. reconstructed fundamental wave , C. disturbance signal defined as A-B, a clearly visible pulse of reversed polarisation

Waveforms of the absolute value of disturbance signal qualitatively shows a considerable structural similarity to waveforms of pressure changes recorded by means of piezoelectric sensors for identical conditions of cavitational load at the same laboratory stand (figure 6). This similarity is particularly evident in the range of basic series of pulses, duration time of main pulse, as well as the presence of preceding pulses.

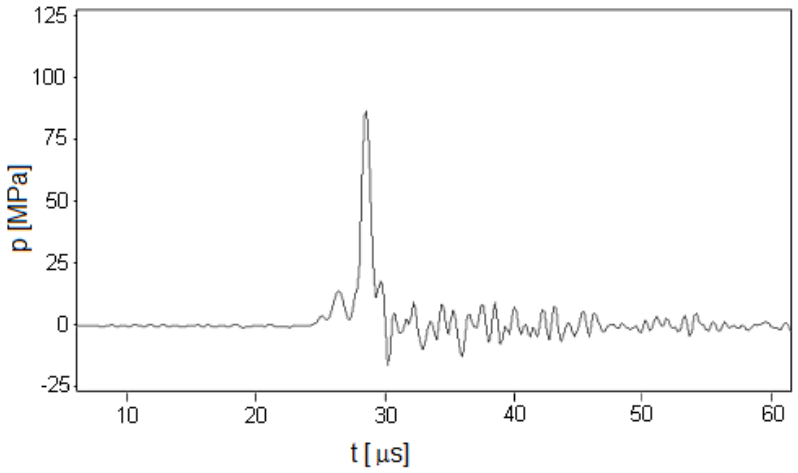

Fig. 6. Example pulse pressure variations in the conditions of cavitation [15]

Because qualitative relationship with pressure pulses and electrical signals variations is beyond doubt, an attempt to describe the quantitative relationships between two types of signals was taken under.

In the preliminary phase of the analysis, the identification of pressure pulses acting on the membrane was carried out. This was done in the Dasylab program, using Pre-post Trigger and Relay modules. The level of discrimination, length of the time window and anticipation of the beginning of the time window were used as variable parameters. If a pulse was identified, descriptor 1, written in the fourth column of the matrix, was assigned to a sequence of signals belonging to it. The assignment to time interval corresponding to identified pulse the logical variable value, determining membership of a time window being a subject of analysis of the correlation of signals (figure 7 and figure 8). After determining the most favourable values of pulse identification parameters, this stage was realised in Matlab program, without a preview of pulse identification in real time.

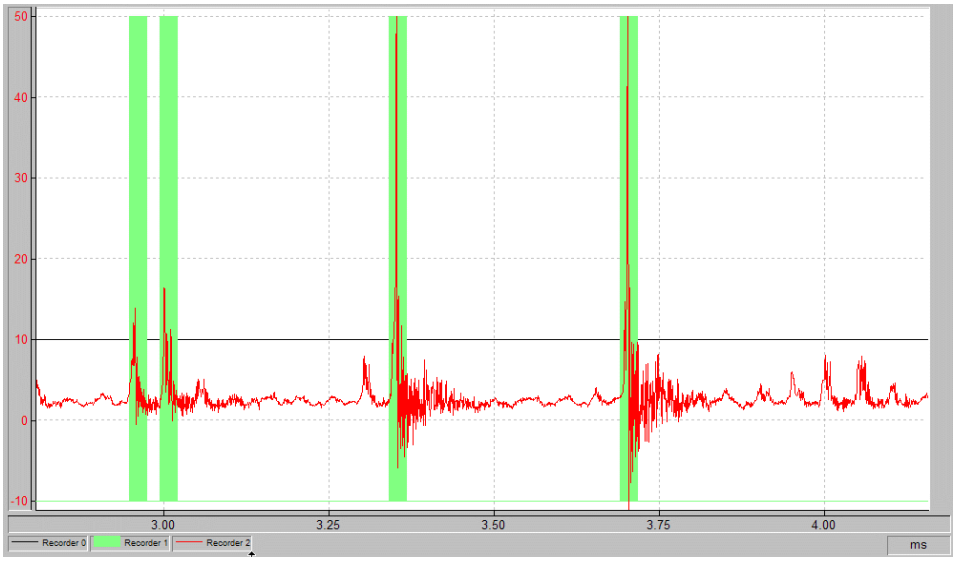

Fig. 7. Qualitative identification (green) of pressure pulse (red) by assumed discrimination level (black), performed in Dasylab software

The processing of electrochemical signals, realised in Scilab and/or Matlab software, included:

1. Median filtration of electric potential variations signal in order to separate disturbing component
2. Reversing and amplification of signal of potential variations
3. Elimination of constant components and cutting negative values of pressure and potential off
4. Analysis of mutual correlation between signals of pressure and potential and determination of Pearson coefficient R_{xy} for the particular time windows.

The general analysis was carried out for the value of levels of discrimination from 4 to 20 MPa and for the width of the time window between 5 and 50 μs. It was found, that the correlation coefficient R_{xy} varies from 0.2 to above 0.8. An increase in the threshold of discrimination was meant to eliminate the phenomena accompanying to pressure pulses (or more accurately, their elements defined as main pulse). Narrowing the time window resulted in elimination from the analysis the preceding pulses and secondary pulses. In both cases, the increase in the coefficient value R_{xy} even above 0.9 was observed. This indicates the significant dependence of electrochemical effects of components related to higher pulse energy. Deviations of peaks maxima location on the time axis, after taking into account delays in signal paths, are lower than 1 μs.

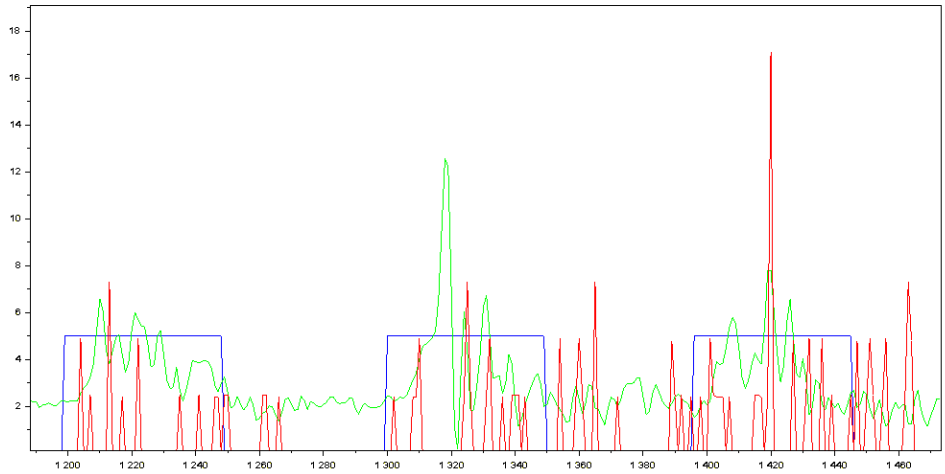

Fig. 8. An example of time windows (blue) and pressure and potential curves (respectively green and red) selected for correlation analysis (discrimination level D = 4 MPa, time widow width 25 µs)

However, a momentary change of potential and current were also observed, which can not be directly associated with changes of pressure. The peaks caused by changes are approx. 30% peaks, extracted from raw signal. This is largely due to the division of electrochemical impulses into four classes, with only two of them being important, associated with implosions near the surface of the pressure transducer diaphragm, as described above. Moreover, due to the relatively large distance between the face of the inductor and the transducer diaphragm, it is possible to register packages of charges reaching these surfaces, but the pressure impulse was no longer recorded as a result of its dissipation. One of explanation includes geometric characteristics of the laboratory stand in which the cavitation cloud is not free, therefore different kinds of interference between current and reflected waves are possible.

Basing on analysis of variations in potential and anode current, the following can be expressed:

1. The decisive parameter for amplitude of variation in difference of potentials between working and reference electrodes is an energy of cavitational influence, being function of exciters oscillation amplitude and width of gap between exciter and working electrode.
2. Peak-to-peak amplitudes reaching 200 mV were recorded for the demineralised water with conductivity in range of 0.1 µS/m. These results are consistent with the references [4, 5]. Simultaneously with increase in conductivity of tested environment, decrease in amplitude of potential pulses was observed, associated among others with the presence of significant amounts of anions in solution.

3. A factor of an influence on pulse sign can be presence of bubble implosion in neighborhood of both working and auxiliary electrodes. The packets of positive charges are moving in opposite directions, and mentioned direction determines pulse sign.
4. The decisive influence on the amplitude of the anode current change has an electrical conductivity of environment and subsequently, cavitational load with related potential oscillations. In conditions of demineralised water the amplitude of the current density changes, was immeasurable small, in the tap water was reached to 0.01 mA/cm^2, and in brine even to 50 mA/cm^2.

4. An analysis of the results

At first stage of measurements no correlation between the forcing potential and the amplitude of disturbing potential was found, contrary to the existing correlation between the amplitude of exciter oscillations and the amplitude of fundamental wave, as well as peak-to-peak amplitudes of raw and disturbance signals. In the range of cavitational load used during the research, the mentioned dependences can be described with polynomials of 1st or 2nd degree.

Variations of pulse sign are caused by properties of the environment i.e. electrolyte, in which positive and negative ions exist. Cavitation bubble implosion in the electrolyte is accompanied by mechanical transfer of ion packet of random composition. The resulting pulse sign is dependent on the sign of ions dominating in the packet.

According to models of interphase zeta potential [16,17], a concentration of positive charges exists on the external surface of particle or bubble. This phenomenon is independent of the value of forcing potential in an open circuit condition (OCP), studied by Chincholle [18], which explains why a majority of observed pulses has positive sign. Negative pulses were observed mainly in an NaCl solution. The domination of pulses with the positive sign causes temporary (up to 5 μs) inversion of system polarisation, and stimulates hydrogen absorption at the electrode surface, regardless of the potential, forcing the anodic nature of the electrode.

Taking into account a close relationship between the location of potential and current pulses on the axis of time, and the fact that the amplitude of current pulses is dependent on liquid conductivity, the following analysis will focus on relationships between pressure and potential.

It is worth noting that the statistical distribution of potential and current pulses may differ significantly from the distribution of the amplitudes of pressure pulses. As shown in references, mechanical movement of portions of electrical charges (ions packets) by the action of microjets and cavitation waves is possible [2]. Ion packet composition is another parameter being a statistical variable. Despite the fact that the expected value of this variable is zero, local fluctuations of concentration at the molecular level are possible [20]. In strong electrolytes it

leads to the observed variability of sign and value of the resultant charge, carried by a microvolume of liquid, accelerated by the cavitational pulse. Under forced polarisation conditions, a momentary reversal of the system polarity may occur.

Presence of a large number of current and potential pulses should be also considered, even though seemingly not related to pulses of pressure which are associated with far implosions and do not give a clear mechanical effect, although they carry a significant electrical charge.

However, an instantaneous change of the potential and current was also observed, which cannot be directly associated with changes in pressure. Peaks of these changes account for about 30% of peaks that are separated from raw signals. A possible explanation of their presence are geometric characteristics of the applied laboratory stand, in which a cavitational cloud is not a free cloud. Therefore, interference of a different kind is possible between incident and reflected waves. The amplitude of pressure changes may be within the limits specified for the cavitation noise [15], but due to relatively greater mass of the moved liquid, amplitudes of current variations may go beyond this range. Amplitudes of potential variations can reach values conforming to the Chincholle model [18].

Analysis of the correlation between signals of pressure and potential indicates that there is no significant delay between enforcement (pressure variations) and response (variations of potential and current). The high compliance of pulses position is obtained when the analysis is performed inside a time window not longer than 15 μs, corresponding to pressure pulses. This relationship was observed regardless of electrochemical conditions, but it is mostly qualitative. An obstacle in determining a quantitative relation is the highly variable and unpredictable composition of an ion packet.

Pulses of positive sign potential (cathodic polarisation) are present regardless of electrochemical conditions, wherein the probability of their occurrence increases with an increase in the cathodic character of forcing potential. A large number of such pulses also occur by forced anodic polarisation. It is, therefore, possible to instantaneously reverse the polarity and hydrogen absorption at the object which nominally is the anode.

The results of the analysis of electrochemical signals make up a basis for planning and execution of an experiment, which will confirm directly the independence of hydrogen absorption from electrochemical conditions in the presence of cavitation [21].

5. Conclusions

The applied filtration method is highly effective and adaptive.Thanks to the use of median filter, the kernel of which is a set of points corresponding to the same phase angle, it is possible to isolate signal disturbances difficult to isolate by other methods.

High compatibility of the "positive – down" group signals with pressure pulses indicated the possibility of mechanically forced hydrogen absorption in cavitation conditions in liquids containing hydrogen or hydronium ions, regardless of other electrochemical conditions.

Acknowledgements

The work was supported by the Polish Ministry of Science and Higher Education, grant no. N509 2925 35.

References

[1] L. Rayleigh, "On the pressure development in a liquid during the collapse of a spherical cavity", *Philosophical Magazine and Journal of Science*, vol. 34, pp. 94–98, 1917.
[2] M. S. Plesset, R. B. Chapman, "Report No. 85-09", *Office of Naval Research*, 1970.
[3] R. T. Knapp, J. Daily, F. G. Hammit, "Cavitation", *McGraw – Hill: New York*, 1970.
[4] J. Chmiel, "Advances in the research into the phenomena of corrosion-cavitation and hydrogen–cavitation wear", *Polish Journal of Environmental Studies*, vol. 18(2A), pp. 33–38, 2009.
[5] J. Steller, "International cavitation erosion test and quantitative assessment of material resistance to cavitation", *Wear*, vol. 233-235, pp. 51–64, 1999.
[6] R. J. K. Wood, "Corrosion of pure copper in flowing seawater under cavitating and noncavitating flow conditions", *Journal of Fluids Engineering*, Transactions of the ASME, vol 112(2), pp. 218–224, 1990.
[7] H. M. Shalaby, A. Al-Hashem, H. Al-Mazeedi, A. Abdullah, "Field and laboratory study of cavitation corrosion of nickel aluminium bronze in sea water", *British Corrosion Journal*, vol. 30(1), pp. 63–70, 1995, https://doi.org/10.1179/000705995798114221
[8] G. Silva, "Wear generation in hydraulic pumps", *SAE Transactions*, vol. 99(2), pp. 635–652, 1990, https://doi.org/10.4271/901679.
[9] J. T. Chang, C. H. Yeh, J. L. He, K. C. Chen,"Cavitation erosion and corrosion behaviour of Ni-Al intermetallic coatings", *Wear*, vol. 255(1-6), pp. 162–169, 2003, https://doi.org/10.1016/S0043-1648(03)00199-6.
[10] C. T. Kwok, F. T. Cheng, H. C. Man, "Synergistic effect of cavitation erosion and corrosion of various engineering alloys in 3.5% NaCl solution source", *Materials Science and Engineering A: Structural Materials: Properties, Microstructure and Processing*, vol. 290(1), pp. 145–154, 2000, https://doi.org/10.1016/S0921-5093(00)00899-6.
[11] G. A. Schmitt, W. Bücken, R. Fanebust, "Modeling microturbulences at surface imperfections as related to flow-induced localized corrosion", *Corrosion*, vol. 48(5), pp. 431-440, 1992, https://doi.org/10.5006/1.3315957.
[12] M. Matsumura, "Erosion-Corrosion. An Introduction to Flow Induced Macro-Cell Corrosion. Bentham Books", 2012, eISBN 978-1-60805-351-3.
[13] O. I. Balyts'kyi, J. Chmiel, L. Doroczyński, "Analysis of electrochemical oscillations in vibration cavitation conditions", *Materials Science*, vol. 47(1), pp. 21–25, 2011, https://doi.org/10.1007/s11003-011-9363-z.

[14] T. Zieliński, “Digital signal processing”, *WKŁ Warszawa*, 2005, pp. 364 (in Polish).
[15] J. Chmiel, W. Janicki, A. Krella, J., “The tests of corrosion-cavitation on the vibratory rig with stationary specimen”, *Problemy eksploatacji (Maintenace problems)*, vol. 76(1), pp. 91–100, 2010 (in Polish).
[16] M. Smoluchowski, “Contribution to the theory of electro-osmosis and related phenomena”, *Bulletin international de l'Académie des sciences de Cracovie*, vol. 3(184), 1903.
[17] R. W. O'Brien and L. R. White, “Electrophoretic mobility of a spherical colloidal particle”, *Journal of the Chemical Society, Faraday Transactions 2,* vol. 74, pp. 1607, 1978.
[18] L. Chincholle, F. Goby, “Etude de la charge electrique des bulles de cavitation. Application eventuelle a la detection du seuil de cavitation”, *In IAHR&SHF Symposium Two Phase Flow and Cavitation in Power Generation. Grenoble*, pp. 138–144, 1976.
[19] A. Barbulescu, V. Marza, “Electrical Effects Induced at the Boundary of an Acoustic Cavitation Zone”, *Acta Physica Poonia Series B.,* vol. 37, pp. 508–518, 2006.
[20] E. G. Sinaiski, L. I. Zaichik, “Statistical Microhydrodynamics”, Wiley-VCH, pp.470, 2008, ISBN 978-3-327-40656-2.
[21] J. Chmiel, E. Łunarska, “Effect of cavitation on absorption and transport of hydrogen in iron”, *Solid State Phenomena*, vol. 183, pp. 25–30, 2012, https://doi.org/10.4028/www.scientific.net/SSP.183.25.